

# **AIMING FOR A WATER INDEPENDENT HOUSEHOLD BY DIRECT REUSE OF GREYWATER USING MBR TECHNOLOGY AND UV DISINFECTION**

Seppe Ongena

Student number: 01608339

Promotors: Prof. dr. ir. Korneel Rabaey, Prof. dr. ir. Arne Verliefde

Tutors: Ir. Arjen Van de Walle, Dr. ir. Leonardo Gutierrez

Master's Dissertation submitted to Ghent University in partial fulfilment of the requirements for the degree of Master of Science in Bioscience Engineering: Environmental Technology

Academic year: 2020-2021





# Copyright notice

The author and the promotor give permission to use this thesis for consultation and to copy parts of it for personal use. Every other use is subject to the copyright laws, more specifically the source must be extensively specified when using results from this thesis.

De auteur en de promotor geven de toelating deze masterproef voor consultatie beschikbaar te stellen en delen van de masterproef te kopiëren voor persoonlijk gebruik. Elk ander gebruik valt onder de beperkingen van het auteursrecht, in het bijzonder met betrekking tot de verplichting de bron uitdrukkelijk te vermelden bij het aanhalen van resultaten uit de masterproef.

Ghent, June 4th, 2021

The promotors,



Prof. dr. ir. Korneel Rabaey



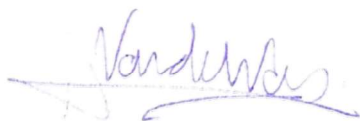
Prof. dr. ir. Arne Verliefde

The author,

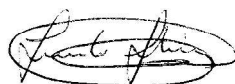


Seppe Ongena

The tutors,



Ir. Arjen Van De Walle



Dr. ir. Leonardo Gutierrez

# Preface

I started this 5-years bioscience engineering programme with the naive intention to ‘better the environment’. Looking back, it is striking to see how much I’ve grown as a person, as I gained more knowledge of the world around me, allowing me to better articulate and substantiate my ideas. I would have never thought I would end up in the water treatment sector, as centralized wastewater treatment plants seemed dreadfully static and boring to me. Instead, my thoughts strayed towards small-scale water treatment systems, as the idea of a water independent house, similar to energy neutral housing, was very intriguing and attractive to me. I began to fantasize about how this could be implemented and was dumbstruck when I found this thesis topic. I was highly motivated to start my research as I delved deeper into the topic with great satisfaction and, admittedly, frequent frustration and sleep deprivation.

The pleasant work environment filled with quick-to-help people and intriguing discussions lightened the workload, for which I would like to thank every researcher, collaborator and colleague-student at CMET. In particular, I would like to thank my tutors, Ir. Van De Walle and Dr. Gutierrez for their excellent guidance, always standing at the ready to answer my questions and listening to my concerns or ideas. I would also like to thank Eng. Mosquera Romero for her support in the microbiological work.

Furthermore, I would like to express my gratitude to my promoters, Prof. Verliefde for allowing me to use the PaInT labs for my analyses, and Prof. Rabaey for his inspirational role and the great opportunities he gave me, allowing me to achieve my personal goals.

I am grateful for the support of my mother, Ann, in all my years of growth towards this moment, and the opportunity to complete these studies in the first place. The support of my friends and family was indispensable, including the late-night laughs and the short, but welcome visits. Lastly, I would like to thank my love, Hülya, for her shoulder to rest on, her words and arms to soothe my stress, and her ears to listen to my incessant babbling about this thesis.

# Contents

<b>Table of Contents</b>	<b>1</b>
<b>List of figures</b>	<b>3</b>
<b>List of tables</b>	<b>4</b>
<b>Abbreviations</b>	<b>7</b>
<b>Abstract</b>	<b>8</b>
<b>Joint thesis subject</b>	<b>9</b>
<b>1 Introduction</b>	<b>10</b>
1.1 Water scarcity: a contemporary problem . . . . .	10
1.2 Water reuse: a solution? . . . . .	11
1.2.1 Water reuse and resource recovery . . . . .	11
1.2.2 Centralized and decentralized water treatment . . . . .	13
1.2.3 Source separation . . . . .	15
1.2.4 Challenges to implementation . . . . .	16
1.3 Greywater as an alternative water resource . . . . .	17
1.3.1 Greywater characterization . . . . .	17
1.3.2 Health and environmental concerns . . . . .	19
1.4 Disinfection of effluent . . . . .	20
1.4.1 The rationale of disinfection . . . . .	20
1.4.2 UV disinfection . . . . .	22
1.5 Membrane technologies for greywater treatment . . . . .	25
1.5.1 Cleaning and fouling . . . . .	27
1.5.2 Polymeric membranes . . . . .	28
1.5.3 Ceramic membranes . . . . .	30
<b>2 Objectives and hypotheses</b>	<b>33</b>
<b>3 Materials and methods</b>	<b>34</b>
3.1 Synthetic greywater composition and preparation . . . . .	34
3.2 Reactor design and operation . . . . .	37
3.3 Analysis methods . . . . .	40
3.3.1 Sampling procedure . . . . .	40
3.3.2 Sample analysis . . . . .	40
3.4 Process kinetics . . . . .	41
3.5 Disinfection assessment methodology . . . . .	43
3.5.1 <i>E. coli</i> removal efficiency . . . . .	43
3.5.2 UV reactor characterization . . . . .	44

3.5.2.1	UV reactor residence time . . . . .	44
3.5.2.2	UV dose determination . . . . .	45
<b>4</b>	<b>Results</b>	<b>47</b>
4.1	Synthetic greywater characterization . . . . .	47
4.2	Phase I: troubleshooting and optimization . . . . .	50
4.2.1	Sludge related problems . . . . .	50
4.2.2	Treatment performance . . . . .	52
4.3	Phase II and III: polymeric and ceramic membrane testing . . . . .	53
4.3.1	Sludge characteristics during operation and kinetics . . . . .	53
4.3.2	Membrane performance . . . . .	54
4.3.3	Treatment performance . . . . .	56
4.4	UV <sub>254</sub> absorbance correlations . . . . .	59
4.5	<i>E. coli</i> removal efficiency . . . . .	60
4.5.1	Spike test 1: polymeric membranes . . . . .	60
4.5.2	Spike test 2: method comparison for polymeric membranes and UV . . . . .	60
4.5.3	Spike test 3: ceramic membranes, UV and EC . . . . .	60
4.6	UV reactor characteristics . . . . .	62
4.6.1	UV reactor residence time . . . . .	62
4.6.2	UV dose . . . . .	63
<b>5</b>	<b>Discussion</b>	<b>64</b>
5.1	Treatment performance . . . . .	64
5.2	Membrane performance . . . . .	65
5.3	Disinfection performance . . . . .	65
5.4	Water fit for reuse . . . . .	67
5.5	Comparison with MBBR . . . . .	69
<b>6</b>	<b>Conclusion</b>	<b>71</b>
6.1	General conclusions . . . . .	71
6.2	Perspectives . . . . .	73
	<b>Appendix</b>	<b>74</b>
<b>A</b>	<b>Sustainability</b>	<b>74</b>
<b>B</b>	<b>Supplementary figures</b>	<b>75</b>
<b>C</b>	<b>Supplementary tables</b>	<b>78</b>
	<b>References</b>	<b>81</b>

# List of Figures

1.1	Areas of physical and economic water scarcity in 2007	10
1.2	Overview of potable and non-potable municipal recycled water, including direct and indirect reuse.	12
1.3	The two most common MBR configurations.	25
1.4	Schematic representation of a composite ceramic membrane	31
1.5	TMP increase due to reversible and irreversible fouling for different membrane materials.	31
3.1	Overview of the MBR setup	37
3.2	Manometer installation height.	39
4.1	Turbidity of the influent during all three phases.	48
4.2	MLSS and MLVSS content of the MBRs during Phase I.	50
4.3	Transmembrane pressures during Phase I.	51
4.4	MLSS and MLVSS content of the MBRs during Phases II and III.	53
4.5	Transmembrane pressures during Phases II and III.	55
4.6	The fouling rates for the polymeric and ceramic membranes.	55
4.7	The tCOD and sCOD for MBR 1 during Phase II and III.	56
4.8	The nitrogen speciation for MBR 1 during Phase II and III.	58
4.9	The carbon fractions for MBR 1 during Phase II and III.	58
4.10	Relation between $UV_{254}$ , TOC and sCOD for the effluent of Phase I and III.	59
4.11	<i>E. coli</i> concentration throughout the treatment train.	61
4.12	Cumulative RTD and RTD of the UV reactor.	62
B.1	Microscopic images of algae in the MBR.	75
B.2	Male nematode tail.	75
B.3	Composite image of a female nematode.	75
B.4	Ciliate protozoa.	75
B.5	Macroscopic view of nematodes and algae.	76
B.6	Progression of the overflow events.	76
B.7	Dispersed growth at the end of Phase I.	77
B.8	The ceramic membranes used in Phase III.	77
B.9	The polymeric membranes used, before and after cleaning.	77
B.10	Overview of the MBR setup.	77
B.11	Diagram of the UV reactor.	77

# List of Tables

1.1	Household wastewater quantities per source. . . . .	17
1.2	General composition of mixed greywater. . . . .	18
1.3	Microbial contamination of greywater. . . . .	20
1.4	Reclaimed water requirements for nonpotable water reuse. . . . .	21
1.5	Required UV doses for untreated greywater disinfection. . . . .	24
1.6	Overview of the operating parameters and major removal efficiencies for studies on GW treatment with polymeric flat sheet MF membranes in submerged MBRs. . . . .	29
1.7	The major advantages and disadvantages of ceramic membranes over polymeric membranes. . . . .	30
3.1	Composition of the synthetic greywater. . . . .	34
3.2	Summary of PCP usage based on risk assessment studies. . . . .	35
3.3	Detergent usage in the EU in 1998. . . . .	35
3.4	Properties of the PCP and detergents used. . . . .	36
3.5	Operational parameters for the three phases. . . . .	39
4.1	Characteristics of fresh greywater and influent. . . . .	47
4.2	Comparison between the synthetic greywater and real mixed greywater. . . . .	49
4.3	Treatment performance during Phase I. . . . .	52
4.4	Treatment performance during Phase II and III. . . . .	57
4.5	Summary of <i>E. coli</i> spike tests 2 and 3. . . . .	61
5.1	Comparison between the observed MBR effluent quality and a selection of nonpotable water reuse quality targets. . . . .	68
5.2	Comparison between MBR and MBBR effluent quality. . . . .	69
C.1	Main differences between membrane polymers. . . . .	78
C.2	Main properties of different ceramic top-layer materials. . . . .	79



# Abbreviations

<i>A</i>	Area
$A_\lambda$	Absorbance at Wavelength $\lambda$
AOP	Advanced Oxidation Processes
AS	Activated Sludge
<i>b</i>	Sludge Decay Rate
bCOD	biodegradable COD
BOD <sub>5</sub>	5-day Biological Oxygen Demand
<i>c</i>	Concentration or the Speed of Light
CASO	Casein Peptone and Soybean Flour Peptone
CCA	Coliform Chromogenic Agar
CFU	Colony Forming Units
CIP	Cleaning-In-Place
COD	Chemical Oxygen Demand
CPD	Cyclobutyl-pyrimidine dimers
C-PE	Chlorinated Polyethylene
CSO	Combined Sewer Overflow
CW	Clothes Washing
<i>D</i>	UV Dose
$d_p$	Pore Diameter
DBP	Disinfection By-products
DO	Dissolved Oxygen
DOC	Dissolved Organic Carbon
$\varepsilon$	Surface Porosity or Molar Absorption Coefficient
<i>E</i> , RTD	Residence Time Distribution
$E_\lambda$	Proton Energy at Wavelength $\lambda$
EC	Electrochemical Cell
EDTA	Ethylenediaminetetraacetic Acid
<i>F</i>	Cumulative Residence Time Distribution
$F_b$	Fraction Biodegradable COD
<i>g</i>	Gravitational Constant
GW	Greywater
<i>h</i>	Planck's Constant
HAA	Halogenated acetic acids
HMBR	Hybrid Membrane Bioreactor

HRT, $\theta_H$	Hydraulic Retention Time
$I$	UV Lamp Intensity
IC	Inorganic Carbon or Ion Chromatography
$J$	Flux
$\kappa$	Electrical conductivity
$l$	Cell Path Length
$\lambda$	Wavelength
LMH	$L\ m^{-2}\ h^{-1}$
LOQ	Limit of Quantification
LP/MP-Hg	Low or Medium Pressure Mercury Vapor Lamps
LRV	Log Removal value
LRT	Log Removal Target
NTU	Nephelometric Turbidity Units
$\mu$	Dynamic Viscosity or Specific Growth Rate
$M$	Manometer height above water level
MBR	Membrane Bioreactor
MBBR	Moving Bed Biofilm Reactor
MBB(C)MR	Moving Bed Biofilm (Ceramic) Membrane Reactor
MF	Microfiltration
ML(V)SS	Mixed Liquor (Volatile) Suspended Solids
$\nu$	Frequency
$N_{immob}$	Immobilised Nitrogen
N.D.	Not Detectable
N/A	Not Applicable
$P$	Pressure
$p$	p-Value at the 95% Confidence Level
$\Phi$	Quantum Yield
PA	Polyamide
PBS	Phosphate Buffered Saline solution
PE	Polyethylene
PES	Polyethersulfone
PFU	Plaque Forming Units
(P)PCP	(Pharmaceuticals and) Personal Care Products
PVDF	Polyvinylidene Difluoride
$Q$	Flow rate

$q$	Specific Substrate Removal Rate
$\rho$	Density or Correlation
$R_f$	Fouling Resistance
$R_m$	Membrane Resistance
$S$	Effluent Substrate Concentration
$S_0$	Influent Substrate Concentration
SA	Sanitary Appliances
sCOD	soluble COD
SLR, $B_x$	Sludge Loading Rate
SRT, $\theta_x$	Solids Retention Time
$T$	Temperature
$t$	Time
$\tau$	Theoretical Residence Time
$\tau_m$	Mean Residence Time
TC	Total Carbon
TDS	Total Dissolved Solids
TF	Toilet Flushing
THM	Trihalomethanes
TKN	Total Kjeldahl Nitrogen
TMP	Transmembrane Pressure
TN	Total Nitrogen
TP	Total Phosphorus
TOC	Total Organic Carbon
TSS	Total Suspended Solids
UR	Unrestricted Reuse
$UV_{254}$	Ultraviolet Light Absorbance at 254 nm
$V$	Volume
VLR, $B_V$	Volumetric Loading Rate
VSS	Volatile Suspended Solids
WKM	Water Kilometres
WWTP	Wastewater Treatment Plant
$X$	Sludge Concentration
$x$	Distance under the Water Level
$\Delta x$	Pore length
$Y_{COD}$	Sludge Growth Yield

# Abstract

## English abstract

The reclamation of greywater for non-potable reuse by a small-scale membrane bioreactor (MBR) treatment system with UV disinfection was studied. No direct comparison between polymeric and ceramic membranes for the treatment of greywater in an MBR was available. Therefore, lab-scale MBR setups were operated for 204 days on synthetic greywater, using C-PE polymeric and SiC ceramic membranes. Fouling rates were determined by monitoring of the transmembrane pressure at a constant flux. General wastewater parameters were analysed, such as chemical oxygen demand, nitrogen speciation, and turbidity. *E. coli* log removals for the membranes and UV reactor were assessed through spike tests, and the UV reactor was characterized in terms of residence time distribution and applied UV dose. A 6.85 times lower linear fouling rate was observed for the SiC membranes, caused by differences in surface material and roughness. The MBR effluent met the strictest water quality targets for unrestricted urban reuse, except for nitrogen limits. Average removal efficiencies for the ceramic membranes were 99.2%, 94.7%, 53%, and 95.7% for turbidity, chemical oxygen demand, total nitrogen, and ammonium-nitrogen, with similar results for the polymeric membranes. No *E. coli* were detected in the effluent, with log removals of 2.7–3.0 and 3.1–3.7 for the ceramic and polymeric membranes, respectively, and a log removal for the UV reactor of >10 at a dose of 875 mJ cm<sup>-2</sup> or 726 J L<sup>-1</sup>. These results indicate a high application potential of ceramic MBR for the treatment and reuse of greywater.

## Dutch abstract

Het hergebruik van grijswater voor niet-drinkbare toepassingen werd bestudeerd met behulp van kleinschalige membraanbioreactoren (MBR) met UV-desinfectie. Een directe vergelijking tussen polymerische en keramische membranen voor dergelijke doeleinden was niet beschikbaar. Daarom werd synthetisch grijswater gedurende 204 dagen gezuiverd door MBRs op laboschaal, gebruik makend van C-PE polymerische en SiC keramische membranen. De *fouling*-snelheid werd bepaald door opvolging van de transmembraandruk bij een constante flux. Algemene waterkwaliteitsparameters werden geanalyseerd, zoals chemische zuurstofvraag, stikstofspeciatie en troebelheid. Verder werd de *E. coli* log reductie voor de membranen en de UV-reactor bepaald, alsook de UV dosis en de distributie van de verblijftijd van de UV-reactor. De SiC membranen vertoonden een 6.85 keer lagere lineaire *fouling*-snelheid, veroorzaakt door verschillen in oppervlaktemateriaal en -ruwheid. Het MBR-effluent voldeed aan de strengste kwaliteitseisen voor stedelijk waterhergebruik, buiten een onvoldoende stikstofverwijdering. De gemiddelde verwijderingsefficiëntie bij de keramische membranen was 99.2%, 94.7%, 53% en 95.7% voor troebelheid, chemisch zuurstofvraag, totale stikstof en ammoniumstikstof, met gelijkaardige resultaten voor de polymerische membranen. *E. coli* werd niet gedetecteerd in het effluent, met log reducties van respectievelijk 2.7–3.0 en 3.1–3.7 voor de keramische en polymerische membranen, en een log reductie voor de UV-reactor van >10 bij een dosis van 875 mJ cm<sup>-2</sup> of 726 J L<sup>-1</sup>. Deze resultaten wijzen op een hoge geschiktheid van MBR met keramische membranen voor het zuiveren en hergebruik van grijswater.

# Joint thesis subject

This thesis subject was divided under two students, Seppe Ongena (the author of this thesis) and Nele Driesen [Driesen, 2021]. Both theses considered the treatment of greywater for non-potable reuse, but applied two different technological treatment trains on the same greywater influent. This thesis focuses on the combination of a membrane bioreactor (MBR) and UV disinfection, while Nele Driesen's thesis regards a moving bed biofilm reactor (MBBR) and electrochemical cell for in-situ chlorine generation. Due to this difference in technology, the operation, characterization, and specific performance assessment of the systems were vastly different, *e.g.*, fouling rate for MBR versus sludge volume index for sludge settling after the MBBR, and UV dose versus residual chlorine concentration for the electrochemical cell.

Although the analyses performed for the effluent quality were the same, as they are common analyses for wastewater treatment, all analyses were performed independently. Only for the *E. coli* spike test, the work load was divided between the two students, with both students performing all required techniques at least once.

# 1

## Introduction

### 1.1 Water scarcity: a contemporary problem

By 2050, 49–59% of the global population will live in water-scarce areas [UNESCO, 2018; UN Population Division, 2019b]. Even now, an estimated 3.6 billion people experience the effects of physical water scarcity at least one month per year [UNESCO, 2018]. Physical water scarcity can be defined as the water demand exceeding the availability, either through the absence of water in, *e.g.*, arid regions, or through overuse of the available sources [Molden, 2007]. Economic scarcity is a different type of water scarcity caused by mismanagement of water resources or lack of adequate infrastructure [Molden, 2007].

Water scarcity is expected to increase in the future. Unrelenting population growth will inevitably cause an increase in demand, with most growth occurring in developing regions, *e.g.*, in Sub-Saharan Africa [Burek *et al.*, 2016; UN Population Division, 2019b]. Furthermore, the per capita water demand will rise with an increasing degree of development, caused by the availability of piped water [UNESCO, 2015]. Urban environments will be the epicentre of population growth, with increased pressures on local water sources [UN Population Division, 2018]. Due to climate change, weather patterns will become more variable and extreme weather events become more frequent, causing increased variation in water availability [UNESCO, 2018]. Furthermore, surface water availability is expected to decrease by 2050, albeit with high regional variability in severity [Burek *et al.*, 2016].

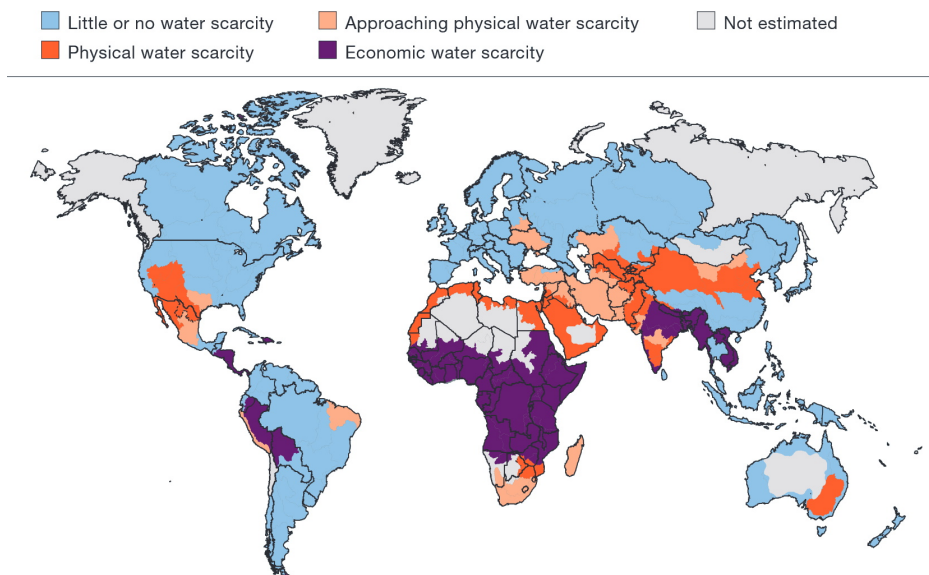


Figure 1.1: Areas of physical and economic water scarcity in 2007. Reprinted from Molden [2007]

However, water scarcity is not a problem of the far future (Figure 1.1). Seasonal droughts, a form of physical water scarcity, already profoundly affect local ecosystems and communities. Wildfire seasons are longer, with more frequent and larger fires [Shukla *et al.*, 2019; Weber *et al.*, 2017]. These wildfires can, in turn, contaminate water supplies, affecting both the quality and available quantity of drinking water [Emmerton *et al.*, 2020; Ice *et al.*, 2004; Lane *et al.*, 2010; Yu *et al.*, 2019]. Droughts in Australia and the Middle East have led to

increased investments in seawater desalination technology and centralized potable water reuse [Meindertsma *et al.*, 2010; Napoli and Rioux, 2016; Palmer, 2011]. Cape Town (South Africa) has experienced serious shortages of the drinking water supply due to a long period of drought (2015–2018) and mismanagement, to a point where some inhabitants reused untreated shower- and bathwater, washing machine water, and kitchen sink water, compromising human health and the environment [Nel and Jacobs, 2019; Simpson *et al.*, 2019]. Many countries in Sub-Saharan Africa suffer from economic water scarcity caused by a lack of water infrastructure and quality [Molden, 2007].

Belgium receives an average annual precipitation of 925 mm [RMI Belgium, s.d.], giving the impression that there is plenty of water in supply. However, in this highly urbanized and concreted environment, rainwater drains act as a highway towards the sea, bypassing infiltration and groundwater replenishment [Willems and Renson, 2019]. This leads to a type of economic scarcity, where the current infrastructure is not adapted to deal with the increasing frequency and duration of droughts and increasing pressure from population growth [Coördinatiecommissie Integraal Waterbeleid, 2019; De Nocker *et al.*, 2017; Vlaamse Milieumaatschappij, 2020b]. Extreme governmental measures were described, the *assessment framework for priority water use during drought, i.e.*, who gets disconnected from the water net first in the event of an extreme drought [Vlaamse Milieumaatschappij, 2020a]. Other factors such as garden irrigation, agriculture, industry, and drinking water production from groundwater increase pressure on groundwater levels [Databank Ondergrond Vlaanderen, s.d.]. Flanders uses surface water for 50% of its drinking water production to limit this pressure, but this supply is also variable and vulnerable to droughts [Vlaamse Milieumaatschappij, 2020c]. Nevertheless, the ratio of total water withdrawals to renewable water availability is expected to be 40–80% by 2040, which puts the country at high risk of water shortages [Luo *et al.*, 2015].

## 1.2 Water reuse: a solution?

### 1.2.1 Water reuse and resource recovery

As a consequence of this increased pressure on water supplies, water is increasingly considered a precious resource that cannot be wasted and needs to be reused [Daigger, 2009; Hering *et al.*, 2013; Puchongkawarin *et al.*, 2015]. Water reuse can be defined as the use of reclaimed water for beneficial use [Asano *et al.*, 2007]. Reclaimed water, also called recycled water, is municipal wastewater that has gone through treatment processes to meet specific water quality criteria [Asano *et al.*, 2007]. This water can then be used for (in)direct potable or non-potable applications (Figure 1.2). Examples of non-potable use are park, garden and agricultural irrigation, toilet flushing, and car and pavement washing [Gonçalves *et al.*, 2020; Goodwin *et al.*, 2019; Schwaller *et al.*, 2021]. For potable reuse, the reclaimed water is purified to drinking water standards, either directly, or indirectly after passing through a natural buffer (Figure 1.2).

What is currently considered wastewater is an almost pure water resource, since it typically contains only  $0.72 \text{ g L}^{-1}$  total dissolved solids [Asano *et al.*, 2007], which means it is 99.9% pure water. The dissolved solids contain, among other constituents: nutrients (nitrogen and phosphorus) and organics (proteins, fats, carbohydrates), which are resources that can be recovered [Alloul *et al.*, 2018; Cruz *et al.*, 2019].



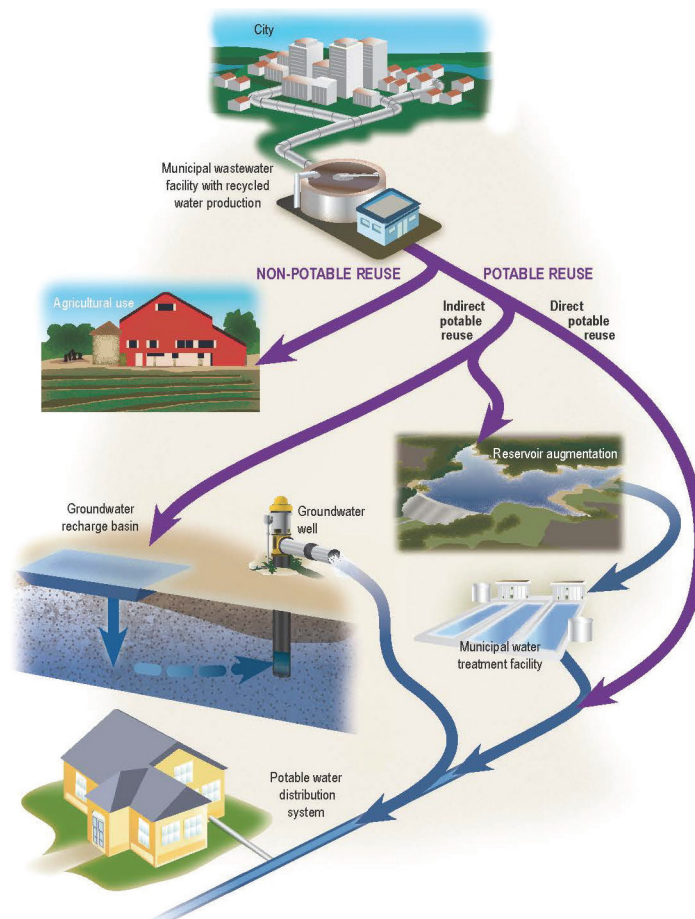


Figure 1.2: Overview of potable and non-potable municipal recycled water, including direct and indirect reuse. Reprinted from the [California Department of Water Resources](#) [2016].

While water reuse can certainly alleviate water stress, there are several concerns when regarding water reuse schemes. Firstly, salts and organic micropollutant accumulation can occur, which might affect human health and the applicability of these streams as *e.g.*, cooling water or agriculture irrigation [Asano *et al.*, 2007; Gomez *et al.*, 2012; Yangali-Quintanilla *et al.*, 2010]. It is evident that, unless purged from the system, these constituents can accumulate in closed-loop reuse systems of households through input by faeces, urine, and use of pharmaceuticals and personal care products (PPCP) [Escudero *et al.*, 2021; Westhof *et al.*, 2016]. Second, there is often a social reluctance to direct reuse of water, despite the fact that reclaimed water for potable or non-potable reuse must comply to high quality standards [Larsen *et al.*, 2016; Leong and Lebel, 2020]. In this context, a differentiation is needed between planned and unplanned reuse of water. With planned reuse, water is deliberately treated and reused [Asano *et al.*, 2007]. Oftentimes, the current drinking water production systems pump up surface water that contains previously discharged treated wastewater of upstream communities, albeit heavily diluted [Asano *et al.*, 2007; Beard *et al.*, 2019; Rice *et al.*, 2016; Verliefe *et al.*, 2007]. This is considered unplanned or *de facto* reuse of water, yet there is little social reluctance regarding the reuse aspect of our current drinking water sources, and more focus on the presence of micropollutants [Rabaey *et al.*, 2020; Rice *et al.*, 2016]. It is important to overcome reluctance and increase public acceptance for water reuse through clear and constant communication on the treatment principles of systems for reuse and human health risks, or more likely lack thereof [Domènech and Saurí, 2010; Fielding *et al.*, 2019; Flint and Koci, 2021; Hartley *et al.*, 2019].



## 1.2.2 Centralized and decentralized water treatment

Besides the treatment of wastewater for reuse and the accompanying public acceptance issues, the economic and infrastructural feasibility of water reuse schemes is an important consideration. It is not cost-effective to use potable water for applications requiring non-potable water quality [Ray *et al.*, 2010]. Should non-potable water reuse and distribution occur through a centralized distribution network, extra pipelines will be necessary for a dual-quality water system since potable water and non-potable water cannot be mixed [Ray *et al.*, 2010]. When considering source separation of wastewater streams (Subsection 1.2.3), the number of required pipelines would increase even more. It might therefore be beneficial to shift towards a decentralized approach. The following subsection provides definitions of centralized water management and decentralization and delves deeper into the differences between the two.

Centralized wastewater management systems collect wastewater from urban environments by means of a sewage network, comprising of pumps and pipelines, whereafter it is treated in a central facility (wastewater treatment plant, WWTP) and often discharged in surface waters [Brown *et al.*, 2009; Larsen *et al.*, 2013]. These centralized systems have proven reliable, efficient, and relatively cheap through an economy of scale [Larsen *et al.*, 2013]. Continuous improvements were made, with sewage networks growing alongside populations and cities. This gradual growth makes it difficult to assess the total value of the infrastructure [Maurer *et al.*, 2010]. As the size of the distribution network increases, so does the costs of maintaining it and the required energy for operation, which is a known diseconomy of scale [Larsen *et al.*, 2013; Maurer, 2009]. Therefore, centralized systems are good for densely populated areas, where the population density compensates for the size of the network [Maurer *et al.*, 2010]. However, the construction rate of sewer networks might not be able to keep up with rapid population growth in urban areas [Öberg *et al.*, 2020]. Furthermore, the costs for sewage pumping and sewer networks can be more costly than the treatment itself, in some cases amounting up to 81% of the capital expenditures and 50% of the operational expenditures [Pabi *et al.*, 2013; Shukla and Tare, 2019]. The costs further increase as the age of the system increases due to an increased number of failures [Folkman, 2018]. System failures such as pipe leakage increase water losses, leading to inefficient use of resources [Bonthuys *et al.*, 2020; Lemos *et al.*, 2013; Shabangu *et al.*, 2020].

Water transport is a key attribute of centralized systems, as evident from the reliance on a sewage network and water distribution network [Marlow *et al.*, 2013]. Worldwide, 504 billion litres of water are transported over  $27\,000 \pm 3800$  km every day [McDonald *et al.*, 2014]. When expressed in water-kilometres (WKM, Rabaey and Van De Walle [2020]), being the amount of water transported ( $\text{m}^3$ ) over a certain distance (km) in one year, the world total reaches  $5 \cdot 10^{18}$  WKM. Large amounts of energy are needed to transport water over long distances [Rezaei *et al.*, 2019], which in the case of Mexico City makes water transport the major contributor to the global warming potential through energy consumption [García-Sánchez and Güereca, 2019]. On average, the energy requirements for transport can be 4 times higher than treatment [Guo *et al.*, 2014]. Furthermore, this transport might increase the effect of water scarcity since the withdrawal location is spatially separated from the discharge location, the latter often being surface water such as rivers or the sea [Larsen *et al.*, 2013; Mbavarira and Grimm, 2021].

As the shortcomings of centralized treatment are increasingly recognized, a (partial) decentralization of urban water management aims to provide a solution. Decentralization can be defined as collection, treatment, and discharge or reuse of wastewater at or near the point of wastewater generation on the scale of individual homes, buildings, communities, industries, or institutional facilities [Asano *et al.*, 2007]. These systems do not require the large distribution and collection systems of centralized treatment, leading to classifications such as non-grid, small-grid and hybrid systems, the latter being partially decentralized systems for the separate collection and treatment of, *e.g.*, urine [Hoffmann *et al.*, 2020; Larsen *et al.*, 2016]. As these modularized systems take on an economy of numbers, advances in manufacturing technology can give them a competitive advantage compared to centralized systems [Dahlgren *et al.*, 2013; Eggimann *et al.*, 2018]. This advantage is further enforced when considering non-grid solutions, which avoid costs and energy consumption associated with large distribution systems.

Most importantly, decentralization can facilitate water reuse and lead to more efficient use of water resources [Larsen *et al.*, 2016]. Water can be infiltrated locally after treatment, relieving pressures on groundwater tables [Rabaey *et al.*, 2020]. Furthermore, decentralized systems can be run on locally produced renewable energy, directly coupling energy availability and demand [Baghaei Lakeh *et al.*, 2017; Cai and Schäfer, 2020]. The energy requirements can be equal to centralized treatment, or in some cases even lower, such as with hybrid systems [Jeong *et al.*, 2018; Zang *et al.*, 2021]. However, a study from Cornejo *et al.* [2016] indicates higher energy requirements per volume treated wastewater compared to centralized treatment. The treatment system may still rely on a central facility for, *e.g.*, regeneration of active carbon, replacement of membrane modules, or treatment of biosolids [Hasik *et al.*, 2017; Larsen *et al.*, 2013]. The environmental impacts of decentralized treatment and reuse systems can be higher, equal or lower than those of centralized systems, varying on a case-by-case basis [Cornejo *et al.*, 2016; Hasik *et al.*, 2017; Opher and Friedler, 2016].

Flanders, with a population density of 480 inhabitants per km<sup>2</sup>, still lacks sewer infrastructure for 1/8<sup>th</sup> of its population [Vlaamse Milieumaatschappij, 2019b]. Furthermore, 40000 households do not have a drinking water connection [De Watergroep, 2019]. This contradicts the expectation that centralized water management always works well in densely populated regions [Maurer *et al.*, 2010]. Recently, a modelling study was performed for the water infrastructure of Flanders, where about 50% of the sewer system was found to be 25 to 49 years old, with current yearly replacement costs of about €200 million [Vlaamse Milieumaatschappij, 2018]. The infrastructure consists of 27461 km, with 9533 km expansion planned to connect Flemish citizens with no access to the sewer network. The cost of the expansion project was estimated at €9.3 billion, which is an approximate €26 000 per newly connected household. Using the current revenue of sewer operators, the maximum financially sustainable investment by 2027 was estimated at €1.5 billion, which would cover an expansion by 1051 km. Hence, only a fraction of the approximate 825 000 unconnected inhabitants can be given a sewer connection by 2027. Decentralized systems could more efficiently use these available investments, since they can be installed with the construction of new buildings [Larsen *et al.*, 2013]. Indeed, the high costs for sewer expansion combined with the threat of water scarcity (Section 1.1) have led to an increased interest in decentralization and water reuse projects in the region, such as the housing projects ‘De Nieuwe Dokken’ and ‘The Mobble’, and ongoing applied research into rainwater purification for drinking water applications [De Watergroep, 2019].

### 1.2.3 Source separation

Source separation is a topic heavily interlinked with decentralization and water reuse. It can be defined as the separate collection and/or treatment of wastewater flows from different sources. As it is not feasible to simply downscale centralized treatment plants for decentralized applications, a certain degree of source separation is needed to homogenize the wastewater flows for the use of simplified treatment technology [Larsen *et al.*, 2013].

Rainwater and greywater (household wastewater excluding toilets) are generally favoured to be treated separately for water reuse because of less hygienic concerns and social reluctance [Larsen *et al.*, 2016]. Since greywater does not include toilet or (in most cases) kitchen wastewater, it exhibits a lower organic and microbial load than mixed domestic wastewater, and is therefore relatively easy to treat [Gross *et al.*, 2015; Larsen *et al.*, 2013]. Greywater constitutes on average about 73% of the total household wastewater flow (Table 1.1). While rainwater is generally not considered wastewater, it is often mixed with wastewater in combined sewer systems, and could therefore benefit from source separation [Ahm *et al.*, 2016; Kroll *et al.*, 2018; Schuetze, 2013]. Rainwater is best suited for treatment to drinking water because it is relatively pure, and is increasingly being used for on-site drinking water production [Alim *et al.*, 2020; De Watergroep, 2019; Domènech and Saurí, 2011; Naddeo *et al.*, 2013].

Blackwater (urine and faeces) contains 68% of the total solids, about 85% of the nutrients and 50% of the organic material emitted by a household [Larsen *et al.*, 2013], despite its smaller contribution of on average 27% to the total household wastewater volume (Table 1.1), which makes it an excellent candidate for energy and nutrient recovery [Besson *et al.*, 2021; De Paepe *et al.*, 2020; Gao *et al.*, 2019; McCarty *et al.*, 2011]. A pollutants group of rising concern are pharmaceuticals and personal care products (PPCP), because of their persistence, resistance to conventional treatment, and toxicity to the aquatic environment [Bu *et al.*, 2013; Delgado *et al.*, 2020]. Blackwater has the potential for the highest concentration of PPCP among source separated wastewater streams [Escudero *et al.*, 2021; Westhof *et al.*, 2016]. In some cases up to 90% of the still active parent compounds are excreted unchanged [Lienert *et al.*, 2007].

Source separation favours decentralization, as infrastructural and economical hurdles would arise with centralized water management. When considering on-site reuse or source separation of greywater, reduced wastewater flows in sewer systems result in excessive solids deposition, grease accumulation, and increased rates of corrosion due to anaerobic conditions [Larsen *et al.*, 2013; Penn *et al.*, 2017]. Another possible effect is a decrease in efficiency of the nitrification–denitrification process in WWTP, causing an increase in effluent nitrate concentrations [Penn *et al.*, 2017]. Incorrect connection of sources to their respective pipelines can cause a decrease in treatment or recovery efficiency [Tang *et al.*, 2020], but this might also be the case in decentralized systems.

A major hurdle to source separation and resource recovery on a centralized scale would be the necessity of separate collection and a dual-quality distribution system for potable and non-potable water. Combined sewer systems have historically shown limitations in terms of combined sewer overflow (CSO), where untreated wastewater and stormwater bypass treatment facilities in the event of overwhelming rainfall [Ahm *et al.*, 2016; Kroll *et al.*, 2018]. Sewer separation can be costly megaprojects such as the London Tideway Tunnel, with an estimated

total cost of £3.9bn, not taking into account the increased operational maintenance costs of the separated piping networks [Tideway, 2020]. Stormwater decoupling from the sewer network can be seen as source separation. It is evident that extensive centralized source separation, where urine, faeces, rainwater, and greywater are treated separately, would have similar, if not higher costs. Indeed, transport costs can be greater than the savings by resource recovery in centralized systems [Lundie *et al.*, 2004].

#### 1.2.4 Challenges to implementation

Despite being increasingly implemented, such as in the redevelopment areas Flintenbreite (Lübeck, Germany), Noorderhoek (Sneek, Netherlands), Jenfelder Au (Hamburg, Germany), de Nieuwe Dokken (Ghent, Belgium) and H+ (Helsingborg, Sweden) [Skambraks *et al.*, 2017], there are still challenges to face with water reuse, decentralized systems and source separation [Hoffmann *et al.*, 2020]. Challenges more specific to the respective aspects were described in the previous Subsections 1.2.1, 1.2.2, and 1.2.3.

The water sector is in general very risk averse, since safeguarding human health is a major objective [Kiparsky *et al.*, 2016]. Undetected system failures or point source pollution caused by a lack of knowledge of home-owners on system operation and maintenance can have adverse health effects [Diaz-Elsayed *et al.*, 2019; Marlow *et al.*, 2013]. Therefore, monitoring of the water quality and risk to public health is a major challenge for decentralized treatment systems and reuse scenarios [Hyde and Smith, 2018; Reynaert *et al.*, 2021]. Because of the distributed nature of decentralized treatment plants, monitoring can become more costly both in terms of time and money [Diaz-Elsayed *et al.*, 2019]. Remote digital monitoring can be a valuable tool to support the semi-automatic operation of decentralized systems [Hoffmann *et al.*, 2020].

This change in monitoring implies a fundamental shift in management of water systems towards increased complexity [Hering *et al.*, 2013; Hoffmann *et al.*, 2020; Marlow *et al.*, 2013; Sedlak *et al.*, 2013]. Responsibilities are diffused amongst several stakeholders, *e.g.*, agencies, institutions, and home-owners [Diaz-Elsayed *et al.*, 2019; Kiparsky *et al.*, 2013; Marlow *et al.*, 2013]. It might be beneficial to evaluate which degree of source separation, decentralization and modularization is optimal, *cf.* non-grid, small-grid and hybrid systems (Subsection 1.2.2, Hoffmann *et al.* [2020]).

Another barrier to implementation is large upfront capital investments, which can be difficult to finance if responsibility falls to smaller parties such as home-owners [Diaz-Elsayed *et al.*, 2019]. The rigidity of centralized systems can be explained by the long-term nature of infrastructure investments, with planning horizons of around 30 years [Kiparsky *et al.*, 2013; Maurer, 2009]. This creates so-called lock-in effects on a regulatory level and economic sunk costs, where current widely implemented technologies are favoured over innovative ones [Larsen *et al.*, 2016; Marlow *et al.*, 2013; Rabaey *et al.*, 2020]. Therefore, modularized systems need to be implemented without creating new lock-in effects [Hoffmann *et al.*, 2020; Marlow *et al.*, 2013]. Strong lock-in effects can also be observed in a social context [Reynaert *et al.*, 2021; Sedlak *et al.*, 2013]. Communities can show resistance to change, and public acceptance for new technologies and unfamiliar practices can be low [Hering *et al.*, 2013; Marlow *et al.*, 2013]. Guidelines, standards, and regulations are often non-existing or only partially applicable to small-scale systems (Reynaert *et al.* [2021], Subsection 1.3.2).

## 1.3 Greywater as an alternative water resource

Source separation allows for the selection of wastewater streams to treat [Larsen and Gujer, 1996]. As described in Subsection 1.2.3, greywater has the lowest organics and microbial load, whilst being the largest household wastewater flow. Therefore, greywater is an excellent source to recover water. Subsection 1.3.1 will consider the composition and quantity of greywater, while Subsection 1.3.2 covers human health and environmental concerns, and lists existing water quality targets for non-potable reuse.

### 1.3.1 Greywater characterization

Greywater (GW) is defined as all household wastewater that excluding toilet wastewater, more specifically baths, showers, handwashing basins, laundry machines, kitchen sinks and dishwashing machines [Gross *et al.*, 2015]. GW can be divided based on the sources considered into dark and light GW, with the latter excluding kitchen, dishwashing, and in some definitions laundry wastewater, since washing detergents often contain aggressive ingredients [Gross *et al.*, 2015; Hyde and Smith, 2018; Shaikh and Ahammed, 2020]. The volumetric flows of GW sources can be found in Table 1.1, both for the average of 11 countries as for Flanders separately. In Flanders, baths and showers make up the major fraction of GW, followed by laundry, washbasins, and kitchen sinks and dishwashing.

Table 1.1: Household wastewater quantities per source.

Water source	Flow ( $\text{L p}^{-1} \text{d}^{-1}$ )	
	[Larsen <i>et al.</i> , 2013] <sup>a</sup>	[Vlaamse Milieumaatschappij, 2018]
Toilets (blackwater)	41±16	21.3
Baths and showers	43±16	28.9
Washbasin	14±8	9.40
Laundry	24±15	16.6
Dishwashing and kitchen sink	27±11	8.3
Total greywater	108±29	63.2
Total	148±33	84.5

<sup>a</sup> Countries: AU, BR, DK, IL, MT, NL, OM, PT, CH, GB, US

However, the quantity and composition of greywater is highly dependent on the sources considered, geographical location, building purpose, environmental variables, and continuously shifting socio-economical factors [Boano *et al.*, 2020; Gross *et al.*, 2015; Hyde and Smith, 2018; Larsen *et al.*, 2013; Shaikh and Ahammed, 2020; Wu, 2019]. Both GW flows and composition show diurnal patterns, based on which household appliances are being used, with higher flows generally in the morning and evening, and higher concentrations during the day [Butler *et al.*, 1995; Eriksson *et al.*, 2009; Shaikh and Ahammed, 2020]. Long storage times, *i.e.*, more than 7 days, can lead to sedimentation and biological degradation, with a significant increase in turbidity, colour and fine particles, and a decrease in COD [Abed *et al.*, 2020; Winward *et al.*, 2008]. Furthermore, storage can lead to a reduction of  $\text{PO}_4^{3-}$ -P through precipitation, co-precipitation of dissolved solids, sedimentation of particles, and microbial activity [Abed *et al.*, 2020]. Despite the high variability of influencing factors, some broad ranges of mixed GW composition are given in Table 1.2.



Table 1.2: General composition of mixed greywater. For [Boano \*et al.\* \[2020\]](#) and [Wu \[2019\]](#), the given values are based both on ranges (min-max) and means ( $\pm$  standard deviation), since a uniform reporting was not present. Furthermore, a column is shown which only includes studies from [Boano \*et al.\* \[2020\]](#) and [\[Wu, 2019\]](#) on mixed greywater that reported ranges. This way, the given range in this table is based on actual minima and maxima as opposed to, *e.g.*, the minimum of means.

Parameter		<a href="#">Larsen <i>et al.</i> [2013]</a>	<a href="#">Boano <i>et al.</i> [2020]</a>	<a href="#">Wu [2019]</a>	Mixed GW <sup>a</sup>
pH		6.4 – 10.0	5 – 9.6	6.7 – 9.65	4.9 – 8.41
$\kappa$	( $\mu\text{S cm}^{-1}$ )	100 – 2800		194 – 3000	331 – 2530
Turbidity	(NTU)	20 – 280		5.6 – 4400	29 – 559
COD	( $\text{mg L}^{-1}$ )	7 – 2570	15.00 – 2263	22.9 – 1600	41.0 – 1595
sCOD	( $\text{mg L}^{-1}$ )			59 – 289	86 – 289
BOD <sub>5</sub>	( $\text{mg L}^{-1}$ )	1 – 1060	1.1 – 1240	9 – 392.4	17.7 – 394
TOC	( $\text{mg L}^{-1}$ )	73 – 93		100 – 552	15.0 – 160.4
TN	( $\text{mg L}^{-1}$ )	0.1 – 128	3 – 322	2.13 – 49	1.3 – 63
TKN	( $\text{mg L}^{-1}$ )				2.6 – 32
NH <sub>4</sub> <sup>+</sup> -N	( $\text{mg L}^{-1}$ )	1 – 75		0 – 47	0.1 – 22
NO <sub>2</sub> <sup>-</sup> -N	( $\text{mg L}^{-1}$ )			0.02 – 1	
NO <sub>3</sub> <sup>-</sup> -N	( $\text{mg L}^{-1}$ )	0.1 – 17		0.0 – 7	0 – 12.32
TP	( $\text{mg L}^{-1}$ )	0.1 – 42	0.01 – 51.58	0.5 – 15	1 – 12.1
PO <sub>4</sub> <sup>3-</sup> -P	( $\text{mg L}^{-1}$ )			0 – 8.1	0.0 – 6.7
TSS	( $\text{mg L}^{-1}$ )	2.0 – 1070	11 – 4952	15 – 4250	9.2 – 744
VSS	( $\text{mg L}^{-1}$ )			39 – 40 <sup>b</sup>	9.2 – 149.8
Na <sup>+</sup>	( $\text{mg L}^{-1}$ )	7.4 – 480			52 – 420
Ca <sub>2</sub> <sup>+</sup>	( $\text{mg L}^{-1}$ )			108 – 148	9 – 437.61
Mg <sub>2</sub> <sup>+</sup>	( $\text{mg L}^{-1}$ )			27 – 37	3 – 140.01
K <sup>+</sup>	( $\text{mg L}^{-1}$ )	0.2 – 24			0 – 22
Cl <sup>-</sup>	( $\text{mg L}^{-1}$ )	9 – 227			18 – 50

<sup>a</sup> [Abdel-Shafy and Al-Sulaiman \[2014\]](#); [Atanasova \*et al.\* \[2017\]](#); [Fountoulakis \*et al.\* \[2016\]](#); [Hernández Leal \*et al.\* \[2010\]](#); [Hocaoglu \*et al.\* \[2013\]](#); [Hourlier \*et al.\* \[2010\]](#); [Jabornig and Favero \[2013\]](#); [Jabornig and Podmirseg \[2015\]](#); [Masi \*et al.\* \[2016\]](#); [Oteng-Peprah \*et al.\* \[2018\]](#); [Ramprasad \*et al.\* \[2017\]](#)

<sup>b</sup> Infrequently reported by [Wu \[2019\]](#).

While greywater has a lower organic and micropollutant load compared to blackwater, more than 250 organic xenobiotic compounds may be present [Etchepare and van der Hoek, 2015; Gross *et al.*, 2015; Westhof *et al.*, 2016]. Several classes can be distinguished, *e.g.*, anionic and cationic surfactants present in detergents and soaps, organobromine compounds and organophosphates used as textile flame retardants, biocides as disinfectants and textile preservatives, anti-corrosives in dishwasher detergents, and a broad range of fragrances, odorants, disinfectants, preservatives, and surfactants used in personal care products [Gross *et al.*, 2015; Larsen *et al.*, 2013]. Etchepare and van der Hoek [2015] found that only 14 of the 278 found micropollutants could potentially pose a risk to human health when reclaimed water was used for potable applications.

### 1.3.2 Health and environmental concerns

Guidelines and regulations on the quality requirements for reclaimed wastewater are sparsely available worldwide (Subsection 1.2.4, Reynaert *et al.* [2021]). Most standards exist for agricultural irrigation, such as the WHO guideline for greywater reuse in agriculture [World Health Organization, 2006], which aims to protect the environment from nutrient accumulation and harmful substances, and safeguard human health [Reynaert *et al.*, 2021]. Due to the low nutrient load (N, P, K) of greywater, plant growth and productivity with greywater irrigation can be unaffected or slightly improved compared to tapwater [Finley *et al.*, 2009; Rodda *et al.*, 2011]. However, prolonged irrigation can have increase soil salt content, metal content, and microbial activity, and change microbial community composition [Rodda *et al.*, 2011; Siggins *et al.*, 2016]. Despite high pathogenic microorganism counts, it is possible that no significant contamination occurs when irrigating with untreated greywater, but direct contact between crop and greywater should be avoided [Finley *et al.*, 2009; Gorgich *et al.*, 2020; Siggins *et al.*, 2016].

With increasing focus on urban water reuse (Subsection 1.2.1), standards are being defined more frequently for non-potable and potable urban water reuse applications, with an increased emphasis on safeguarding human health besides removal of pollutants [Reynaert *et al.*, 2021]. Contamination with faecal coliforms and enterococci or faecal streptococci occurs through, *e.g.*, showering, albeit to a lower extent compared to mixed wastewater, being greywater and blackwater [Gross *et al.*, 2015]. Indeed, the use of untreated greywater is accompanied by a low risk for faecal contamination [Kusumawardhana *et al.*, 2021; Schoen *et al.*, 2020]. Pathogen concentrations from other sources can be much higher, *e.g.*, *Salmonella* spp. with food preparation, leading to greater concern than faecal contamination [Gross *et al.*, 2015]. Possible other pathogens are *Pseudomonas aeruginosa*, *Staphylococcus aureus* sp., *Legionella pneumophila* sp., *Clostridium perfringens* sp., and *Cryptosporidium* spp. (Table 1.3).

The main exposure routes when considering non-potable greywater reuse for, *e.g.*, toilet flushing, are inhalation or ingestion through splashes and aerosols when flushing, and ingestion through misconnections [Gross *et al.*, 2015]. Opportunistic pathogens such as *P. aeruginosa* and *L. pneumophila* can grow in the reuse system [Kusumawardhana *et al.*, 2021; Schoen *et al.*, 2018]. Showering and drinking of misconnected water can lead to a high risk due to presence of *S. aureus* and *E. coli*. Mitigation of these risks can include good design of greywater reuse systems including collection and treatment, and correct plumbing installation [Kusumawardhana *et al.*, 2021].

Table 1.3: Microbial contamination of greywater. All values are given in CFU/100 mL (colony forming units), with the units for somatic coliphages in PFU/100 mL (plaque-forming units).

	Larsen <i>et al.</i> [2013]	Gross <i>et al.</i> [2015]	Mixed GW <sup>a</sup>
Total coliforms		$1.6 \cdot 10^7 - 6.3 \cdot 10^8$	$0 - 1.4 \cdot 10^9$
Faecal coliforms	$2 \cdot 10^3 - 10^9$	$10^3 - 10^8$	$0 - 5.7 \cdot 10^6$
<i>E. coli</i>			$0 - 8.1 \cdot 10^6$
Somatic coliphages	$0 - 10^4$	$10^3$	
<i>C. perfringens</i>	$1.30 \cdot 10^3$		
<i>Salmonella</i>			$0 - 7.9 \cdot 10^3$
<i>L. pneumophila</i>		$32 - 7.9 \cdot 10^2$	
<i>Cryptosporidium</i>		$0 - 2 \cdot 10^8$	
<i>P. aeruginosa</i>	$3 \cdot 10^3 - 3 \cdot 10^4$	$2 \cdot 10^2 - 2 \cdot 10^4$	$94 - 3.1 \cdot 10^4$
<i>S. aureus</i>	$2 \cdot 10^3 - 10^4$	$10^4 - 5 \cdot 10^5$	$1.2 \cdot 10^2 - 4.1 \cdot 10^3$
Enterococci and faecal streptococci	$10^3 - 10^5$	$25 - 4 \cdot 10^4$	$8 \cdot 10^3 - 1.2 \cdot 10^6$

<sup>a</sup> Atanasova *et al.* [2017]; Benami *et al.* [2016]; Fountoulakis *et al.* [2016]; Hourlier *et al.* [2010]; Oteng-Peprah *et al.* [2018]

However, the most important threats to human health when reusing greywater are posed by rotavirus, norovirus, and *Cryptosporidium* spp. due to their higher concentrations and therefore higher need for removal [Schoen *et al.*, 2018; Vuppaladadiyam *et al.*, 2019]. Most bacteria are effectively removed through the most common treatment methods compared to viruses and protozoa [Schoen *et al.*, 2020; Sharvelle *et al.*, 2017]. An overview of both physicochemical and microbial reclaimed greywater standards for non-potable water reuse beyond agricultural irrigation can be found in Table 1.4.

## 1.4 Disinfection of effluent

### 1.4.1 The rationale of disinfection

Since microbial contamination can pose a significant health risk, disinfection of wastewater treatment effluent is often required (Subsection 1.3.2). The disinfective capacity of individual technologies is often expressed in log removal values (LRV), while the reduction necessary to meet water quality requirements is expressed in a log reduction target, or LRT [Schoen *et al.*, 2020]. The LRV (or LRT) can be defined as

$$LRV = \log \frac{c_{in}}{c_{out}}, \quad (1.1)$$

with  $c_{in}$  the concentration of a certain pathogen in the influent and  $c_{out}$  the concentration of a certain pathogen after treatment or disinfection (LRV), or the required concentration according to regulations, guidelines or standards (LRT). Treatment technologies aimed at the improvement of physicochemical quality, *e.g.*, membrane separation, can also exhibit removal for bacteria, viruses, and protozoa [Schoen *et al.*, 2018, 2020]. In this subsection, only dedicated disinfection processes will be discussed, *i.e.*, excluding reverse osmosis or other membrane or filtration based processes. The most commonly used disinfection processes are UV, O<sub>3</sub>, peracetic acid, and chlorine disinfection, and more advanced oxidation processes (AOP) are, *e.g.*, TiO<sub>2</sub>-UV (photocatalysis), UV/H<sub>2</sub>O<sub>2</sub>, vacuum-UV/UV-C, O<sub>3</sub>/H<sub>2</sub>O<sub>2</sub>, and O<sub>3</sub>/UV [Dubowski *et al.*, 2020; Gassie and Englehardt, 2017; Linden and Mohseni, 2014; Ragazzo *et al.*, 2020].



Table 1.4: Reclaimed water requirements for nonpotable water reuse. UR: unrestricted reuse, TF: toilet flushing, SA: sanitary appliances, CW: clothes washing, N.D.: not detectable.

Type		ISO 30500:2018 Category A <sup>b</sup> International standard	U.S. EPA [2012] Guideline	Australia (2011) <sup>c</sup> Guideline	Italy (2003) <sup>d</sup> Regulation	Spain (2007) <sup>d</sup> Regulation	Canada (2010) <sup>e</sup> Guideline	China GB/T 18920-2020 Standard
Reuse purpose		UR	UR	TF, CW	TF	SA	TF	TF and UR
pH		6 – 9	6 – 9	6.5 – 8.5	6.0 – 9.5		6.0 – 9.0	6.0 – 9.0
$\kappa$	(mS cm <sup>-1</sup> )				≤3.0	≤3.0		
Turbidity	(NTU)		≤2	≤2 (95 <sup>th</sup> percentile) ≤5 (max)		1 – 15	≤5 (max), ≤2 (median)	≤5
COD	(mg L <sup>-1</sup> )	≤50			≤100			
BOD <sub>5</sub>	(mg L <sup>-1</sup> )		≤10	≤10	≤20		≤20 (max), ≤10 (median)	≤10
TN	(mg L <sup>-1</sup> )	70% reduction			≤15	≤10 <sup>a</sup>		
NH <sub>4</sub> <sup>+</sup> -N	(mg L <sup>-1</sup> )				≤1.6			≤3.9
TP	(mg L <sup>-1</sup> )	80% reduction			≤2	≤2 <sup>a</sup>		
TSS	(mg L <sup>-1</sup> )	≤10		<10	≤10	5 – 35	≤20 (max), ≤10 (median)	≤1000
Cl <sup>-</sup>	(mg L <sup>-1</sup> )				≤250			
Residual chlorine	(mg L <sup>-1</sup> )		>1	0.2 – 2, or UV dose 40 – 70 mJ cm <sup>-2</sup>			≥0.5	≥0.2
Total coliforms	(CFU 100 mL <sup>-1</sup> )							≤0.3
Faecal coliforms	(CFU 100 mL <sup>-1</sup> )		N.D.	<1				
<i>E. coli</i>	(CFU 100 mL <sup>-1</sup> )	≤1 (≥6 LRV)		>5 LRV	≤10	0 – 10 <sup>4</sup>	≤200 (max), N.D. (median)	N.D.
Coliphage MS2	(PFU 100 mL <sup>-1</sup> )	≤1 (≥7 LRV)		<1 (>6.5 LRV)				
Clostridia	(CFU 100 mL <sup>-1</sup> )			<1				
Protozoa	(L <sup>-1</sup> )			>5 LRV				
<i>Salmonella</i> sp.	(CFU 100 mL <sup>-1</sup> )				N.D.	N.D.		
Nematode eggs	(L <sup>-1</sup> )					≤0.1		
<i>Legionella</i>	(CFU 100 mL <sup>-1</sup> )					0 – 10 <sup>2</sup>		

<sup>a</sup> Only required for aquifer recharge and recreational uses.

<sup>b</sup> Reynaert *et al.* [2020]

<sup>c</sup> Western Australia Department of Health [2011]

<sup>d</sup> Alcalde Sanz *et al.* [2014]

<sup>e</sup> Health Canada [2010]

Advanced oxidation processes (AOP) all produce hydroxyl radicals ( $\bullet\text{OH}$ ), which can oxidize most inorganic and organic compounds in a rapid and non-selective way, including micropollutants [Dubowski *et al.*, 2020; Linden and Mohseni, 2014; Ternes and Joss, 2006]. The disinfection in AOP can be mainly attributed to oxidative damage by reactive oxygen species to the cell envelope, enzymes, and intracellular substances, *i.e.*, genetic material of pathogens [di Chen *et al.*, 2021]. The main advantage of AOP is the absence of disinfection by-products (DBPs), but high operational costs are an important disadvantage, for instance high UV energy consumption [Rodríguez-Chueca *et al.*, 2015]. However, high energy use might be a lesser concern when decentralized solar energy is used during the day, allowing for renewable energy storage in the form of treated wastewater [Rabaey *et al.*, 2020].

Chlorine disinfection, whilst being very economical, can lead to the formation of DBPs through the substitution of chlorine and the oxidation of natural organic matter, *e.g.*, carbohydrates, humic acids, and amino acids [Kwarciak-Kozłowska, 2020]. These DBPs are unwanted due to toxicity and mutagenicity and can be classified as trihalomethanes (THMs, *e.g.*, chloroform), halogenated acetic acids (HAAs, *e.g.*, dichloroacetic acid), and chloramines (CAM, *e.g.*, NDMA or N-Nitrosodimethylamine) [Kwarciak-Kozłowska, 2020]. Ozone has no residual disinfectant concentration and can also lead to the formation of DBPs, *e.g.* aldehydes, ketones, and bromate [Collivignarelli *et al.*, 2017]. Peracetic acid increases the effluent COD and can have a high chemical cost, but does not usually lead to any DBPs of concern [Domínguez Henao *et al.*, 2018].

Considering decentralized water treatment on, *e.g.*, a household scale, it might be good practice to avoid reliance on chemicals, including chemical transport, distribution and localized storage. Therefore, in-situ electrochemical chlorine gas ( $\text{Cl}_2$ ) production or UV disinfection are interesting options. In the former, free reactive chlorine is generated in situ [Huang *et al.*, 2016]. Electrochemical chlorine generation can be more effective for the removal of *E. coli*, *Enterococcus* and coliphage MS2 compared to chemical disinfection [Huang *et al.*, 2016]. However, the presence of ammonia in the wastewater can significantly reduce the disinfection efficiency through reaction of chlorine to chloramines [Huang *et al.*, 2016]. Furthermore, a higher applied cell voltage and longer reaction time will generate more organic DBPs such as THMs and HAAs [Huang *et al.*, 2016]. Therefore, UV disinfection will be considered, without AOP for simplicity.

### 1.4.2 UV disinfection

The working principle of UV disinfection is the generation of ultraviolet electromagnetic radiation in the germicidal range, being UV-C (200 – 280 nm) and UV-B (280 – 320 nm). The optimum for bacterial inactivation is about 260 – 265 nm, which coincides with the peak absorption by DNA. Indeed, UV wavelengths below 320 nm are actinic, causing photochemical reactions with proteins, RNA, and DNA, especially in the UV-C range. The main mechanism of micro-organism inactivation is the production of various photoproducts and the cross-linking between nucleic acids, resulting in the formation of intrastrand cyclobutyl-pyrimidine dimers (CPD) in DNA, leading to mutations or cell death [Kowalski, 2009].

However, the sustained DNA damage can be limited with photoreactivation, which is a self-repair process induced by visible and UV wavelengths monomerizing the formed CPDs. Photoreactivation is limited for viruses, since monomerization leaves gaps and defects in the DNA for which many bacterial cells possess repair enzymes such as photolyase. Photoreactivation is dependent on the amount of UV damage and can not completely reverse damage due to the presence of other damaging photoproducts. Enzymes, including photorepair enzymes, can be damaged by broader UV wavelengths in the UV-C and UV-B range, excluding 253.7 nm [Kowalski, 2009]. Furthermore, advanced oxidation processes with UV, *e.g.*, TiO<sub>2</sub>-powder/UV or even TiO<sub>2</sub>-coated ceramic membranes/UV, can reduce photoreactivation through the production of hydroxyl radicals [Fang *et al.*, 2014].

Three main types of UV lamps exist [Kowalski, 2009]: low pressure (LP) mercury vapour (Hg) lamps producing a wavelength of 253.7 nm, medium pressure (MP) Hg lamps with generally broader emission patterns in the UV-C and UV-B spectrum, and light-emitting diodes (LEDs) that have a variety of possible wavelengths. LP-Hg lamps can also be called monochromatic lamps, while MP-Hg lamps can be called polychromatic lamps [Hijnen *et al.*, 2006]. The optimum wavelength for *E. coli* inactivation is roughly 265 nm, with the bacterial absorbance at 253.7 nm being 84% of the optimal absorbance, leading to high germicidal effectiveness of LP-Hg lamps. UV wavelengths of 175 – 210 nm can lead to the formation of ozone from oxygen, which is only a problem with MP-Hg lamps since these can exhibit a weak spectral line at 185 nm and LP-Hg lamps only emit strongly at 253.7 nm. However, MP-Hg lamps show enhanced prevention of photoreactivation due to their broad spectrum nature. LED-UV lamps are small, but can be organized into arrays. LED-UVs can produce an optimum wavelength of 265 nm and do not require the toxic heavy metal mercury [Kowalski, 2009]. Furthermore, 280 nm LEDs can limit photoreactivation and dark repair of *E. coli* compared to LP-Hg lamps and 265nm LED-UVs due to the inactivation of aforementioned repair enzymes [Li *et al.*, 2017]. A disadvantage of LED-UVs is their more expensive nature compared to mercury vapour lamps [Crook *et al.*, 2014].

The irradiance of the UV lamp, which is the power of the lamp at a certain wavelength over a surface area, is often expressed in  $\text{mW cm}^{-2}$  or  $\text{W m}^{-2}$  due to the measurement methods typically used. In the case of water treatment, however, both the irradiation field and micro-organisms are present in a volume, and UV intensity is rapidly reduced (attenuated) within the first 15 cm of water [Kowalski, 2009]. Therefore, an irradiance unit of  $\text{W m}^{-3}$  or  $\text{mW L}^{-1}$  is a more appropriate choice [Kowalski, 2009; Müller *et al.*, 2014]. The corresponding UV dose or fluence, being the photonic energy in joules absorbed per unit area or volume, is then typically expressed in  $\text{mJ cm}^{-2}$  or  $\text{mJ L}^{-1}$ . This UV dose is linearly related to the LRV, although this relationship can plateau at higher UV doses for some micro-organisms, *e.g.*, *Cryptosporidium* [Hijnen *et al.*, 2006].

The required UV dose to completely inactivate the micro-organisms present in greywater can be found in Table 1.5, which is based on maximum pathogen concentrations in untreated greywater (Table 1.3) and linear regressions for UV dose and inactivation relations found in Hijnen *et al.* [2006]. However, these values only serve as an indication, since dose-inactivation data was found to be sparse except for the study of [Hijnen *et al.*, 2006], which is primarily based on data for drinking water disinfection with lower pathogen loads. Therefore, the log removal targets (LRT) for greywater can be higher than the maximum observed log removal values

(LRV) in the reviewed studies for drinking water, and the calculated UV doses were higher than the tested ranges. Since greywater could contain more UV-absorbing organic compounds than drinking water, a correction would be required, which is not taken into account for Table 1.5. Furthermore, the effect of photoreactivation, the use of environmental species (*i.e.*, not lab-grown pure cultures), and partial removal through prior wastewater treatment is not considered. *P. aeruginosa* and *S. aureus* were not reviewed in Hijnen *et al.* [2006], which might be due to a lower health risk [Friedler and Gilboa, 2010].

Table 1.5: Required UV doses for untreated greywater disinfection, with  $c_{GW, max}$  the maximum concentrations for mixed greywater from Table 1.3, the LRT the required log removal for full disinfection,  $D_{used}$  and  $LRV_{max}$  the used UV dose range and maximum observed log removal of the reviewed studies in Hijnen *et al.* [2006], respectively, and  $D_{LRT}$  the required UV dose for the specified log removal target.

	$c_{GW, max}$ (CFU 100 mL <sup>-1</sup> )	LRT	$D_{LRT}$ (mJ cm <sup>-2</sup> )	$LRV_{max}$	$D_{used}$ (mJ cm <sup>-2</sup> )
Total coliforms <sup>a</sup>	1.4·10 <sup>9</sup>	9.1	18.1	6.0	1 – 15
Faecal coliforms <sup>a</sup>	10 <sup>9</sup>	9.0	17.8	6.0	1 – 15
<i>E. coli</i>	8.1·10 <sup>6</sup>	6.9	13.7	6.0	1 – 15
Somatic coliphages <sup>b</sup>	10 <sup>4</sup>	4.0	72.7	4.9	5 – 139
<i>C. perfringens</i>	1.30·10 <sup>3</sup>	3.1	69.9	3.0	48 – 64
<i>Salmonella</i> <sup>c</sup>	7.9·10 <sup>3</sup>	3.9	7.6	5.6	2 – 10
<i>L. pneumophila</i>	7.9·10 <sup>2</sup>	2.9	7.2	4.4	1 – 12
<i>Cryptosporidium</i> <sup>d</sup>	2·10 <sup>8</sup>	8.3	32.1	3.0	0.9 – 13.1
<i>P. aeruginosa</i>	3.1·10 <sup>4</sup>	4.5			
<i>S. aureus</i>	5·10 <sup>5</sup>	5.7			
Enterococci and faecal streptococci <sup>e</sup>	1.2·10 <sup>6</sup>	6.1	19.5	4.6	2.5 – 16

Represented as <sup>a</sup>*E. coli*, <sup>b</sup>MS2 coliphage, <sup>c</sup>*Salmonella typhi*, <sup>d</sup>*C. parvum*, and <sup>e</sup>*Streptococcus faecalis*

UV was first used for drinking water disinfection in 1906 [von Recklinghausen, 1914]. However, preference was given to chlorination, which was being implemented quasi-simultaneous and had lower costs, a higher reliability and the presence of a disinfectant residual [Hijnen *et al.*, 2006]. Almost non-existent DPBs and higher inactivation of *Cryptosporidium*, *Giardia*, and viruses compared to chlorination and ozonation led to increased application of UV disinfection in recent decades [Friedler and Gilboa, 2010; Hijnen *et al.*, 2006]. Therefore, UV is highly effective against all pathogens, bacteria, protozoa and viruses present in wastewater treatment effluent and drinking water [Hijnen *et al.*, 2006]. However, no residual disinfectant is present, which can enable regrowth of pathogens [Crook *et al.*, 2014; Fenner and Komvuschara, 2005; Friedler and Gilboa, 2010]. Furthermore, UV disinfection is highly sensitive to UV scattering and absorption by particles or large flocs, meaning that high TSS and turbidity levels can reduce disinfection effectiveness and increase the UV dose demand [Azimi *et al.*, 2014; Friedler *et al.*, 2021; Kowalski, 2009]. Therefore, removal of particles prior to UV irradiation is favoured. LED-UVs might be less affected when multiple diodes are present at different angles, compared to more traditional UV configurations with a single lamp or parallel irradiation [Crook *et al.*, 2014].

## 1.5 Membrane technologies for greywater treatment

Key challenges for greywater treatment are the high variability, both in terms of flows and loads, and the presence of xenobiotic compounds (Subsection 1.3.1). Decentralized treatment systems should be able to overcome these difficulties, whilst being compact and robust [Gross *et al.*, 2015]. A most promising technique are membrane bioreactors (MBR), since on-site MBR systems have shown good reliability and produce good water quality fit for reuse in terms of turbidity, bacteria, TSS, and BOD<sub>5</sub> [Gross *et al.*, 2015; Jabornig, 2014]. MBRs have a high potential for micropollutant removal [Ma *et al.*, 2018; Tadkaew *et al.*, 2011; Trinh *et al.*, 2012], but this will not be elaborated upon any further in this work.

Membrane bioreactors are defined by Judd [2011] as an integration of a permselective membrane with a biological treatment process. This selectivity is achieved by either sieving (porous membranes for microfiltration, ultrafiltration, and nanofiltration) or by dissolving and diffusion (dense membranes for nanofiltration or reverse osmosis). The following work will be limited to microfiltration (MF), where the membrane acts as filter with a pore size of 0.05  $\mu\text{m}$  to approximately 5  $\mu\text{m}$ , rejecting the solid materials developed by the biological process to provide a clarified permeate (partially) free of larger microbial cells [Hyde *et al.*, 2016; Judd, 2011]. This retention of biomass can cause a high solids retention time (SRT), leading to reduced sludge production and the ability to treat a large volume of water with low hydraulic retention time (HRT) [Gross *et al.*, 2015; Park *et al.*, 2015].

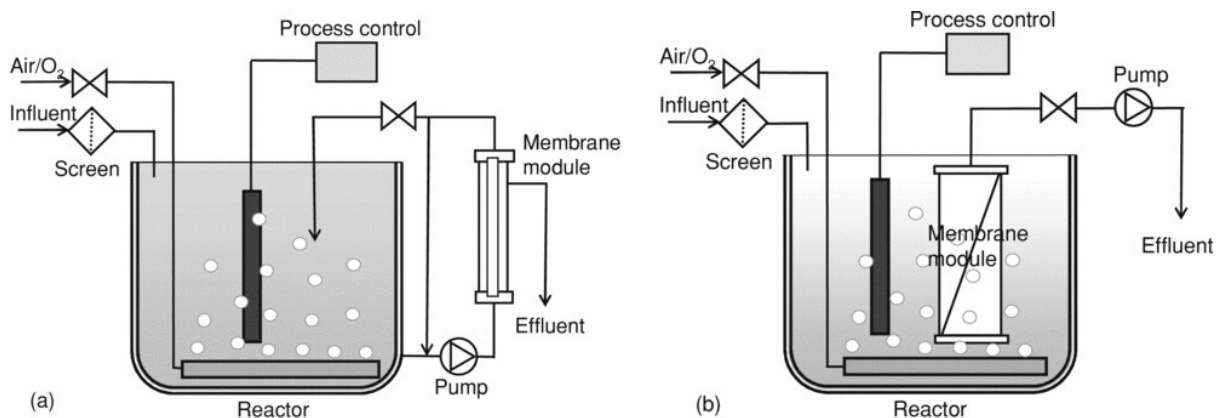


Figure 1.3: The two most common MBR configurations: (a) external configuration with cross-flow filtration, (b) submerged configuration in dead-end filtration mode. Reprinted from Lin *et al.* [2012].

The combination of the biological reactor with the membrane itself can occur in different configurations (Figure 1.3). The membranes can be submerged (internally) in the reactor, often with dead-end filtration, *i.e.*, filtration flow is perpendicular to the membrane [Atanasova *et al.*, 2017; Fountoulakis *et al.*, 2016], or they can be situated in an external compartment, where a tangential shear force often acts on the membrane, *i.e.*, cross-flow filtration [Friedler *et al.*, 2008; Sun *et al.*, 2010]. The ratio between permeate (effluent) and feed (influent) is known as the recovery [Judd, 2011]. When the recovery is  $< 1$ , the concentrate can be defined as the retained mixed liquor which can be recirculated or disposed of.

Control of permeation can be based on flux or pressure, since both are correlated through the relationship

$$J_w = \frac{\Delta P}{\mu \cdot R_m} = \frac{\varepsilon \cdot d_p^2 \cdot \Delta P}{32\mu \cdot \Delta x}, \quad (1.2)$$

where  $J_w$  is the water flux ( $\text{m}^3 \text{m}^{-2} \text{s}^{-1}$  or more commonly LMH,  $\text{L m}^{-2} \text{h}^{-1}$ ),  $\Delta P$  the transmembrane pressure or TMP (Pa),  $\mu$  the dynamic viscosity of water (Pa s), and  $R_m$  the clean membrane resistance ( $\text{m}^{-1}$  or equivalent),  $\varepsilon$  the surface porosity,  $d_p$  the pore diameter (m) and  $\Delta x$  the pore length or membrane thickness [Gitis and Rothenberg, 2016; Park *et al.*, 2015]. Therefore, by setting either  $J_w$  or  $\Delta P$ , the other can be controlled. The membranes can be constructed as flat sheets, hollow fibres, (capillary) tubes, pleated filter cartridges, or spiral wound modules. There are two main material classes for use in membrane bioreactors, being polymeric and ceramic membranes [Judd, 2011]. Their application for GW treatment will be described in detail in Subsections 1.5.2 and 1.5.3.

To increase the treatment performance of MBRs, they can be integrated with other biological treatment technologies to obtain hybrid-MBR or HMBR. On such option is the use of biocarriers from moving bed biofilm reactors (MBBR) for moving bed biofilm (ceramic) membrane reactors, or MBB(C)MR [Palmarin and Young, 2019; Palmarin *et al.*, 2020; Wang *et al.*, 2019]. This can lead to an increase in removal efficiency for TN and ammonia due to enhanced simultaneous nitrification and denitrification in the deeper, anoxic layers of the biofilm on the carriers [Palmarin and Young, 2019].

Microbial growth on GW can be limited due to surfactants and biocides present in the GW, causing low sludge concentrations of 2 to 3.6 g MLSS  $\text{L}^{-1}$  [Hasan *et al.*, 2015; Lamine *et al.*, 2012; Palmarin *et al.*, 2020]. However, the lower MLSS levels can in some cases be attributed to a low organic load in the GW, dependent on the type and composition of the GW [Lieberman *et al.*, 2016]. Therefore, enhanced biomass retention is a major advantage of MBRs, besides their compact operation. MBRs can effectively overcome long periods of starvation, which is beneficial for decentralized water treatment regarding, *e.g.*, absence of household inhabitants during holiday periods. Palmarin *et al.* [2020] found that, after a starvation period of two months, the MLVSS concentration decreased by 35%, but the lost biomass was recovered within 2 weeks. Furthermore, a decrease in the removal of ammonia, total nitrogen, and total phosphorus from 88%, 58%, and 90%, to -46%, 19%, and 9%, respectively was observed, also recovering to the baseline treatment performance after two weeks. Lastly, starvation led to an increase in soluble microbial products (SMP), which caused immediate fouling during the first four days after reactivation. Again, the fouling rate returned to normal after two weeks of reactivation.

MBRs generally have high energy consumptions [Gross *et al.*, 2015; Judd, 2011]. Indeed, decentralized greywater reuse can increase energy consumption for MBR compared to centralized systems [Besson *et al.*, 2021]. Energy use can vary from around 0.4 kWh  $\text{m}^{-3}$  to as high as 3.3 kWh  $\text{m}^{-3}$  [Atanasova *et al.*, 2017; Atasoy *et al.*, 2007; Jeong *et al.*, 2018; Lamine *et al.*, 2012]. Despite aeration contributing about 90% of the energy requirements in submerged MBRs [Judd, 2011], fouling control and reduction of maintenance is an important and often-researched topic.



### 1.5.1 Cleaning and fouling

From Equation 1.3, it follows that an increase in membrane resistance will lead to either a reduced flow through the membrane ( $J_w$ ) or an increase in TMP, dependent on the operational control (Subsection 1.5). This increase in membrane resistance is defined as *fouling*, and can be modelled as a resistance in series, with  $R_f$  the fouling resistance (Equation 1.3, Park *et al.* [2015]).

$$J_w = \frac{\Delta P}{\mu \cdot (R_m + R_f)} \quad (1.3)$$

Fouling is caused by deposition over time of solid particles on the membrane surface, being cake filtration, or within the pores, being clogging [Gitis and Rothenberg, 2016; Judd, 2011]. These particles can be inorganic scaling, organic, colloidal, and microbial in nature [Gitis and Rothenberg, 2016]. The accumulation of inorganic precipitates on the membrane surface is uncommon for microfiltration, and colloidal fouling with inert material such as sand or clay is limited and reversible if the particle size is large relative to the membrane pore size [Gitis and Rothenberg, 2016]. Fouling is more commonly caused by organic solutes through solute-membrane interactions such as electrostatic and hydrophobic or hydrophilic interactions. Important factors are the hydrophobicity and iso-electric point of the solutes and membrane, surface roughness and porosity of the membrane, and pH, ionic strength and metal concentration of the water [Gitis and Rothenberg, 2016]. The most common type of membrane fouling, especially in MBRs, is biofilm formation on the membrane surface leading to cake filtration [Gitis and Rothenberg, 2016; Judd, 2011; Park *et al.*, 2015].

To remove fouling, some sort of cleaning is necessary, which can be physical or chemical and is performed either in-situ (cleaning-in-place, CIP) or ex-situ (cleaning-out-of-place, COP) [Judd, 2011]. Fouling that can be removed by physical cleaning is called reversible, while any fouling requiring chemical intervention is called irreversible [Gitis and Rothenberg, 2016]. Oftentimes, despite being less effective than chemical cleaning, physical cleaning is preferred due to a reduced cost, time needed for cleaning, and likeliness to induce membrane degradation [Judd, 2011]. For similar reasons as with disinfection (Subsection 1.4.1), chemical usage and chemical waste should be avoided when considering non-grid water reuse, thereby favouring maximum possible physical cleaning.

Typically, physical cleaning is done on a periodic basis, while chemical cleaning is performed once a certain pressure threshold is achieved [Judd, 2011]. Physical cleaning methods include backwashing and relaxation. Backwashing involves the reversal of flow or blowing of air towards the feed side to wash-off or blow out fouling constituents, and is not possible for most flat sheet polymeric membranes. Relaxation is the stopping of the permeate flow on a periodic basis whilst continuing membrane aeration to induce shear stress, *i.e.*, air scouring [Gitis and Rothenberg, 2016; Judd, 2011; Yusuf *et al.*, 2015]. A wide range of chemical cleaning agents can be used, dependent on the nature of the foulant. Examples are bases and acids (NaOH, citric/oxalic acid) for the hydrolysis and solubilization of organic and microbial fouling, acids (HCl, H<sub>2</sub>SO<sub>4</sub>, citric/oxalic, HNO<sub>3</sub>) for inorganic fouling removal, oxidants (HOCl, H<sub>2</sub>O<sub>2</sub>) for decomposing organic matter, chelating agents (EDTA) to weaken fouling layer strength by removal of divalent cations (*e.g.*, Ca<sup>2+</sup>), surfactants to solubilize the foulants, and enzymes to remove fouling caused by proteins [Gitis and Rothenberg, 2016; Judd, 2011].

### 1.5.2 Polymeric membranes

The most commonly used membranes are polymeric, *i.e.*, being constructed from a large range of possible polymers, with commercial use of predominantly polyethersulfone (PES), polyvinylidene difluoride (PVDF), or derivatives of polyethylene (PE). Polymer materials can differ mainly in mechanical strength, hydrophilicity, and chemical resistance, of which an overview can be found in Table C.1 for 6 polymer families. Most polymeric membranes are asymmetric, which means that a layer with a larger pore size supports a separation layer with a smaller pore size, which provides the necessary selectivity [Judd, 2011]. Polymeric membranes show widespread implementation in industry, and studies for the treatment of greywater with polymeric membranes are ubiquitous in literature [Wu, 2019]. More recent research focused mainly on ultrafiltration and hollow fibre membranes [Atanasova *et al.*, 2017; Ding *et al.*, 2016; Fountoulakis *et al.*, 2016; Jabornig and Podmirseg, 2015; Palmarin *et al.*, 2020], due to higher packing densities possible [Judd, 2011; Park *et al.*, 2015].

However, this study considers microfiltration. A selection of studies concerning GW treatment with polymeric flat sheet MF membranes in submerged MBRs is given in Table 1.6, with operational regimes mostly based on sequencing batch reactors, except the study of Huelgas and Funamizu [2010], which was operated in a continuous mode. All studies except Scheumann and Kraume [2009] relied on gravitational permeation based on a water level difference, which means both flux and pressure differed throughout the operational cycle. Huelgas and Funamizu [2010] controlled permeation through a constant water level, *i.e.*, a constant pressure head. Scheumann and Kraume [2009] used peristaltic pumps, leading to a flux-controlled system. All recoveries were 100% with no sludge wastage, except for a SRT of 55 days set by Hocaoglu and Orhon [2010]. Atasoy *et al.* [2007] and Lamine *et al.* [2012] observed no requirement of membrane cleaning for 50 days, while for Huelgas and Funamizu [2010] this was 87 days and the membranes used by Scheumann and Kraume [2009] required cleaning every 6 months. Furthermore, Scheumann and Kraume [2009] studied intermittent aeration, with the introduction of anoxic and oxic periods to enhance nitrogen removal.



Table 1.6: Overview of the operating parameters and major removal efficiencies for studies on GW treatment with polymeric flat sheet MF membranes in submerged MBRs. The relaxation is expressed in minutes of pumping per total pumping cycle during the permeation step.

	Huelgas and Funamizu [2010]	Atasoy <i>et al.</i> [2007]	Hocaoglu <i>et al.</i> [2013]	Scheumann and Kraume [2009]	Lamine <i>et al.</i> [2012]
Greywater source	Synthetic kitchen sink and washing machine wastewater	Lodging houses	Lodging and guest houses	Synthetic GW excluding kitchen sink and dishwasher	Bathwater
<i>Operational parameters</i>					
$V_{\text{reactor}}$ (L)	10, lab scale	600, pilot scale	630, pilot scale	500, pilot scale	17, lab scale
Membrane type	Polyolefin <sup>a</sup> , Kubota A4	C-PE, Kubota plate and frame	C-PE, Kubota plate and frame	Polyphenol resin plate (0.4 $\mu\text{m}$ ), PES (UF) and PVDF (MF)	PE, Kubota A3
$d_p$ ( $\mu\text{m}$ )	0.4	0.4	0.4		0.4
Relaxation ( $\text{min min}^{-1}$ )	2/12	None	None	1/10	1/6
Specific aeration ( $\text{m}^3 \text{air m}^{-2} \text{h}^{-1}$ )		6		1.3	8
$J_w$ (LMH)	7.5 – 11.7	26 – 36		9 – 12	<7
HRT (h)	13.6	18	21	12	13
SLR ( $\text{kg COD kg}^{-1} \text{MLSS d}^{-1}$ )	0.07			0.05	0.09
VLR ( $\text{kg COD m}^{-3} \text{d}^{-1}$ )	1.21	0.3			0.318
MLSS ( $\text{g L}^{-1}$ )	16	4 – 12	4.6	5.0 – 8.0	3.5
DO ( $\text{mg L}^{-1}$ )	4		7	8 – 9 (oxic) and <0.3 (anoxic)	
<i>Removal efficiencies</i>					
COD	96%	95%	97%	92%	87%
$\text{NH}_4^+\text{-N}$	6%	82%	89.5%	97%	97%
TN	52.4% <sup>b</sup>	92%		76%	Presumably low
TSS		94%	>96%		100%
<i>Log removal values</i>					
Total coliforms		>4.13			>5.0
Faecal coliforms		>3.55			>4.7

<sup>a</sup> 'Polyolefins' can refer to PE or PP.

<sup>b</sup> Total Kjeldahl nitrogen, not including nitrite and nitrate.

### 1.5.3 Ceramic membranes

Ceramic membranes are a subcategory of membranes made from (at least one layer) of inorganic material [Gitis and Rothenberg, 2016]. This distinguishes them directly from polymeric membranes, resulting in significantly different properties (Table 1.7). While polymeric membranes can be either porous or dense (Section 1.5), ceramic membranes are most often porous and asymmetric (Figure 1.4), *i.e.*, ceramic membranes are usually composites with a support layer giving strength to the membrane. Aluminium oxide ( $\alpha$ -Al<sub>2</sub>O<sub>3</sub>) is commonly used as support, but this is being increasingly replaced by TiO<sub>2</sub>, due to its higher corrosion resistance [Buekenhoudt, 2008]. Other possible substrate materials are glass (SiO<sub>2</sub>) and stainless steel [Nyamutswa *et al.*, 2018; Zeuner *et al.*, 2020].

The intermediate layers usually consist of  $\gamma$ -Al<sub>2</sub>O<sub>3</sub>, TiO<sub>2</sub>, ZrO<sub>2</sub>, or mixtures thereof and serves as a transition between the large pores of the support and the small pore size of the top layer [Buekenhoudt, 2008]. The material of the active top layer determines the main properties of the ceramic membrane. Possible options are  $\gamma$ -Al<sub>2</sub>O<sub>3</sub>, SiO<sub>2</sub>, SiC, TiO<sub>2</sub>, ZrO<sub>2</sub>, other metal oxides and metal oxide mixtures, and zeolite [Arndt *et al.*, 2016; Gitis and Rothenberg, 2016; Richter *et al.*, 2003]. Hybrid organic-inorganic materials for the top layer aim to combine the best aspects of ceramic and polymeric membranes [Merlet *et al.*, 2020]. An overview of the different materials and characteristics can be found in Table C.2. It is evident that the selection of an appropriate material (*e.g.*, materials with low fouling) can impact the system performance for a chosen application.

Table 1.7: The major advantages and disadvantages of ceramic membranes over polymeric membranes. Adapted from Gitis and Rothenberg [2016]

Advantages	Disadvantages
Higher thermal stability (>200°C)	Low hydrothermal stability of composite membranes with a silica top layer
Higher resistance to organic solvents	More expensive source materials, complex processing; relatively high capital installation costs
Chemical stability over a wider pH range	Difficult sealing and module construction
Long-time operational stability, no ageing, higher lifespan (15–20 years vs. 7–10 years); potentially lower life cycle cost	Low packing density
Higher mechanical stability and structural integrity under large pressure gradients, allowing for operation and backwashing at high flux (up to 500 LMH)	The innate brittleness requires specialized configurations and supporting systems
More uniform pore size distribution, no deterioration of selectivity at higher flux	Relatively high installation and modification costs in case of defects
(Electro)catalytic and electrochemical activity easily realizable.	Low permeability of high-selectivity (dense) membranes at medium temperatures

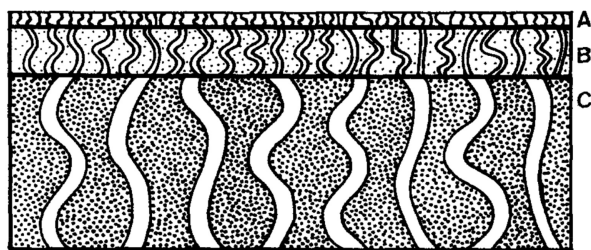


Figure 1.4: Schematic representation of a composite ceramic membrane: (A) top layer. (B) intermediate layer, and (C) porous support. Reprinted from Lindqvist and Lidén [1997].

Due to increased chemical and thermal stability, ceramic membranes can withstand harsh chemical cleaning, and can be sterilized and autoclaved [Issaoui and Limousy, 2019]. Furthermore, because of the rigid structure, ceramic membranes are backwashable.  $\text{TiO}_2$  membranes with glass  $\text{SiO}_2$  support can be used for its photocatalytic properties as an alternative to chemical cleaning [Nyamutswa *et al.*, 2018].

Hofs *et al.* [2011] compared polymeric and ceramic membranes in terms of fouling susceptibility when treating lake water. The small tubular membranes tested were  $\text{Al}_2\text{O}_3$ ,  $\text{TiO}_2$ , and  $\text{ZrO}_2$  ceramic membranes and a polyethersulfone/polyvinylpyrrolidone mixture polymeric membrane. From Figure 1.5, it becomes clear that the tested membranes differ significantly in terms of fouling. Firstly, it can be noted that the ceramic membranes show less irreversible fouling than the polymeric, but this difference can be explained by the lower volume-to-area ratio of the polymeric membranes [Hofs *et al.*, 2011].  $\text{TiO}_2$  and especially SiC have significantly lower fouling susceptibility among the ceramic membranes, both irreversible and reversible. de Wit *et al.* [2015] attribute this to the low iso-electric point and high hydrophilicity for the case of SiC. However, Hofs *et al.* [2011] regard the larger pore size of the  $\text{TiO}_2$  and SiC membranes as the cause of the lower fouling susceptibility. All membranes should have similar pore sizes, but the measured pore sizes were found to be vastly different and up to 24 times higher than those given by the manufacturers [Hofs *et al.*, 2011]. It is worth noting, however, that the porosity of the SiC membrane was determined for a different membrane type (flat disc) than the membrane used for the fouling experiments [Hofs *et al.*, 2011].

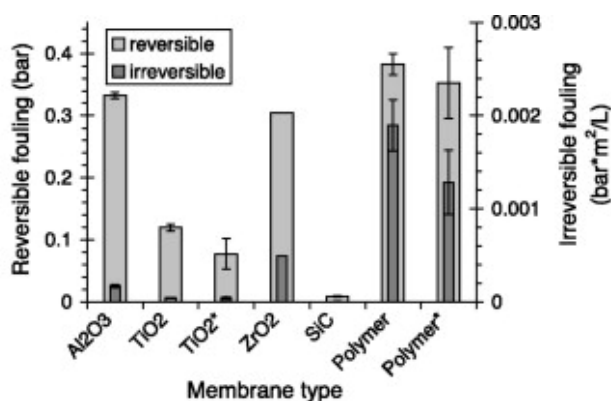


Figure 1.5: TMP increase due to reversible and irreversible fouling for different membrane materials. Reprinted from Hofs *et al.* [2011].

The high costs of raw materials and energy consumption for the sintering-based production process of ceramic materials have led to the preference of polymer-based membranes over ceramics, especially for small-scale systems [Li, 2007]. Therefore, ceramic membranes are more often used for niche applications where its advantages are a requirement, *e.g.*, high load industrial wastewaters [Eom *et al.*, 2015; Issaoui *et al.*, 2016], food and beverage industry [Yang *et al.*, 2020; Yazdanshenas *et al.*, 2010], and microbial fuel cells [Burmistrov *et al.*, 2013; Daud *et al.*, 2018]. To counter this, there is a strong focus on the use of low-cost raw materials such as kaolin clay, coal fly ash, illite clay, and apatite to reduce production costs [Hubadillah *et al.*, 2018; Jedidi *et al.*, 2009; Khemakhem *et al.*, 2007; Sahoo *et al.*, 2016].

There have been few studies on the applicability of ceramic membranes for (non-biological) greywater treatment [Ahn *et al.*, 1998; Bhattacharya *et al.*, 2013; Das *et al.*, 2018]. Concerning MBRs for GW treatment, Sun *et al.* [2010] studied a biofilm-MBR, being a biofilm reactor and an external submerged membrane unit, using Al<sub>2</sub>O<sub>3</sub> ceramic membranes with a pore size of 0.2 µm. The treated wastewater streams were the greywater, blackwater, and bilge water of a ship. Bilge water is the oily, surfactant-rich water found in the bilge, *i.e.*, lowest part of a ship, generated by draining of deck water into the ship, internal (oil) leaks, or other spillage. For the case of black- and greywater only, removal efficiencies of 88% and 72% for respectively COD and NH<sub>4</sub><sup>+</sup>-N were achieved with a recovery of 93% and a flux of 13.5 LMH. Furthermore, both recoveries of 70% and 93% showed similar values for TSS near the membranes, as well as similar effluent quality [Sun *et al.*, 2010].

Another study was made by Hasan *et al.* [2015], where a low-cost ceramic membrane was prepared using a mixture of dried clay soil (80 w%) and rice bran (20 w%), resulting in a porosity of 60±1% and a pore size of 1–5 µm. Synthetic greywater, composed of shampoo, dish cleaner and laundry detergent was treated. Removal efficiencies of >97% and >88% were found for respectively BOD<sub>5</sub> and TOC, but no removal of TN or TP was observed. Anionic surfactant removal was found to be >99% for methylene blue and 93% for linear alkylbenzene sulfonates (C<sub>10</sub> – C<sub>14</sub>). The ceramic filter was not heavily susceptible to fouling, since it could be operated at a stable flux of 11.5 LMH without cleaning or backwash for the total duration of the experiment.

The limited amount of available literature on ceramic membrane bioreactors for greywater treatment might be due to the perceived high cost of ceramic membranes compared to polymeric membranes (Table 1.7). However, interest in more general applications such as wastewater treatment is increasing. The robustness, *i.e.*, mechanical strength and lifespan, could be an advantage for household-scale submerged MBR for greywater treatment, allowing low maintenance requirements. Furthermore, the ability to clean the membranes without the need for chemicals allows for a more safe operation for household applications. To the best of the author's knowledge, a direct comparison between ceramic and polymeric membranes for small-scale greywater treatment in MBRs has not been performed, and no LRV has been determined for ceramic membranes in this scenario.

# 2

## Objectives and hypotheses

As the title of this thesis implies, the focus will be on the reclamation of greywater for non-potable reuse and the application potential of an MBR treatment system with UV disinfection on a small scale, *e.g.*, single households. A continuous flow submerged MBR was chosen as opposed to a sequencing batch reactor to monitor fouling more effectively through constant flux application and the measurement of the transmembrane pressure. Microfiltration was chosen due to lower operating pressures, fouling, energy and maintenance requirements caused by the larger pore size. Flat sheet membranes were selected since this membrane type can be more easily cleaned manually by wiping or brushing of the filter cake layer. The main objectives and hypotheses are, in order of importance:

1. Comparing C-PE polymeric and SiC ceramic flat sheet membranes in terms of fouling rate and treatment performance. Due to the superior surface characteristics of ceramic membranes, it is expected that the SiC membranes will be less susceptible to fouling and therefore have a higher applicability to small-scale treatment systems.
2. Evaluating the microbial disinfection performance with the indicator organism *E. coli*, to ensure low human health risk of the treated effluent. This includes the determination of a LRV for the polymeric and ceramic flat sheet membranes, and UV disinfection. The LRV for the membranes are expected to be in line with literature, while the UV reactor is expected to effectively remove *E. coli* to non-detectable levels. Furthermore, the UV reactor will be characterized to link the determined LRV with the applied UV dose.
3. Maintaining a stable operation of an MBR with UV disinfection, treating synthetic greywater and producing effluent quality fit for non-potable reuse. It is hypothesized that the influent buffer or storage drum will contribute to degradation, as would be expected in a real-life situation. As MBRs are a proven technology that are being often applied in centralized WWTP, it is hypothesized that the MBR can effectively treat the greywater to water quality targets for non-potable reuse.
4. Confirming the advantages of MBRs compared to different treatment systems for decentralized greywater treatment. These include the smaller required reactor size, effective retention of biomass, high effluent clarity, and better process control. The activated sludge concentration is expected to be limited due to the inhibitive nature of surfactants and biocides present in greywater.
5. Determining a correlation between  $UV_{254}$  absorbance of the effluent and water quality parameters sCOD and TOC, to allow for on-line monitoring. It is expected that strong correlations will be found, although the specific relations are expected to be different for the influent and effluent.

## 3

# Materials and methods

## 3.1 Synthetic greywater composition and preparation

Due to practical constraints, synthetic greywater was chosen as reactor feed, of which the composition and aimed-for COD and TN can be found in Table 3.1. The composition was based on risk assessment studies for personal care product (PCP) use [Ficheux *et al.*, 2019], economic data on detergent use [Madsen and Miljøstyrelsen, 2001], greywater quantity dependent on source for Flanders [Vlaamse Milieumaatschappij, 2018], and Aiyuk and Verstraete [2004] and Larsen *et al.* [2013] for chemical compounds concentration. The GW was prepared weekly in concentrate batches of 10 L and stored at 4°C, which could be diluted with tap water to 280 L fresh influent when needed. To analyse the composition of the synthetic greywater, fresh GW was prepared once using demineralized water (Milli-Q) as diluent. Furthermore, the composition of tap water was analysed once to assess its contribution to synthetic GW in terms of COD, TN and ions.

Table 3.1: Composition of the synthetic greywater, including aimed-for COD and TN concentrations.

Component	Concentration (mg L <sup>-1</sup> )
<i>PCP and detergents</i>	
Shampoo	53.48
Shower gel	142.60
Toothpaste	35.65
Shaving foam	53.48
Liquid laundry	208.49
Dishwasher tablets	87.43
<i>Chemical compounds</i>	
NaAc	394.00
NH <sub>4</sub> Cl	83.00
K <sub>2</sub> HPO <sub>4</sub>	3.00
Na <sub>2</sub> SO <sub>4</sub>	51.08
CaCl <sub>2</sub>	50.00
NaCl	50.00
<i>Overall parameters</i>	
COD <sub>PCP and detergents</sub>	204
COD <sub>NaAc</sub>	300
COD <sub>total</sub>	504
TN <sub>PCP and detergents</sub>	1.3
TN <sub>NH<sub>4</sub>Cl</sub>	21.73
TN <sub>total</sub>	23.0

For rinse-off PCP usage, risk assessment studies were selected from [Ficheux \*et al.\* \[2019\]](#), of which a summary can be found in [Table 3.2](#). For each PCP, an intermediate value was selected for further calculations. For detergents, no risk assessment studies were found, which is likely due to the indirect nature of exposure contrary to PCP, which are often applied directly to the body. The daily usage per person was therefore based on economic data. Even then, little data was available for each category of detergent, with the most recent data found from 1998 [[Madsen and Miljøstyrelsen, 2001](#)]. A summary can be found in [Table 3.3](#).

Table 3.2: Summary of PCP usage based on risk assessment studies.

PCP	Consumption (g p <sup>-1</sup> d <sup>-1</sup> )			Selected values
	<a href="#">Biesterbos <i>et al.</i> [2013]<sup>a</sup></a>	<a href="#">Garcia-Hidalgo <i>et al.</i> [2017]<sup>b</sup></a>	<a href="#">Gomez-Berrada <i>et al.</i> [2017]<sup>c</sup></a>	
Shampoo	2.4	2.9	7.8	3
Conditioner	2.1	2.9		2.5
Shower gel	4.5	8.3	11.9	8
Bathing foam	1.2	0.8		1
Toothpaste	2.2	1.8		2
Shaving foam	1.3			1.3
Shaving gel	1.7			1.7
Liquid hand soap		10.3	6.1	7.5
Solid soap			3.2	3.2

Countries: <sup>a</sup> NL; <sup>b</sup> CH; <sup>c</sup> FR, MK, ES, NL, PL, PT, MU, ZA, and BR

The calculated product usage (g p<sup>-1</sup> d<sup>-1</sup>) can be divided by the total water usage for greywater (L p<sup>-1</sup> d<sup>-1</sup>) as discussed in [Subsection 1.3.1](#) to obtain concentrations in g L<sup>-1</sup>. The water usage data for Flanders was used [[Vlaamse Milieumaatschappij, 2018](#)]. Water requirements for textile handwashing (1.1 L p<sup>-1</sup> d<sup>-1</sup>) and hand dishwashing (6 L p<sup>-1</sup> d<sup>-1</sup>) were not included. The missing COD and TN contained within food particulates often present in kitchen sink and machine dishwasher wastewater was approximated by acetate and ammonium chloride. The values for shaving gel and foam were summed, and shaving foam was used. Similarly, for hand and machine dishwashers, dishwashing tablets were used. The value for powder laundry was used as liquid laundry, while the value for liquid laundry itself was dropped.

Table 3.3: Detergent usage in the EU in 1998 [[Madsen and Miljøstyrelsen, 2001](#)]. Values in g p<sup>-1</sup> d<sup>-1</sup> were converted using the population size in 1998 [[UN Population Division, 2019a](#)].

Detergents	Consumption (ton y <sup>-1</sup> )	Consumption (g p <sup>-1</sup> d <sup>-1</sup> )
Powder laundry	3100000	11.70
Liquid laundry	560000	2.11
Fabric softener	1000000	3.77
Hand dishwasher	800000	3.02
Machine dishwasher	500000	1.89



For the chemical compounds (NaAc, NH<sub>4</sub>Cl, K<sub>2</sub>HPO<sub>4</sub>, Na<sub>2</sub>SO<sub>4</sub>, CaCl<sub>2</sub>, NaCl), a previous composition was continued, which was partly based on [Aiyuk and Verstraete \[2004\]](#). The used products (detergents and PCP), together with their properties, can be found in Table 3.4. Density was determined by adding a known weight of the product to a measuring cylinder filled with water and measuring the volume increase. COD and TN were determined by dissolving a certain weight of the product (dependent on expected COD and TN values) in 100 mL volumetric flasks, after which analyses were performed as described in Section 3.3.

Table 3.4: Properties of the PCP and detergents used.

<b>Product</b>	<b>Density (g mL<sup>-1</sup>)</b>	<b>COD (mg g<sup>-1</sup>)</b>	<b>TN (mg g<sup>-1</sup>)</b>
Shampoo (L'Oréal Elseve Extraordinary Oil)	1.057	377	0.7
Shower gel (Tahiti Tropical wood)	0.9649	374	0.59
Toothpaste (Sensodyne Fresh Mint)	1.777	385	7.1
Shaving foam (Gillette Series 3x Sensitive Skin)	0.175	478	0.87
Liquid laundry (Persil Power Gel Summer Garden)	1.036	331	0.39
Dishwasher tablets (Sun Classic)	2.03	253	8.6



## 3.2 Reactor design and operation

Two identical MBRs with a volume of 10 L were constructed out of acrylic panels (Figures 3.1 and B.10). The reactors could be bolted closed by a lid, to avoid aerosol dispersion in the lab. The polymeric membranes used were flat sheet chlorinated polyethylene (C-PE) membranes with a pore size of 0.4  $\mu\text{m}$ , surface area of 0.11  $\text{m}^2$  (A4 size), and initial membrane resistance ( $R_m$ ) of  $2.75 \cdot 10^{11} \text{ m}^{-1}$  (Kubota, Japan, Figure B.9). A hydrophilic agent was applied to the C-PE membrane by the manufacturer (Kubota), which increases hydrophilicity and reduces fouling susceptibility (Subsection 1.5.2). The ceramic membranes used were flat sheet SiC membranes with a surface area of 0.165  $\text{m}^2$ , a pore size of 0.56  $\mu\text{m}$ , and a porosity of 42% (confidential supplier, Figure B.8). The clean water membrane resistance was not estimated for the ceramic membranes. Each MBR was outfitted with either a polymeric or ceramic membrane. The membranes were suspended by a metal wire at an appropriate height in the middle of the reactor. The reactors were set up in a temperature-controlled room, being  $22 \pm 1 \text{ }^\circ\text{C}$ .

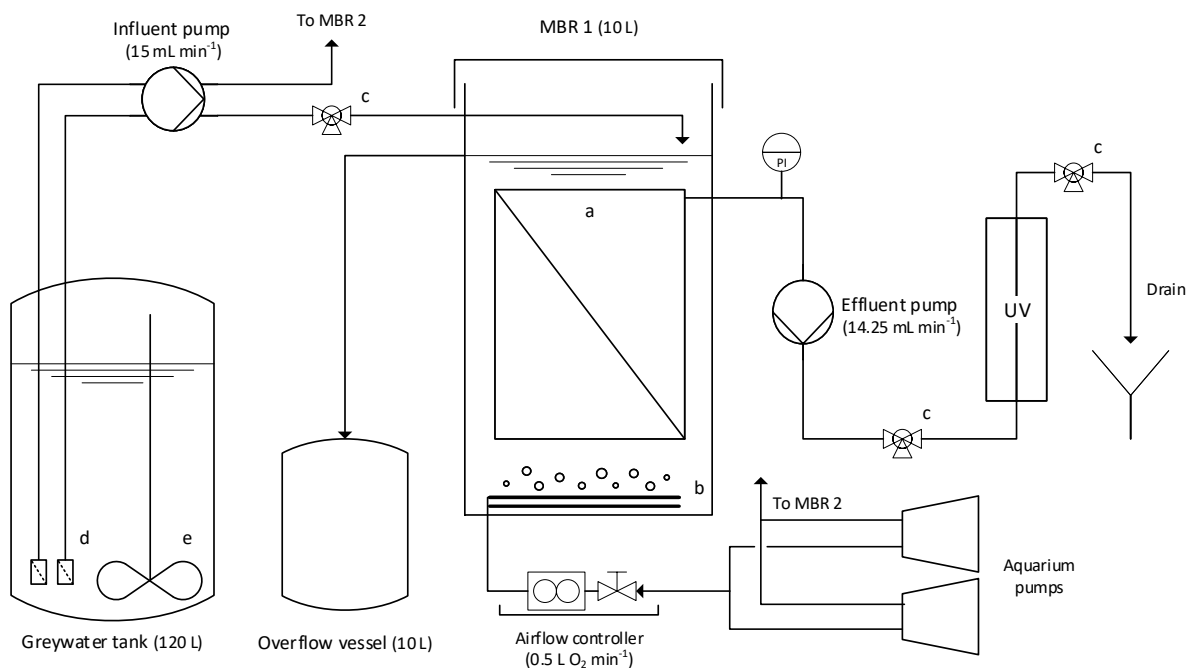


Figure 3.1: Overview of the membrane bioreactor (MBR) setup, with PI: pressure indicator (manometer), a: membrane, b: aeration stones, c: sample valves, d: 1 mm mesh filter, and e: overhead stirrer.

The reactors were inoculated at  $1 \text{ g L}^{-1}$  MLSS with activated sludge from a nearby WWTP (Ossemeersen, Ghent). The initial start-up was performed on a previous greywater composition, which was diluted 1:10 due to excessive foaming. Starting at day 0, the new composition as described in Subsection 3.1 was used. The reactor operation can be divided into 3 phases, with a first phase of operation and heavy optimization using the polymeric membranes (Phase I: day 0–74). Between day 75 and day 95, there was a bridge period when reactor operation continued, but no analysis results are available. Due to sludge problems during Phase I (Subsection 4.2.1), the reactors were reinoculated on day 96 at  $4 \text{ g L}^{-1}$  MLSS, *i.e.*, the reactor contents were replaced with undiluted activated sludge from the WWTP. Sample analysis resumed on day 123. Polymeric membrane operation continued until day 164 (Phase II: day 96–164). On day 165, the ceramic membranes were installed (Phase III), and operation was continued until day 204.

The MBRs were continuously aerated by aquarium pumps (Eheim 400), one for each MBR. Initially, two cylinder shaped aeration stones of length 120 mm were used per MBR ('Hi-Oxy', unknown supplier). These were replaced on day 63 by two bar-shaped aeration stones of length 200 mm (SuperFish Air-Stone 200 mm). Starting day 62, the aeration flow rate was set at  $0.5 \text{ L O}_2 \text{ min}^{-1}$  by a gas flow controller, which led to a specific aeration flow (per membrane surface area) of  $0.27$  and  $0.18 \text{ m}^3 \text{ O}_2 \text{ m}^{-2} \text{ h}^{-1}$  for the polymeric and ceramic membranes, respectively.

Two 60 L blue plastic drums were used for synthetic greywater storage. The greywater tanks were refilled whenever the level was low, which was usually every other day. Two home-made mesh filters, consisting of a 1 mm metal mesh screen fitted inside a PVDF tube connector, were placed on the influent tubing to protect the membranes from any coarse particles. Starting day 19, the influent drums were continuously stirred at 500 rpm using overhead stirrers with 4-bladed propellers (IKA Eurostar 20). On day 39, the barrels were replaced with one single 120 L blue plastic drum, to save space and provide exactly the same influent to both reactors. Two peristaltic pumps with each two pumpheads (Watson Marlow 530S with type-313 pumpheads) were used for influent and effluent. The effluent pump was replaced by two similar pumps on day 150, to more accurately set the recovery, since the pumpheads could show deviation.

The influent flowrate was set according to the greywater drum storage capacity and the set recovery. The gross flow rate ( $Q_g$ ) is defined as the instantaneous flow rate measured when pumping, while the net flow rate ( $Q_n$ ) accounts for relaxation. The fluxes were calculated as the effluent flow rates divided by the membrane surface area. The hydraulic retention time (HRT,  $\theta_H$ , h) was calculated as the reactor volume ( $V$ , L) divided by the net influent flowrate ( $Q_{n, in}$ ,  $\text{L h}^{-1}$ ). The solids retention time (SRT,  $\theta_X$ , d) was calculated as the reactor volume ( $V$ , L) divided by the net overflow rate or wastage flowrate ( $Q_{n, w}$ ), being the difference between net influent ( $Q_{n, in}$ ,  $\text{L d}^{-1}$ ) and net effluent ( $Q_{n, out}$ ,  $\text{L d}^{-1}$ ) flowrates. The greywater entered the MBR above the water level. The excess was removed through overflow at a constant water level into a 10 L plastic can to allow for sludge wastage. The recovery was increased during Phase I when MLSS concentrations were too low. A home-made cycle timer was installed for the pumps (based on an Omron H3CR-F) on day 13 and set initially at 1 minute of membrane relaxation and 9 minutes of operation in cycles of 10 minutes (1 min / 10 min). Relaxation was increased 2 days later to 2 min / 10 min. An overview of the used operational parameters, not including the bridge period at the end of Phase I, can be found in Table 3.5.

The transmembrane pressure (TMP) was manually monitored using a manometer. Therefore, measurement time resolution is in the range of a few hours to days. Initially, an analog manometer was used (dry pressure gauge  $-1$  to  $0$  bar, Mega). Since the resolution of these pressure gauges was only 20 mbar and the lowest reading was 40 mbar suction pressure, the switch was made on day 29 to a digital manometer (Dwyer DPGW-00). These digital manometers had a range of  $0$  to  $-1013$  mbar, with a resolution of 1 mbar. The transmembrane pressures are reported as absolute values, *i.e.*, in mbar suction pressure.

Table 3.5: Operational parameters for the three phases. A bridge period of 20 days is present between Phase I and II for which no operational parameters are known.

Membrane type Surface area (m <sup>2</sup> )	Phase I (74 days total)					Phase II (68 days)		Phase III
	Polymeric (C-PE)					Polymeric (C-PE)		Ceramic (SiC)
	0.11					0.11		0.165
Duration (days)	13	2	31	7	21	30	38	40
Recovery (%)	95	95	95	80	98.6	90	95	95
Gross flux, $J_g$ (LMH)	7.2	8.0	9.0	6.5	8.1	8.0	7.8	5.2
Net flux, $J_n$ (LMH)	7.2	7.2	7.2	5.2	6.5	6.4	6.2	4.1
Relaxation (min/min)	None	1/10	2/10	2/10	2/10	2/10	2/10	2/10
HRT (h)	12	12	12	13.9	13.9	10.24	13.9	13.9
SRT (d)	10	10	10	2.9	41.3	5.3	11.6	11.6

The manometers were installed at the height of the water level, so hydrostatic effects would cancel out. The reasoning is as follows: suppose the manometer is installed at a certain height  $M$  above the water level, and let  $x$  be a variable distance below the water level,  $P_{atm} = 0$  the atmospheric pressure and  $P_m$  the measured pressure at the manometer (Figure 3.2). The pressure both inside and outside the membrane can be calculated using the Bernoulli equation simplified for static liquids (Equation 3.1), since water flow speed inside and outside the membrane are assumed equal, and the effect of aeration on the pressure is assumed negligible. The transmembrane pressure is then given by Equation 3.2, from which it is evident that when  $M = 0$ , the pressure measured at the manometer will equal the transmembrane pressure.

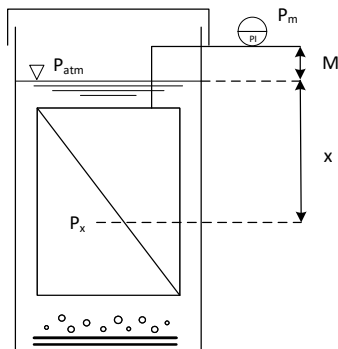


Figure 3.2: Manometer installation height.

$$P_{x,in} = (x + M) \cdot \rho \cdot g + P_m \quad (3.1)$$

$$P_{x,out} = x \cdot \rho \cdot g$$

$$\Delta P = P_{x,in} - P_{x,out} \quad (3.2)$$

$$= P_m + M \cdot \rho \cdot g$$

One UV reactor was installed per MBR (Xclear UV-C multimax), which is designed for ponds with a capacity of 7000 L. The maximum design flow of the UV reactor is 3000 L h<sup>-1</sup>. Low pressure mercury-vapor (LP-Hg) UV-C lamps with a power rating of 9W and a UV-C output of 2.3 W were used (Philips TUV PL-S 9W 2P UV-C). Sample ports were installed after the influent pump, effluent pump, and UV reactor (Figure 3.1). Treated greywater effluent was disposed of through a connection with the drain.

The membranes were cleaned when membrane suction pressure generally exceeded 100 mbar, *i.e.*, when manometer readings were below  $-100$  mbar. Cleaning was performed chemically during Phase I, using a solution of 0.375 g L<sup>-1</sup> active chlorine, prepared by adding 1 commercial javel tablet (1.5 g active chlorine per tablet) to 4 L of tap water. During Phase II, only manual cleaning was performed by gently wiping the sludge cake layer from the membrane surface by hand. All cleaning for Phases I and II occurred *ex-situ*. For the ceramic membranes (Phase III), no cleaning was necessary.

## 3.3 Analysis methods

### 3.3.1 Sampling procedure

Samples were taken three times per week on Monday, Wednesday and Friday. Each sampling day, 50 mL of influent, effluent (after UV), and the MLSS was sampled using falcon tubes. For the influent and effluent, additional 30 mL samples were taken to analyse turbidity, conductivity, UV<sub>254</sub>, and carbon fractions (total, total organic, and inorganic) at PaInT (UGhent). The samples were stored at 4°C until further analysis. Pump flows were monitored during sampling in Phase I and II. If large deviations from the operational settings were observed, the pump tubing was replaced and the pumps were recalibrated. During Phase III, pumps were consistently recalibrated during sampling to obtain more constant and precise flow rates. Before sampling, the reactors were stirred using a long pole to resuspend settled sludge.

### 3.3.2 Sample analysis

The samples were analysed weekly. Turbidity, conductivity and UV<sub>254</sub> were analysed in batches per month, and carbon was analysed in batches of 3 months. Temperature and pH were measured on the day of sampling. The pH was measured for influent, reactor and effluent samples using a 744 pH meter (Metrohm) calibrated for pH 7–10. The pH probe used was a Unitrode combined pH electrode with integrated Pt1000 temperature sensor and a 3 M KCl reference electrode (Metrohm).

Turbidity and conductivity was measured for influent and effluent, using a HI 98713 ISO portable turbidity meter (Hanna Instruments) and a C3020 multi-parameter analyser (Consort), respectively. UV-absorbing organic constituents were measured for influent and effluent at 254 nm using a UV-1600PC spectrophotometer (VWR) and a quartz cuvette (path length 1 cm) zeroed with distilled water, following Standards Method 5910 [[American Public Health Association \*et al.\*, 2017](#)]. For the influent, the samples were filtered through 0.45 µm polyamide filters (Chromafil Xtra) to exclude turbidity effects on absorbance [[APHA, 2017](#)]. Correlations were determined between UV<sub>254</sub> absorption, TOC, and COD, but these correlations are specific to the greywater studied and are not comparable with other wastewaters [[APHA, 2017](#)]. Total carbon, total organic carbon and inorganic carbon samples were prepared for analysis by using glass vials and stored at 4°C until analysed using a TOC-5000 total organic carbon analyser (Shimadzu Corp.) and processed according to Standard Method 5310 [[APHA, 2017](#)].

Total nitrogen and (s)COD were determined using nanocolor tube tests (Macherey-Nagel). For the influent and effluent, TN was measured using the TN<sub>b</sub> 220 and TN<sub>b</sub> 22 test kits, respectively. The COD of the influent samples was determined using COD 1500 test kits, while for the effluent COD 160 and later COD 40 test kits were used. Soluble COD measurements were performed for influent and reactor samples by filtering through 0.45 µm polyamide filters (Chromafil Xtra) and analysed using the COD 1500 and 160 test kits, respectively. The test tubes were digested using either a HC 6040 digester (WPA), a COD reactor 16500 (Hach), or nanocolor vario 4 (Macherey-Nagel) and determined using a nanocolor 500 D spectrophotometer (Macherey-Nagel).

TSS and VSS (MLSS and MLVSS for the reactors) measurements were performed according to Standard Methods 2540D and E, by filtering a 10 mL sample over a glass fibre filter and weighing the mass difference of the filter after drying for 2 hours at 105°C for TSS and incinerating for 1.5 hours at 550°C for VSS [APHA, 2017]. Since the scales on which the measurements were performed showed fluctuation, a limit of quantification (LOQ) was determined by weighing 10 blank samples before and after the complete method procedure. The average mass difference was determined to be 0.06 mg, with a standard deviation of 0.25 mg. The method's limit of detection was defined as the average with 10 standard deviations added, which is 3 mg. Therefore, when filtering 10 mL samples, the minimum quantifiable amount of TSS or VSS is 0.3 g L<sup>-1</sup>. For the MLSS and MLVSS of the reactors, 3 replicates were analysed per sample. For the TSS and VSS measurements of the effluent after membrane filtration, 265.05 mL was filtered for a LOQ of 0.01 g L<sup>-1</sup>.

The cations (Na<sup>+</sup>, NH<sub>4</sub><sup>+</sup>, K<sup>+</sup>, Ca<sup>2+</sup>, Mg<sup>2+</sup>) and anions (Cl<sup>-</sup>, NO<sub>2</sub><sup>-</sup>, NO<sub>3</sub><sup>-</sup>, PO<sub>4</sub><sup>3-</sup>, SO<sub>4</sub><sup>2-</sup>) were analysed using ion chromatography (IC). The samples were filtered through 0.20 µm PVDF filters (Chromafil Xtra), diluted 1:2 with deionized water (Milli-Q), and stored at 4°C until further analysis by the technical staff. For the cations, an IC 761 chromatograph (Metrohm) was used, with a LOQ of 0.2 mg L<sup>-1</sup> for all cations, including the dilution factor. For the anions, this was a Compact IC Flex 930 (Metrohm) with a LOQ of 0.1 mg L<sup>-1</sup> for all anions.

If sample results are given by a mean and standard deviation ( $\bar{x} \pm \sigma$ ), this means that the normality was checked using both a quantile-quantile (Q-Q) plot and the Shapiro-Wilk test for normality. In some cases, the Shapiro-Wilk test was negative for normality, while the Q-Q plot showed clear indication of normality, except outliers. In that case, normality was assumed. When the data was not normally distributed, a range and mean, *i.e.*, min – max ( $\bar{x}$ ) are given. When stating statistical significance, a p-value will be given. For the correlations, a pearson correlation  $\rho$  and p-value for significance is given. For linear models (linear regression), a residual analysis was done to check for normality, linearity, and homoscedasticity by plotting the residuals versus the fitted values and a Q-Q plot of the residuals. All statistical analyses were made on a 5% significance level using RStudio.

### 3.4 Process kinetics

All calculations for kinetics will be based on the book of Rittmann [2001]. The mixed liquor volatile suspended solids (MLVSS) was assumed to be representative of the active biomass. The flows used were the net flows, accounting for relaxation. The sludge loading rate (SLR,  $B_X$ ) in kg COD kg<sup>-1</sup> MLVSS d<sup>-1</sup> and volumetric loading rate (VLR,  $B_V$ ) in kg COD m<sup>-3</sup> d<sup>-1</sup> can be calculated using the following equations:

$$SLR = B_X = \frac{S_0 \cdot Q_{in}}{X} \quad (3.3)$$

$$VLR = B_V = \frac{S_0 \cdot Q_{in}}{V}, \quad (3.4)$$

with  $S_0$  the influent COD concentration (kg L<sup>-1</sup>),  $Q_{in}$  the influent flow rate (L d<sup>-1</sup>),  $X$  the sludge concentration (kg MLVSS L<sup>-1</sup>), and  $V$  the reactor volume (m<sup>3</sup>). The calculations for kinetic parameters were performed for each data point and averaged to obtain an average parameter. These average parameters were then used in further calculations.

The sludge specific growth rate ( $\mu$ ) in  $\text{d}^{-1}$  can be calculated by

$$\mu = \frac{1}{X(t)} \frac{dX(t)}{dt} = \frac{1}{\bar{X}} \frac{X(t) - X(t - \Delta t) + \bar{X} \cdot \bar{Q}_w \cdot \Delta t / V}{\Delta t}, \quad (3.5)$$

with  $X(t)$  the sludge concentration ( $\text{g MLVSS L}^{-1}$ ) at time  $t$ ,  $\bar{X}$  the average sludge concentration between time  $t$  and the previous sample  $t - \Delta t$ ,  $\bar{Q}_w$  the average sludge wastage ( $\text{L d}^{-1}$ ) between  $t$  and  $t - \Delta t$ ,  $V$  the reactor volume ( $\text{L}$ ), and  $\Delta t$  the time step ( $\text{d}$ ). The first part of the numerator ( $X(t) - X(t - \Delta t)$ ) is the sludge growth that can be observed through measurements of reactor MLVSS. The second part,  $\bar{X} \cdot \bar{Q}_w \cdot \Delta t / V$ , represents the sludge growth that is removed through sludge wastage, *i.e.*, the average amount of sludge removed ( $\bar{X} \cdot \bar{Q}_w \cdot \Delta t$ ) that would have been in a reactor volume  $V$  otherwise. The sludge growth rate is a measure for the solids retention time  $\theta_X$ , since  $\theta_X$  is the inverse of  $\mu$ . The net sludge growth yield ( $Y_{n,COD}$ ), being the mass of cell dry weight (MLVSS) grown per mass of consumed substrate (COD), incorporating sludge decay, can be calculated using

$$Y_{n,COD} = \frac{V \cdot \bar{X} \cdot \mu}{(\bar{S}_0 - \bar{S}) \cdot \bar{Q}_{in}}, \quad (3.6)$$

with  $\bar{Q}_{in}$  the net influent flow rate ( $\text{L d}^{-1}$ ) and  $(\bar{S}_0 - \bar{S})$  the average COD removal between time  $t$  and  $t - \Delta t$  ( $\text{g COD L}^{-1}$ ), since  $S_0$  and  $S$  are the influent and effluent substrate concentrations ( $\text{g COD L}^{-1}$ ), respectively. The numerator represents the amount of sludge grown per day ( $\text{g MLVSS d}^{-1}$ ), while the denominator is given by the amount of substrate removed per day ( $\text{g COD d}^{-1}$ ). Substituting Equation 3.5 yields

$$Y_{n,COD} = \frac{V \cdot (X(t) - X(t - \Delta t)) + \bar{X} \cdot \bar{Q}_w \cdot \Delta t}{(\bar{S}_0 - \bar{S}) \cdot \bar{Q}_{in} \cdot \Delta t}. \quad (3.7)$$

If the yield ( $Y_{COD}$ ) would be known, the amount of nitrogen removed through microbial uptake and immobilisation in the cell biomass ( $N_{immob}$ ,  $\text{g d}^{-1}$ ) can be calculated using

$$N_{immob} = (\bar{S}_0 - \bar{S}) \cdot \bar{Q}_{in} \cdot Y_{COD} \cdot 0.08 \frac{\text{g N}}{\text{g biomass}}, \quad (3.8)$$

About 0.08 g nitrogen is required for every g of biomass grown [Rittmann, 2001].  $N_{immob}$  can be calculated in another way when the amount of sludge removed ( $\Delta X$ ,  $\text{g d}^{-1}$ ) is known, by using

$$N_{immob} = 0.08 \frac{\text{g N}}{\text{g biomass}} \cdot \Delta X = 0.08 \frac{\text{g N}}{\text{g biomass}} \cdot \bar{X} \cdot \bar{Q}_w. \quad (3.9)$$

From Equations 3.8 and 3.9, the yield can be inferred. The yield and net yield are related through Equation 3.10, where  $b$  is the biomass decay rate ( $\text{d}^{-1}$ ) and  $q$  is the specific substrate removal rate ( $\text{g COD g}^{-1} \text{MLVSS d}^{-1}$ ). The decay rate  $b$  is the only unknown variable and can therefore be calculated.

$$Y_{n,COD} = Y_{COD} - \frac{b}{q} = Y_{COD} - b \cdot \left( \frac{(\bar{S}_0 - \bar{S}) \cdot \bar{Q}_{in}}{\bar{X}} \right)^{-1} \quad (3.10)$$



The expected biomass concentration can then be calculated using Equation 3.11, while the required reactor volume for a desired sludge concentration can be calculated by using Equation 3.12, with  $\bar{t}$  the ratio of HRT to SRT ( $\theta_H/\theta_X$ ).

$$X_{expected} = \frac{Y_{COD} \cdot \bar{Q}_{in} \cdot (\bar{S}_0 - \bar{S})}{(1 + b \cdot \theta_X) \cdot \bar{t}} \quad (3.11)$$

$$V_{required} = \frac{Y_{COD} \cdot \bar{Q}_{in} \cdot \theta_X \cdot (\bar{S}_0 - \bar{S})}{X_{desired} \cdot (1 + b \cdot \theta_X)} \quad (3.12)$$

## 3.5 Disinfection assessment methodology

### 3.5.1 *E. coli* removal efficiency

To assess disinfection performance, a known concentration of *E. coli* LMG 8063 (ATCC 8739) was spiked to the synthetic greywater influent. Three spike test were performed: two on the polymeric membranes during part two of Phase II and one for the ceramic membranes, UV, and electrochemical cell (EC) of Driesen [2021] during Phase III (Table 3.5). The total chlorine concentration for the EC was 0.77 mg Cl<sub>2</sub> L<sup>-1</sup>, determined with Standard Methods 4500-Cl G [APHA, 2017] using a Lightwave II UV-vis Spectrophotometer (Biochrom WPA).

For the first spike test on the polymeric membranes, MacConkey agar was used based on Standard Method 9222 B [APHA, 2017]. Standard Method 9222 B is a standard total coliform procedure using, in this case, MacConkey agar. A spread plate method was used contrary to the membrane filter method of Standard Method 9222 B, by adding 100 µL of sample and spreading. The influent was spiked to a concentration of 10<sup>8</sup> CFU 100 mL<sup>-1</sup> *E. coli* as total coliforms (Table 1.3). Total coliform counts for the influent and effluent were determined, for both blank and spiked influent.

The second spike test was used to compare three different methods (on MacConkey, m-FC and CCA agars) for their efficacy of *E. coli* strain LMG 8063 detection. These methods are the Standard Methods 9222 B and D, and the ISO 9308–1:2014 method [APHA, 2017; ISO, 2014]. Standard Method 9222 D is a membrane filter method for thermotolerant (faecal) coliforms using m-FC agar. The ISO 9308–1:2014 method is based on membrane filtration using coliform chromogenic agar (CCA). All three methods were adapted as spread plate methods, by adding 20 µL sample to the respective agar plate and spreading. Total coliform counts for the influent, effluent and effluent after disinfection were determined, with an influent spike of 10<sup>8</sup> CFU 100 mL<sup>-1</sup>. Two duplicates were used per MBR per sample point (four in total per sample point). No blanks were analysed.

The third spike test on ceramic membranes, UV, and EC was performed using CCA. The spike was performed as before for the second spike test for the polymeric membranes, but no duplicates were taken per MBR. Separate spikes were performed for the UV and EC using the unspiked effluent. For the UV, additional spike solutions of 10<sup>4</sup>, 10<sup>8</sup>, and 10<sup>10</sup> CFU 100 mL<sup>-1</sup> were prepared. For the UV and EC samples, 10 and 100 mL were filtered according to the ISO 9308–1:2014 method using sterile membrane filters with a 0.45 µm pore size (Millipore S-Pak) and a stainless steel filter holder (Microsart Manifold) disinfected with EtOH and rinsed with a phosphate buffered saline solution (PBS).

All operations (*e.g.*, media preparation and plating) were performed using standard sterile microbial techniques. The selected *E. coli* strain was inoculated on MacConkey agar to obtain a pure culture plate, incubated for 24 hours at 37°C, and stored at 4°C until further use. A single isolated colony from the pure culture plate was used to inoculate casein peptone and soybean flour peptone broth (CASO broth) in two steps, starting at 10 mL CASO broth in a falcon tube. Fully grown CASO broth was determined to contain  $3.27 \cdot 10^{11}$  CFU 100 mL<sup>-1</sup> of *E. coli*. Therefore, to obtain approximately  $10^8$  CFU 100 mL<sup>-1</sup> of *E. coli* as total coliforms in 120 L synthetic greywater (Section 3.2), a final volume of 40 mL CASO broth is needed after the second growth step. For both steps, the CASO broth was allowed to incubate overnight at 37°C in a shaker. When the media was fully grown, the falcon tubes were centrifuged at 1500 rcf (relative centrifugal force) for 5 minutes using an Eppendorf centrifuge 5430. The obtained pellets were subjected to three washing steps using PBS, followed by vortexing and centrifugation. The final *E. coli* solution was stored at 4°C until further use.

The falcon tubes containing *E. coli* were added to a full 120 L greywater drum. The samples were taken 1 HRT later for the first spike test and 1.5 HRT later for the latter two spike tests (Section 3.2). For all samples of the influent, effluent, and effluent after disinfection, 2 to 4 dilutions were prepared in microwell plates using PBS as diluent, with the dilution factor dependent on the expected *E. coli* concentrations. Plating was performed as described above. The MacConkey and CCA agar were incubated for 24 hours at 37°C, and the m-FC for 24 hours at 44.5°C. The measured plate counts were used to calculate *E. coli* concentrations, and LRV were calculated using Equation 1.1.

## 3.5.2 UV reactor characterization

### 3.5.2.1 UV reactor residence time

The theoretical residence time ( $\tau$ ), being the HRT of the UV reactor, can be determined by dividing the reactor volume by the flow rate. The UV reactor volume was determined by filling both UV reactors twice (4 measurements), measuring the reactor volume by pouring its contents in a measuring cylinder, and taking the average. However, since the HRT does not represent the actual exposure time to UV irradiation, the mean residence time ( $\tau_m$ ) was determined following the book of Fogler [2016]. When applying a step input of a tracer with measurable properties (*e.g.*, concentration, fluorescence, conductivity), the outlet measurement will follow the cumulative residence time distribution (RTD)  $F(t)$ . As the conductivity will be measured by using a salt solution, the cumulative RTD is given by:

$$F(t) = \frac{\kappa(t)}{\int_0^\infty \kappa(t)} = \frac{\kappa(t)}{\kappa_0}, \quad (3.13)$$

with  $\kappa(t)$  the outlet tracer conductivity at time  $t$  and  $\kappa_0$  the maximum tracer conductivity, which is equal to the tracer conductivity at the inlet. A salt solution of 100 mS cm<sup>-1</sup> was prepared by dissolving 10.83 g NaCl in demineralized water ( $\kappa = 0.24$  μS cm<sup>-1</sup>). Conductivity was measured using a HI edge equipped with a HI/63100 conductivity probe (Hanna Instruments). For the step tracer experiment, the UV reactor was filled with demineralized water (Milli-Q) and a flow rate of 14.25 mL min<sup>-1</sup> was used. Each 4 mL eluted from the system, with a total of 372 mL, was sampled in a glass test tube and measured for conductivity.



Derivation of the cumulative RTD  $F(t)$  yields the residence time distribution function

$$E(t) = \frac{dF(t)}{dt} \quad (3.14)$$

As the derivative is very sensitive to small errors in the conductivity measurements, a moving average was calculated with a window size of 3. The moving average is given by

$$\kappa_{avg}(t) = \frac{\kappa_{t-1} + 2\kappa_t + \kappa_{t+1}}{4}, \quad (3.15)$$

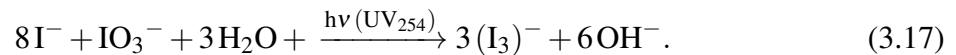
With  $t$  indicating the relevant 4 mL sample,  $t - 1$  the previous sample and  $t + 1$  the next sample. The RTD function  $E(t)$  can provide insight in the type of flow regime, *e.g.*, plug flow, continuously stirred-tank reactor behaviour, dead volumes, and bypasses. The mean residence time  $\tau_m$  is given by

$$\tau_m = \frac{\int_0^\infty t \cdot E(t) dt}{\int_0^\infty E(t) dt} = \int_0^\infty t \cdot E(t) dt, \quad (3.16)$$

which can provide further insights in the reactor flow regime when comparing to the theoretical residence time  $\tau$ .

### 3.5.2.2 UV dose determination

The dose determination was performed by iodide-iodate actinometry [Müller *et al.*, 2014; Rahn, 1997; Rahn *et al.*, 2003]. When exposed to UV<sub>254</sub> irradiation, triiodide is formed in the following reaction:



A solution of iodide-iodate consisting of 0.6 M KI, 0.1 M KIO<sub>3</sub> and 0.01 M borax (Na<sub>2</sub>B<sub>4</sub>O<sub>7</sub> · 10H<sub>2</sub>O) was prepared by dissolving 49.7990 g KI, 10.6997 g KIO<sub>3</sub> and 1.9069 g borax in 500 mL demineralized water (Milli-Q), using a volumetric flask. The prepared iodide-iodate solution was measured before irradiation at a wavelength of 300 nm using a UV-1600PC spectrophotometer (VWR) and a quartz cuvette with path length of 1 cm. This gives an additional measure of the iodide concentration, using

$$c_{\text{KI}} = \frac{1.061 M}{A_{300}}, \quad (3.18)$$

with  $c_{\text{KI}}$  the concentration of potassium iodate in the solution (M), and  $A_{300}$  the absorbance at 300 nm (unitless). The UV reactor was pre-rinsed with demineralized water and the actinometric solution was pumped through the reactor at a flow rate of 14.25 mL min<sup>-1</sup>, which is the same as for the residence time determination. The irradiated solution was sampled after 1.5  $\tau_m$  (Subsection 3.5.2.1), to ensure adequate mixing and steady-state. The UV<sub>254</sub> dose on a volumetric basis  $D_v$  (J L<sup>-1</sup>) can be calculated by measuring the absorbance of the solution at 352 nm before and after irradiation in the UV reactor, using Equation 3.19. The UV dose is traditionally expressed in J cm<sup>-2</sup>, which can be calculated from the volumetric dose ( $D_v$ ) using Equation 3.20.

$$D_v = \frac{E_{254} \cdot \Delta A_{352}}{l \cdot \varepsilon \cdot \Phi} \quad (3.19)$$

$$D = I \cdot \tau_m = \frac{D_v \cdot V_{UV \text{ reactor}}}{A_{surface}} \quad (3.20)$$

With  $D_v$  the volumetric UV dose ( $\text{J L}^{-1}$ ),  $D$  the UV dose ( $\text{J cm}^{-2}$ ),  $E_{254}$  the photon energy at 254 nm ( $\text{J einstein}^{-1}$ ),  $\Delta A_{352}$  the absorbance difference at 352 nm before and after radiation,  $l$  the cuvette path length (cm),  $\varepsilon$  the molar absorption coefficient for the iodide-iodate solution ( $\text{M}^{-1} \text{cm}^{-1}$ ),  $\Phi$  the quantum yield for the iodide-iodate solution ( $\text{mol Einstein}^{-1}$ ),  $I$  the lamp radiation intensity ( $\text{mW cm}^{-2}$ ),  $\tau_m$  the mean residence time (s),  $V_{UV \text{ reactor}}$  the reactor volume (L), and  $A_{surface}$  the surface area exposed to UV radiation ( $\text{cm}^2$ ).

The photon energy at 254 nm ( $E_{254}$ ) can be determined using the Planck-Einstein relation (Equation 3.21), with the speed of light  $c$  being  $3 \cdot 10^8 \text{ m s}^{-1}$ , and Planck's constant  $h$  being  $6.6262 \cdot 10^{-34} \text{ J s}$  [French and Taylor, 1978]. For a wavelength  $\lambda$  of 254 nm ( $2.54 \cdot 10^{-7} \text{ m}$ ), the photon energy  $E_{254}$  will be  $7.83 \cdot 10^{-19} \text{ J}$ . Expressed per moles of photons (einsteins), this becomes  $4.71 \cdot 10^5 \text{ J einstein}^{-1}$ .

$$E_\lambda = h\nu = \frac{hc}{\lambda} \quad (3.21)$$

The reactor volume ( $V_{reactor}$ ) and mean residence time ( $\tau_m$ ) were determined as described in Subsection 3.5.2.1. A cylindrical shape of the lamp casing was assumed to calculate the exposed surface area  $A_{surface}$ . Both the area of the lower base and the mantle of the cylinder up to the water level were included.

The molar absorption coefficient  $\varepsilon$  for a iodide-iodate solution containing 0.6 M KI was determined to be  $27600 \text{ M}^{-1} \text{cm}^{-1}$  by Rahn *et al.* [2003]. The quantum yield  $\Phi$ , being the moles of triiodide formed per moles of photons absorbed (einsteins), is 0.75 at a KI concentration of 0.577 M and a temperature of  $20.7^\circ\text{C}$  [Rahn, 1997]. To correct for different concentrations and temperatures, Equation 3.22 can be used, for which the KI concentration ( $c_{\text{KI}}$ ) was determined as described above, and the average temperature measurement ( $T_{avg}$ ) between the sample before and after irradiation was used.

$$\Phi = 0.75 (1 + 0.02 (T_{avg} - 20.7)) (1 + 0.23 (c_{\text{KI}} - 0.577)) \quad (3.22)$$

Furthermore, the lamp intensity  $I$  was estimated using both Equation 3.20 and by dividing the lamp power output at 254 nm by the estimated surface area. Transmission effects of the lamp casing or reflection effects of the aluminium reactor lining were not accounted for.

# 4

## Results

### 4.1 Synthetic greywater characterization

The synthetic greywater was characterized to validate the correctness of using it as a substitute for real GW. The composition of fresh GW and of the influent after storage in the 120 L drum can be found in Table 4.1. Both total nitrogen (TN) and the chemical oxygen demand (COD) of the synthetic greywater prepared with demineralized water (Milli-Q) were close to the calculated values in Table 3.1. The tap water used only added a small amount of COD (1.2%), but the TN contribution was more significant (12.7%).

The tap water was a major contributor of  $K^+$ ,  $Ca^{2+}$ ,  $Mg^{2+}$ ,  $NO_3^-$ -N, and  $SO_4^{3-}$  to the (expected) fresh greywater composition.  $Na^+$  and  $Cl^-$  were mainly provided by the chemical compounds added in the synthetic GW, since they can be found in the majority of the added salts as counterions. Ammonium was provided almost exclusively through the addition of  $NH_4Cl$ . It is important to note that no  $PO_4^{3-}$  was detected in both the fresh GW (Milli-Q) and the tap water ( $<0.1 \text{ mg L}^{-1}$ ), despite  $1.6 \text{ mg L}^{-1}$  being added through  $K_2HPO_4$ . It is possible that the phosphate was precipitated by organics or other chemicals present in the detergents and subsequently filtered when preparing the samples for IC analysis (Subsection 1.3.1).

When comparing the measured influent composition after storage in the 120 L drum with the expected concentrations, it is clear that the total COD (tCOD) of the influent was significantly lower than 516 ( $p < 2.2 \cdot 10^{-16}$ ), which indicates that degradation was already occurring (Subsection 1.3.1). Furthermore,  $K^+$ ,  $Ca^{2+}$ , and  $NH_4^+$ -N differ significantly from the expected values ( $p < 2.2 \cdot 10^{-16}$ ), while the TN does not ( $p = 0.3$ ). The nitrogen was mainly present as organic nitrogen (TN – all other species) and ammonium, since  $NO_3^-$ -N and  $NO_2^-$ -N are on average only  $0.2$  and  $0.3 \text{ mg L}^{-1}$ , respectively. Phosphate was, again, not detected in the influent, except in 10 out of 109 measurements.

Table 4.1: Characteristics of fresh greywater and influent. The fresh GW (Tap) represents the sum of the first two columns, *i.e.*, the expected influent concentrations. All values in  $\text{mg L}^{-1}$ , except pH.

	Fresh GW (Milli-Q)	Tap Water	Fresh GW (Tap)	Influent
pH	8.5	8.07		$8.2 \pm 0.3$
COD	510	6	516	$395 \pm 83$
TN	22	3.2	25.2	$25 \pm 3$
$NH_4^+$ -N	20.8	$<0.2$	20.8	$16 \pm 2$
$NO_2^-$ -N	$<0.03$	$<0.03$	$<0.03$	$<0.03 - 1.3$ (0.3)
$NO_3^-$ -N	0.4	5.7	6.1	$<0.02 - 2.2$ (0.2)
$PO_4^{3-}$	$<0.1$	$<0.1$	$<0.1$	$<0.1 - 6.1$ (0.6)
$Na^+$	175.1	54.0	229.1	$185.6 - 282.2$ (220.3)
$K^+$	2.7	7.3	10.0	$4.9 - 10.1$ (6.9)
$Ca^{2+}$	18.7	121.2	139.8	$57.8 - 116.2$ (79.4)
$Mg^{2+}$	0.5	12.6	13.1	$5.1 - 11.7$ (8.0)
$Cl^-$	109.8	67.4	177.1	$132.0 - 219.6$ (167.4)
$SO_4^{2-}$	46.3	93.6	139.8	$23.3 - 140.2$ (90.5)

The suspended solids content of the influent was measured on day 157 (Phase II). The TSS and VSS concentrations were  $0.67$  and  $0.27 \text{ g L}^{-1}$ , respectively, which is another indication of precipitation, since only powders and liquids were used to prepare the synthetic GW. Furthermore, the turbidity of the influent increased for the entire duration of the experiment (Figure 4.1).

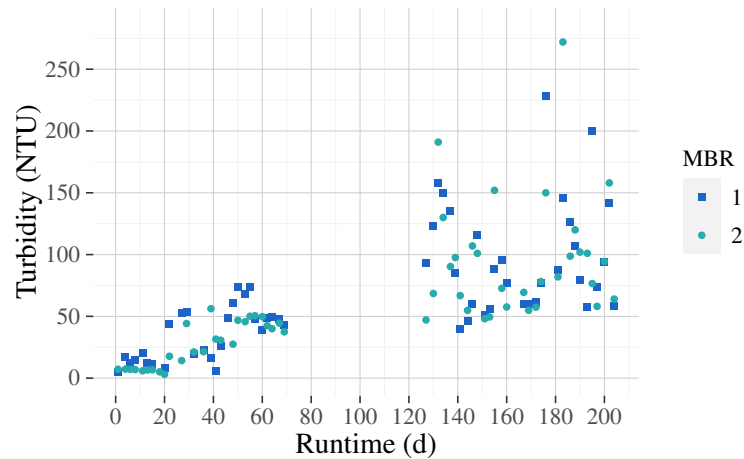


Figure 4.1: Turbidity of the influent during all three phases. NTU: nephelometric turbidity units.

There are clear trends for the influent, which voided the normality assumption so no mean and standard deviation could be given in Table 4.1. Sodium and chloride concentrations were lower ( $p$  both  $< 1 \cdot 10^{-15}$ ) in Phase II and III compared to Phase I. Calcium concentrations were significantly lower ( $p < 2.2 \cdot 10^{-16}$ ) during Phase II compared to Phase I and III. Magnesium, sulphate, and potassium concentrations decreased continuously over time in the ranges given in Table 4.1. Soluble COD (sCOD) was measured for the influent, which was also lower ( $p = 5 \cdot 10^{-10}$ ) in Phase II and III ( $194 \pm 76 \text{ mg L}^{-1}$ ) compared to Phase I ( $293 \pm 40 \text{ mg L}^{-1}$ ) and overall lower than the influent tCOD, although the tCOD showed large variation.

Significant correlations between the turbidity and sodium ( $p = 1 \cdot 10^{-4}$ ), potassium ( $p = 2 \cdot 10^{-5}$ ), calcium ( $p = 3 \cdot 10^{-3}$ ), magnesium ( $p = 4 \cdot 10^{-12}$ ), and sulphate ( $p = 1 \cdot 10^{-13}$ ) concentrations were found, but no significant correlations for sCOD and  $\text{NH}_4^+$  ( $p > 0.05$ ). It is not clear exactly which salts or organics were precipitating to cause the observed differences and trends of sCOD, ammonium, and aforementioned ions since, *e.g.*, magnesium and sulphate have the highest correlation with turbidity, but magnesium sulphite is very soluble in water. However, anoxic conditions prevailed in the influent drum during Phases II and III, which was observed by the slightly noticeable smell of  $\text{H}_2\text{S}$ . Therefore, different speciation may occur compared to fresh influent, which influences precipitation behaviour.

A comparison between the synthetic GW and real mixed GW can be found in Table 4.2, with the values for mixed GW taken from literature (Table 1.2). All values were situated approximately in the reported ranges, with high concentrations for pH,  $\text{NH}_4^+\text{-N}$ , and especially  $\text{Cl}^-$ .

Table 4.2: Comparison between the synthetic greywater used in this study and real mixed greywater compiled from literature.

Parameter		This study		Mixed GW <sup>a</sup>
pH		7.41 – 8.72	(8.16)	4.9 – 8.41
$\kappa$	( $\mu\text{S cm}^{-1}$ )	1091 – 1730	(1280)	331 – 2530
Turbidity	(NTU)	3.12 – 272	(66.2)	29 – 559
tCOD	( $\text{mg L}^{-1}$ )	225 – 623	(395)	41.0 – 1595
sCOD	( $\text{mg L}^{-1}$ )	100 – 389	(231)	86 – 289
BOD <sub>5</sub>	( $\text{mg L}^{-1}$ )			17.7 – 394
TOC	( $\text{mg L}^{-1}$ )	11.7 – 117	(50.0)	15.0 – 160.4
TC	( $\text{mg L}^{-1}$ )	87.8 – 193	(146)	
IC	( $\text{mg L}^{-1}$ )	62.0 – 143	(96.5)	
TN	( $\text{mg L}^{-1}$ )	19 – 36	(25)	1.3 – 63
TKN	( $\text{mg L}^{-1}$ )			2.6 – 32
NH <sub>4</sub> <sup>+</sup> -N	( $\text{mg L}^{-1}$ )	9.4 – 22.1	(16.2)	0.1 – 22
NO <sub>2</sub> <sup>-</sup> -N	( $\text{mg L}^{-1}$ )	<0.03 – 1.3	(0.3)	
NO <sub>3</sub> <sup>-</sup> -N	( $\text{mg L}^{-1}$ )	<0.02 – 2.2	(0.2)	0 – 12.32
TP	( $\text{mg L}^{-1}$ )			1 – 12.1
PO <sub>4</sub> <sup>3-</sup> -P	( $\text{mg L}^{-1}$ )	<0.03 – 1.4	(0.1)	0.0 – 6.7
TSS	( $\text{mg L}^{-1}$ )		670	9.2 – 744
VSS	( $\text{mg L}^{-1}$ )		270	9.2 – 149.8
Na <sup>+</sup>	( $\text{mg L}^{-1}$ )	185.6 – 282.2	(220.3)	52 – 420
Ca <sub>2</sub> <sup>+</sup>	( $\text{mg L}^{-1}$ )	57.8 – 116.2	(79.4)	9 – 437.61
Mg <sub>2</sub> <sup>+</sup>	( $\text{mg L}^{-1}$ )	5.1 – 11.7	(8.0)	3 – 140.01
K <sup>+</sup>	( $\text{mg L}^{-1}$ )	4.9 – 10.1	(6.9)	0 – 22
Cl <sup>-</sup>	( $\text{mg L}^{-1}$ )	132.0 – 219.6	(167.3)	18 – 50

<sup>a</sup> Abdel-Shafy and Al-Sulaiman [2014]; Atanasova *et al.* [2017]; Fountoulakis *et al.* [2016]; Hernández Leal *et al.* [2010]; Hocaoglu *et al.* [2013]; Hourlier *et al.* [2010]; Jabornig and Favero [2013]; Jabornig and Podmirseg [2015]; Masi *et al.* [2016]; Oteng-Peprah *et al.* [2018]; Ramprasad *et al.* [2017]

## 4.2 Phase I: troubleshooting and optimization

As mentioned before, Phase I of reactor operation with the polymeric membranes is characterized by heavy optimization and problems with the mixed liquor suspended solids (MLSS) quality and quantity (Subsection 3.2). Therefore, Phase I will be discussed separately, while the comparison between polymeric and ceramic membranes will be based on Phases II and III.

### 4.2.1 Sludge related problems

Both reactors were inoculated at  $1 \text{ g MLSS L}^{-1}$ . During the first 15 days, 5 overflow events occurred in MBR 1, *i.e.*, the effluent flow rate was too low, causing excessive overflow and sludge loss of often more than half the MLSS content (Figures 4.2a and B.6). If this occurred, both reactor contents were mixed, causing a decrease in MBR 2 MLSS as well. The cause of the overflow events was an airstone in MBR 1 that was broken, which only caused air bubbling in one location of the stone, and none for the second stone. Thus, membrane air scouring was not sufficient, which caused higher transmembrane pressures. The tubing connections of the effluent were initially not air-tight, leading to air intrusion at higher pressures, loss of effluent flow rate and excessive overflow. This excessive overflow lowered MLSS concentrations, leading to dispersed growth (fine sludge particles) since only the fastest growing micro-organisms could persist, which are not necessarily good floc-formers [Rittmann, 2001]. This in turn caused even higher transmembrane pressures (Figure 4.3).

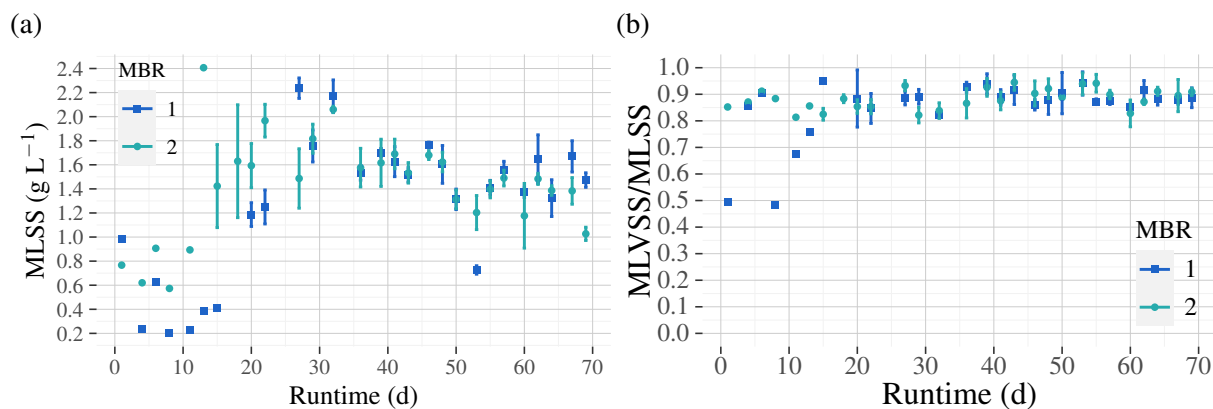


Figure 4.2: MLSS (a) and MLVSS (b) content of the MBRs during Phase I.

Tightening the connections and introducing a relaxation regime caused sludge concentrations to increase to about  $1.6 \text{ g MLSS L}^{-1}$  and pressures to normalize after day 15. However, the MLSS content was still lower than that of an activated sludge system (generally  $4 \text{ g MLSS L}^{-1}$ ), and especially low for MBRs (Rittmann [2001] and Table 1.6). The ratio of mixed liquid volatile suspended solids (MLVSS) to MLSS was sufficiently high ( $>0.8$ ). After stabilisation, the calculated sludge and volumetric loading rates (SLR and VLR) using Equations 3.3 and 3.4 were  $0.5 \pm 0.1 \text{ kg COD kg}^{-1} \text{ MLVSS d}^{-1}$  and  $0.7 \pm 0.1 \text{ kg COD kg}^{-1} \text{ MLVSS d}^{-1}$ , respectively. Since the SLR and VLR for typical activated sludge (AS) treatment of raw domestic wastewater are usually around  $0.25 \text{ kg bCOD kg}^{-1} \text{ MLVSS d}^{-1}$  and  $1 \text{ kg bCOD kg}^{-1} \text{ MLVSS d}^{-1}$  [Rittmann, 2001], the reactor biomass does not seem limited in terms of substrate in such a way that the MLSS would be expected lower than that of a typical AS system. It should

be noted that the biodegradable fraction of the COD (bCOD) is not known for this synthetic greywater. However, since the majority of the COD is provided by acetate (60%), the fraction biodegradable COD ( $F_b$ , bCOD/COD) is expected to be very high. Even with an  $F_b$  of 0.6, the biomass would not be more substrate limited than in an AS system.

The COD:TN:P ratio of the influent for all three phases was 100:4.9:0.3–100:10.5:0.7 (100:6.3:0.4), with the values for phosphorus assumed to be the added phosphate in the synthetic greywater, not accounting for precipitation. However, additional phosphorus is added with the detergents as, *e.g.*, phosphonates in the dishwasher tablets and liquid laundry detergent. If the phosphate precipitate in the influent is bioavailable, there is no immediate indication of nutrient deficiency.

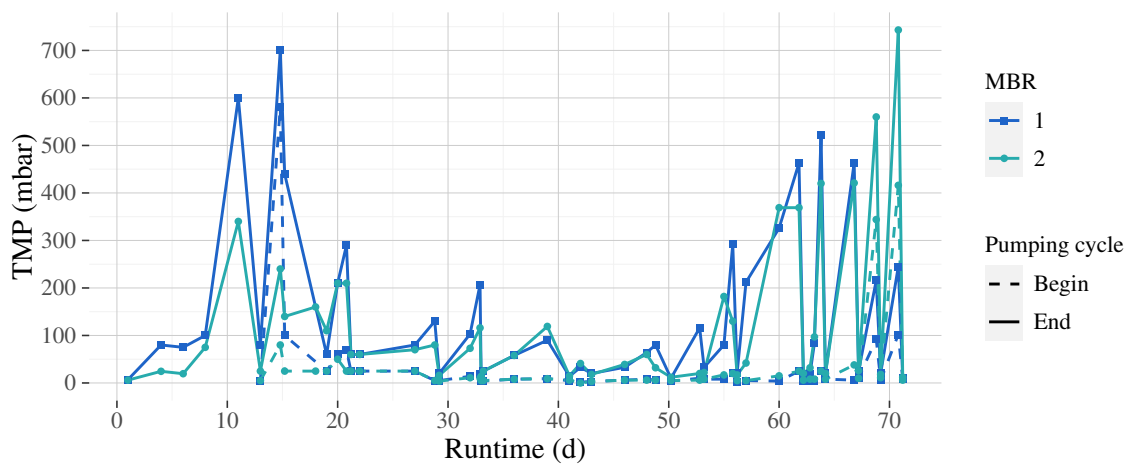


Figure 4.3: Transmembrane pressures (TMP) during Phase I. The pressures at the beginning of the pumping cycle were measured at the end of relaxation, while the pressures at the end of the pumping cycle were measured just before relaxation.

During the stable operation (Day 15–46), sludge bulking was observed, which was later found to be caused by excessive aeration. There was no effect on membrane performance. Towards the end of Phase I, the recovery was accidentally set to 80%. This caused a very low sludge retention time of 2.9 days and excessive sludge wastage. Combined with the excessive aeration, this led again to the formation of dispersed growth, *i.e.*, weak, small flocs with a turbid supernatant, which caused a dramatic increase in transmembrane pressures (Figures 4.3 and B.7). By consequence, the membranes needed to be cleaned nearly every other day. The turbid supernatant was removed (wash-out of non-flocculating cells), the recovery was increased to 98.6%, and the dissolved oxygen concentration was lowered from 9.77 to 2.75 mg O<sub>2</sub> L<sup>-1</sup> whilst still ensuring sufficient air scouring of the membranes. Nevertheless, no improvement of membrane performance and sludge characteristics was observed, which led to the reinoculation of the reactors at the start of Phase II.



## 4.2.2 Treatment performance

The effluent characteristics and removal efficiencies of both MBRs can be found in Table 4.3. High average removal efficiencies for tCOD (92.4%), turbidity (96.3%), and TOC (91.9%) were observed. No significant conductivity or ion concentration shifts occurred besides nitrogen species. Total nitrogen removal was limited to 34.9% on average, while ammonium was mainly removed (77.7%) through nitrification. A comparison between the reactor performances for polymeric and ceramic membranes is more meaningful when reactor operation is more stable and on the same sludge inoculum. Therefore, a more in-depth analysis will be made on the treatment performance results of Phases II and III.

Table 4.3: Treatment performance of both MBRs during Phase I. All values are in  $\text{mg L}^{-1}$ , except pH, the conductivity  $\kappa$  ( $\mu\text{S cm}^{-1}$ ), and the turbidity (NTU).

Parameter	Influent (Phase I)		Effluent (Phase I)		Removal efficiency (%)	
pH	7.41 – 8.56	(8.15)	7.20 – 8.66	(8.08)		
$\kappa$	1123 – 1549	(1353)	849 – 1455	(1311)		
Turbidity	3.12 – 73.7	(30.9)	0.26 – 1.28	(0.57)	83.5 – 99.5	(96.3)
tCOD	225 – 502	(384)	15 – 92	(29)	79.0 – 96.6	(92.4)
TOC	16.6 – 117	(52.8)	0.0 – 26.8	(3.0)	7.4 – 100	(91.9)
TC	87.8 – 186	(146)	44.6 – 112	(83.3)	3.7 – 64.0	(42.0)
IC	67.2 – 114	(93.3)	42.7 – 109	(80.4)	–2.4 – 54.4	(13.5)
TN	20 – 31	(24)	5 – 20.6	(15.7)	0.0 – 77	(35)
$\text{NH}_4^+\text{-N}$	9.4 – 20.7	(17.0)	<0.2 – 17.9	(3.7)	–27.9 – 99.2	(77.7)
$\text{NO}_2^-\text{-N}$	<0.03 – 1.1	(0.2)	<0.03 – 2.5	(0.5)		
$\text{NO}_3^-\text{-N}$	<0.02 – 2.2	(0.2)	<0.02 – 19.1	(8.8)		
$\text{PO}_4^{3-}$	<0.1 – 6.1	(0.3)	<0.1 – 1.6	(0.1)		
$\text{Na}^+$	192.0 – 282.2	(236.1)	97.3 – 287.1	(231.9)		
$\text{Ca}_2^+$	74.8 – 99.6	(84.5)	74.1 – 98.8	(85.2)		
$\text{Mg}_2^+$	8.6 – 11.7	(10.0)	9.0 – 11.5	(10.1)		
$\text{K}^+$	6.4 – 9.0	(7.6)	6.1 – 14.1	(8.1)		
$\text{Cl}^-$	157.8 – 219.6	(187.0)	101.3 – 214.7	(182.6)		
$\text{SO}_4^{3-}$	60.8 – 140.2	(119.3)	78.2 – 143.6	(125.0)		

## 4.3 Phase II and III: polymeric and ceramic membrane testing

Phase II and III were characterized by a more stable operation in terms of transmembrane pressures and the installation of the ceramic membranes on day 165, starting Phase III. All comparisons between the two membrane types will be based on these results. Since MBR 1 was the most stable, only the treatment performance results of this reactor will be shown in figures, although both reactors showed no noticeable differences for treatment performance, except a difference in trends for TOC and IC (Subsection 4.3.3). The reason for this is to declutter the figures both in contents and quantity of figures.

### 4.3.1 Sludge characteristics during operation and kinetics

After reinoculation on day 96, the MBRs maintained a higher MLSS content of about 2.25 to 3 g MLSS L<sup>-1</sup> (Figure 4.4a). However, MBR 2 showed a decrease in sludge concentration. This was caused by differences in flow rates and was usually fixed by replacing the pump tubing. However, the pump tubing flow rate degrades over the course of two weeks in the order of about 0.08 mL min<sup>-1</sup> d<sup>-1</sup>, and the pump heads themselves could differ 0.3 mL min<sup>-1</sup>. Therefore, two effluent pumps were installed on day 165, the two reactors were mixed, and pump recalibration was performed on every sampling day since.

The calculated SLR and VLR were  $0.3 \pm 0.1$  kg COD kg<sup>-1</sup> MLVSS d<sup>-1</sup> and  $0.7 \pm 0.2$  kg COD m<sup>-3</sup> d<sup>-1</sup>, respectively. The lower SLR is caused by an increase in MLVSS concentration relative to Phase I. Therefore, the SLR is now closer to that of a conventional AS system [Rittmann, 2001]. Between day 184 and 186 (weekend), the influent mesh filter of MBR 1 was clogged. The reactor content of MBR 1 decreased to 2 L, since no influent was provided and the membranes remained operational. The 2 MBRs were mixed and refilled with overflow from the 10 L plastic overflow vessel, which caused an increase in sludge concentration to about 3 to 3.75 g MLSS L<sup>-1</sup> (Figure 4.4a). This increase was temporary, since the increase in MLVSS content caused a significant decrease in SLR ( $p = 2 \cdot 10^{-5}$ ) to a value of  $0.23 \pm 0.04$  kg COD kg<sup>-1</sup> MLVSS d<sup>-1</sup>, limiting sludge growth.

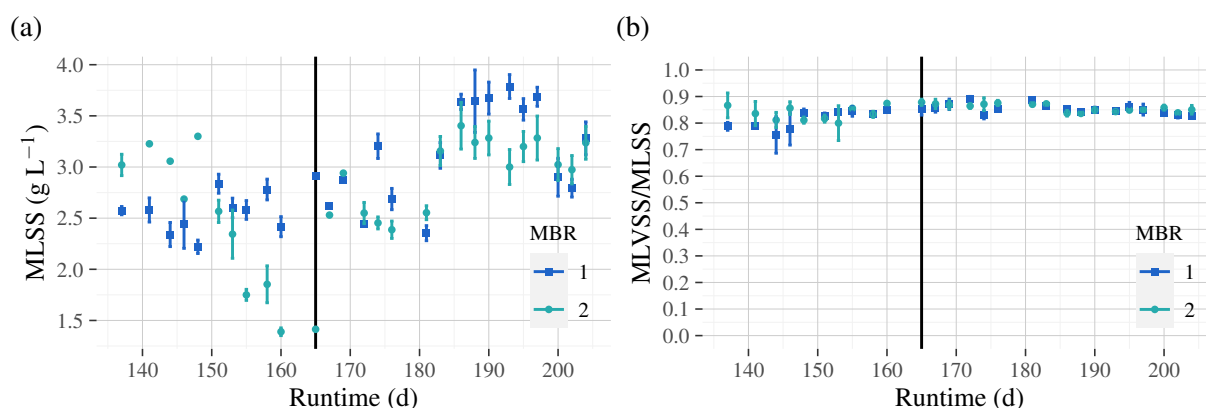


Figure 4.4: MLSS (a) and MLVSS (b) content of the MBRs during Phase II and III. The ceramic membranes were installed on day 165, indicated by the vertical line.

The sludge specific growth rate  $\mu$  was calculated for MBR 1 using Equation 3.5, since the effluent flow rate and thereby sludge overflow was not accurate for MBR 2 during Phase II. The two data points when the overflow was added back into the reactor were not taken into account. The average sludge growth rate was calculated to be  $0.086 \text{ d}^{-1}$ , which relates to a sludge retention time of 11.6 days ( $\mu = \theta_x^{-1}$ ). This is equal to the setpoint of 11.6 days (Table 3.5). Indeed, at steady state without inhibition,  $X(t)$  will equal  $X(\Delta t)$  on average, so Equation 3.5 reduces itself to the inverse of the definition of the sludge retention time. The net sludge growth yield ( $Y_{n,COD}$ ) was calculated using Equation 3.7 and was found to be on average  $0.34 \text{ g MLVSS g}^{-1} \text{ COD}$ , which is in line with typical growth yields of AS [Rittmann, 2001]. The nitrogen removal through immobilization was estimated using Equation 3.9 to be  $0.20 \text{ g N d}^{-1}$ . The growth yield ( $Y_{COD}$ ) was inferred using Equation 3.8 and was found to be  $0.38 \text{ g MLVSS g}^{-1} \text{ COD}$ . The average specific substrate removal rate  $q$  was  $2.7 \text{ g COD g}^{-1} \text{ MLVSS d}^{-1}$  (Equation 3.10). The biomass decay coefficient  $b$  is then  $0.02 \text{ d}^{-1}$ , which is relatively low [Rittmann, 2001], providing no indication of excessive die-off due to the detergents in the GW.

The expected sludge concentration computed using Equation 3.11 was on average  $2.43 \text{ g MLVSS L}^{-1}$ , which corresponds to roughly  $2.9 \text{ g MLSS L}^{-1}$  (Figure 4.4b) and is close to the observed values (Figure 4.4a). Should a sludge concentration of  $4 \text{ g MLSS L}^{-1}$  (AS, Rittmann [2001]) or  $12 \text{ g MLSS L}^{-1}$  (MBR, Judd [2011]; Park *et al.* [2015]) be ideal, reactor volumes of respectively  $5.2 \text{ L}$  and  $1.7 \text{ L}$  would be feasible compared to the reactor volume of  $10 \text{ L}$  used for the experiments (Equation 3.12). This would give rise to respective HRTs of  $7.2$  and  $2.4$  hours, which would still be sufficient to ensure adequate treatment performance [Judd, 2011; Park *et al.*, 2015].

### 4.3.2 Membrane performance

During Phase II, the transmembrane pressures for the polymeric membranes followed the expected pattern of exponential transmembrane pressure increase after cleaning (Figure 4.5, Park *et al.* [2015]). Cleaning was performed manually by gently wiping off the sludge cake, on average every 6.2 days. The ceramic membranes were installed on day 165 (Phase III). After day 180, the pressures increased from around  $7 \text{ mbar}$  to  $25 \text{ mbar}$  due to the increased MLSS concentration (Figure 4.4a). The ceramic membrane of MBR 1 was cleaned once by gently wiping off the filter cake, due to the clogging of the mesh filter of the influent mentioned before. No cleaning was performed for MBR 2. The TMP for the ceramic membranes were generally lower than the TMP for the polymeric membranes (Figure 4.5).

To compare the membrane materials in terms of fouling rate, each cleaning cycle of the polymeric membranes was overlapped, the fouling resistance  $R_f$  was calculated using the gross flux for Equation 1.3, and the initial cleaned membrane resistance taken as  $R_m$  (Figure 4.6a). The average linear fouling rate  $dR_f/dt$  was found to be  $4.6 \cdot 10^{11} \pm 0.9 \cdot 10^{11} \text{ m}^{-1} \text{ d}^{-1}$  ( $p = 5 \cdot 10^{-6}$ ,  $R^2 = 0.43$ ). Due to the exponential nature of fouling development [Gitis and Rothenberg, 2016; Park *et al.*, 2015], high deviations from linear behaviour were found more than 5 days after cleaning (Figure 4.6a). When only looking at the quasi-linear part of membrane fouling ( $<5$  days), the fouling rate was on average  $3.7 \cdot 10^{11} \pm 0.4 \cdot 10^{11} \text{ m}^{-1} \text{ d}^{-1}$  ( $p = 4 \cdot 10^{-9}$ ,  $R^2 = 0.70$ ).

For the ceramic membranes, deviations from the linear behaviour were observable, but this was caused by the temporary increase in sludge concentration (Figure 4.6b). The TMP increase for MBR 1 caused by the mesh filter clogging was not taken into account. After the MLSS content of the reactors decreased, the fouling rate resumed quasi-linear behaviour. Ignoring the temporary increase, the linear fouling rate was  $5.4 \cdot 10^{10} \pm 0.5 \cdot 10^{10} \text{ m}^{-1} \text{ d}^{-1}$  ( $p = 7 \cdot 10^{-11}$ ,  $R^2 = 0.79$ ), which is a factor 6.85 lower than the fouling rate of the polymeric membranes.

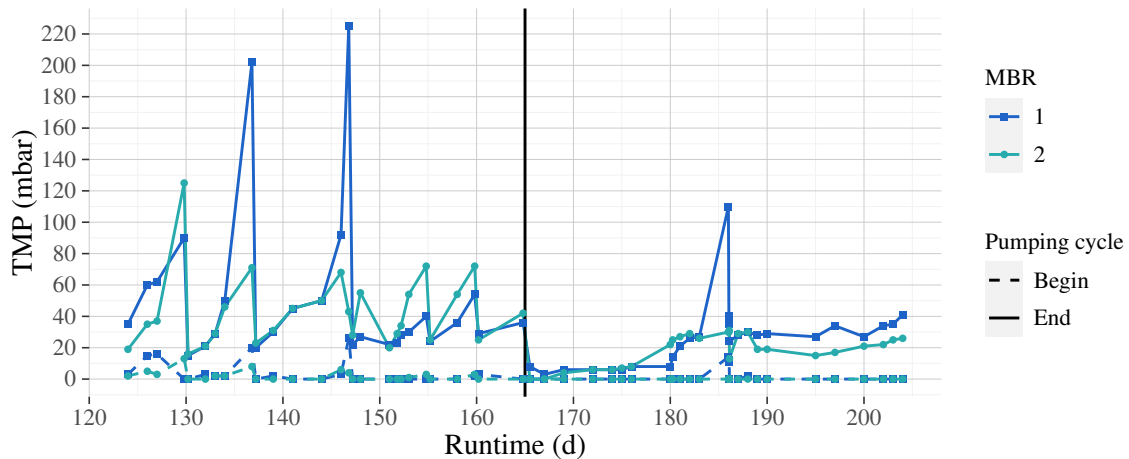


Figure 4.5: Transmembrane pressures (TMP) during Phases II and III. The pressures at the beginning of the pumping cycle were measured at the end of relaxation, while the pressures at the end of the pumping cycle were measured just before relaxation. The ceramic membranes were installed on day 165, indicated by the vertical line.

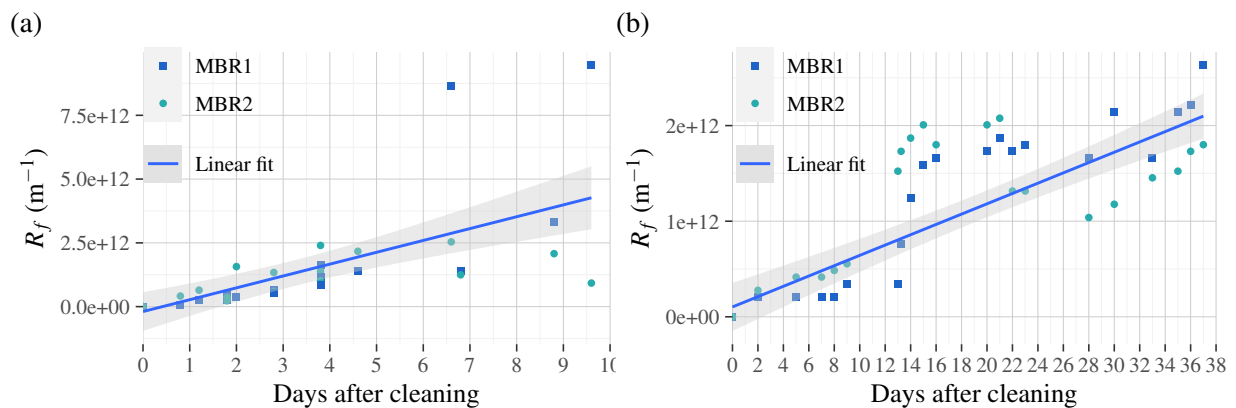


Figure 4.6: The fouling rates in terms of fouling resistance increase  $R_f$  for the polymeric (a) and ceramic (b) membranes. Note the difference in x- and y-axis scales.

### 4.3.3 Treatment performance

The effluent characteristics and removal efficiencies of both MBRs for Phases II and III can be found in Table 4.4. The performance was much higher compared to Phase I except for TOC, TC, and IC. Both polymeric and ceramic membranes showed high turbidity removal efficiencies (98.9% and 99.2%, respectively) with no significant difference ( $p = 0.13$ ), despite the larger pore size of the ceramic membranes. The TSS of the effluent was measured once, but was found to be below the detection limit for both membranes ( $<0.01 \text{ g L}^{-1}$ ). Differences in ions, not including nitrogen species, and conductivity were caused by the trends of the influent as explained in Section 4.1. The pH of the effluent differed on average only 0.1 units, but the difference was significant ( $p = 7 \cdot 10^{-4}$ ).

The tCOD removal of both Phases were very similar, being 95.8% for Phase II and 94.7% for Phase III, although a significant difference of 1% was found ( $p = 0.01$ ). This difference was most likely caused by the addition of the overflowed sludge on day 180 (Figure 4.7a). Indeed, this addition was reflected in a temporary increase of reactor and effluent sCOD (Figure 4.7b). The TN removal rate was on average  $0.20 \text{ g N d}^{-1}$ , which was exactly the same as the previously calculated removal through immobilisation (Subsection 4.3.1). Therefore, the mechanism for TN removal was based on biomass growth and removal, with nitrification of the remaining ammonium in the influent (Figure 4.8). The efficiency of removal was significantly higher ( $p = 0.008$ ) in Phase III (53%) compared to Phase II (43%), which can be seen in Figure 4.8b. A higher MLSS concentration might have led to increased sludge wastage and removal of immobilised nitrogen.

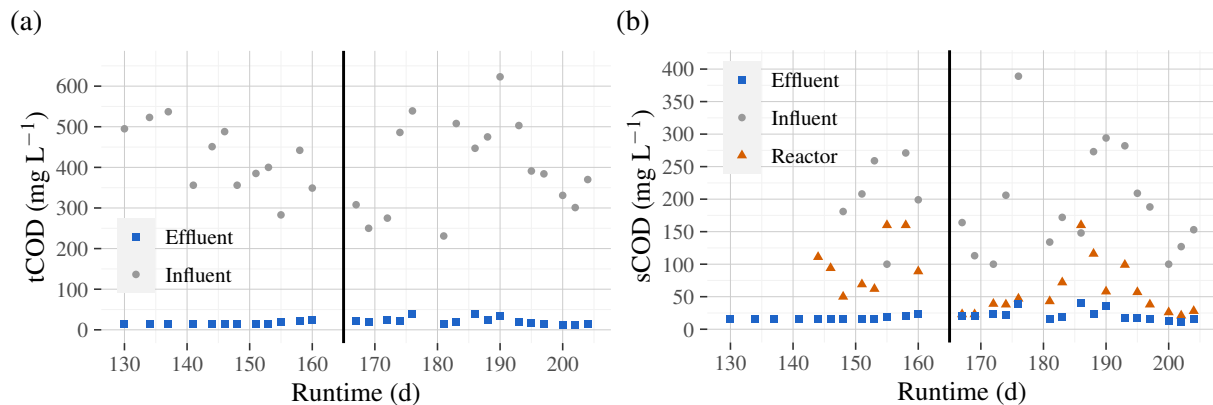


Figure 4.7: The total (a) and soluble (b) COD for MBR 1 during Phase II and III. The ceramic membranes were installed on day 165, indicated by the vertical line. Note the difference in y-axis scale.

Table 4.4: Treatment performance of both MBRs during Phases II and III. All values are in mg L<sup>-1</sup>, except pH, the conductivity  $\kappa$  ( $\mu\text{S cm}^{-1}$ ), and the turbidity (NTU).

Parameter	Influent (Phase II and III)		Effluent (Phase II)		Removal Phase II (%)		Effluent (Phase III)		Removal Phase III (%)	
pH	7.69 – 8.72	(8.17)	7.56 – 8.01	(7.73)			7.62 – 8.12	(7.83)		
$\kappa$	1091 – 1730	(1216)	944 – 1301	(1178)			1005 – 1431	(1107)		
Turbidity	39.8 – 272	(96.8)	0.27 – 3.83	(0.87)	96.1 – 99.7	(98.9)	0.33 – 3.27	(0.83)	98.2 – 99.7	(99.2)
tCOD	231 – 623	(405)	15 – 28	(17)	92.2 – 97.3	(95.8)	10 – 40	(21)	91.1 – 97.3	(94.7)
TOC	7.9 – 149	(56.9)	1.4 – 82.1	(17.4)	–22.6 – 98.5	(68.6)	4.9 – 32.4	(16.8)	8.1 – 86.2	(57.9)
TC	98.5 – 193	(146)	60.9 – 103	(83.3)	3.9 – 62.1	(38.0)	83.5 – 124	(106)	23.0 – 41.0	(31.6)
IC	0.8 – 143	(89.2)	6.6 – 86.3	(65.9)	–24.7 – 89.7	(13.7)	74.8 – 111	(89.0)	–0.2 – 38.6	(20.8)
TN	19 – 36	(25)	9.1 – 20.8	(14.8)	10 – 65	(43)	6.9 – 18.5	(11.6)	29 – 73	(53)
NH <sub>4</sub> <sup>+</sup> -N	14.1 – 28.4	(19.9)	<0.2 – 10.8	(0.8)	48.5 – 99.3	(95.4)	<0.2 – 8.0	(0.8)	55.6 – 99.2	(95.7)
NO <sub>2</sub> <sup>-</sup> -N	<0.03 – 1.3	(0.3)	0.1 – 1.7	(0.4)			0.1 – 3.6	(0.7)		
NO <sub>3</sub> <sup>-</sup> -N	<0.02 – 1.4	(0.1)	0.2 – 18.3	(11.7)			1.6 – 16.1	(8.6)		
PO <sub>4</sub> <sup>3-</sup>	<0.1 – 6.1	(0.8)	<0.1 – 0.2	(0.1)			<0.1 – 4.2	(0.3)		
Na <sup>+</sup>	185.6 – 254.1	(205.1)	142.9 – 221.8	(202.0)			186.0 – 284.8	(203.7)		
Ca <sub>2</sub> <sup>+</sup>	57.8 – 116.2	(74.4)	64.6 – 76.7	(70.8)			57.0 – 128.6	(78.3)		
Mg <sub>2</sub> <sup>+</sup>	5.1 – 10.6	(6.2)	5.5 – 7.2	(6.1)			4.7 – 12.2	(6.2)		
K <sup>+</sup>	4.9 – 10.1	(6.1)	5.7 – 12.1	(6.8)			<0.2 – 16.4	(4.3)		
Cl <sup>-</sup>	132.0 – 174.8	(148.8)	111.7 – 163.4	(149.7)			132.8 – 216.1	(147.1)		
SO <sub>4</sub> <sup>3-</sup>	23.3 – 96.3	(63.3)	72.9 – 95.7	(87.2)			47.6 – 91.9	(70.2)		

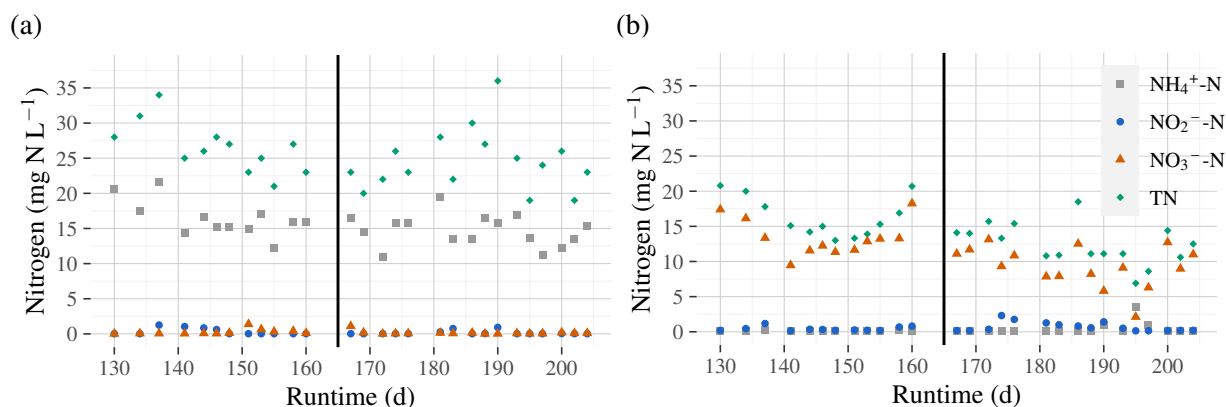


Figure 4.8: The nitrogen speciation for the influent (a) and effluent (b) of MBR 1 during Phase II and III. The ceramic membranes were installed on day 165, indicated by the vertical line.

During Phase II, the TOC of the influent showed a steady increase, while the IC continuously decreased. After replacement of the influent pump tubing on day 166, the values returned to the normal levels observed in MBR 2 and Phase I. No similar pattern was seen for the influent of MBR 2, which is peculiar, since both influent pumps were connected to the same storage drum. Therefore, a comparison between the removal efficiencies of Phases II and III is not representative. Furthermore, both MBR effluents and the influent of MBR 2 showed a gradual increase of all carbon fractions over time, which might be caused by the prolonged storage of the samples until analysis. Indeed, the samples of Phase I (day 50–69) which were analysed during Phase III showed an abrupt decrease of TOC and by consequence also TC.

The total carbon removal in Phase III was based by large on organic carbon removal with an efficiency of 57.9%, followed by inorganic carbon removal with an efficiency of 20.8%. The carbon in the effluent is mainly of an inorganic nature, *i.e.*, carbonate. Inorganic carbon is slightly lower in the effluent, which can be explained by autotrophic microbial growth of, *e.g.*, nitrifying bacteria.

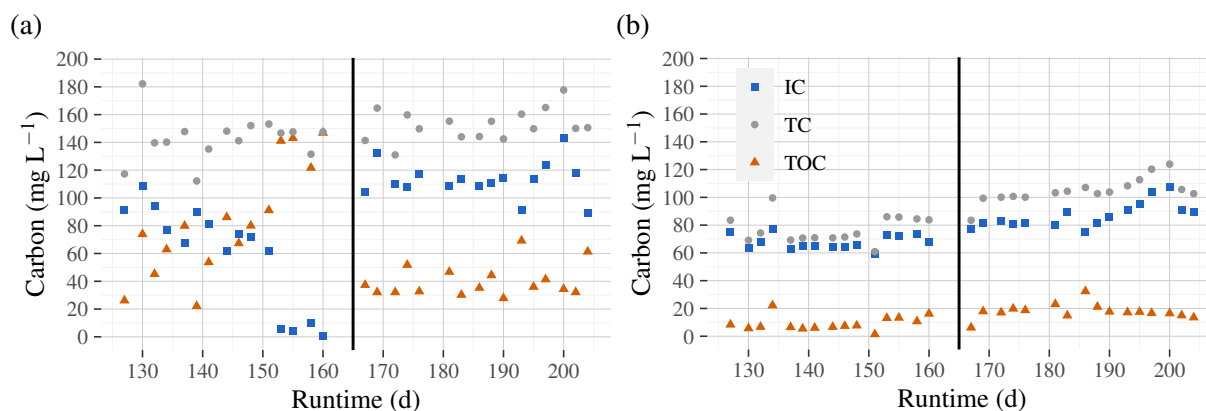


Figure 4.9: The carbon fractions for the influent (a) and effluent (b) of MBR 1 during Phase II and III. The ceramic membranes were installed on day 165, indicated by the vertical line.



## 4.4 UV<sub>254</sub> absorbance correlations

In the context of decentralized water treatment, continuous monitoring of treated greywater is a challenge (Section 1.2.4). The measurement of UV<sub>254</sub> absorbance can be a good *indication* of the aggregate concentration of UV-absorbing organic compounds, and is often correlated with the TOC and sCOD [APHA, 2017]. Therefore, online measuring of UV<sub>254</sub> absorbance could be a valuable tool for monitoring the effluent quality of decentralized systems.

For Phase I, a significant correlation was found between the influent UV<sub>254</sub> and TOC ( $\rho = 0.40$ ,  $p = 0.005$ ), but not between sCOD and UV<sub>254</sub> ( $\rho = 0.04$ ,  $p = 0.8$ ). For the effluent, significant correlations were found between UV<sub>254</sub> and both TOC ( $\rho = 0.62$ ,  $p = 6 \cdot 10^{-6}$ ) and sCOD ( $\rho = 0.70$ ,  $p = 2 \cdot 10^{-7}$ ). During Phase II, no significant correlations were found for both the influent and effluent ( $p > 0.05$ ), except a negative correlation for the influent between TOC and UV<sub>254</sub> ( $\rho = -0.45$ ,  $p = 0.015$ ). Indeed, the TOC was shown to increase during Phase II (Figure 4.9a), while UV<sub>254</sub> absorbance decreased over time. For Phase III, the only significant correlations found were for the effluent between UV<sub>254</sub> absorbance and both sCOD ( $\rho = 0.41$ ,  $p = 0.02$ ) and TOC ( $\rho = 0.36$ ,  $p = 0.04$ ).

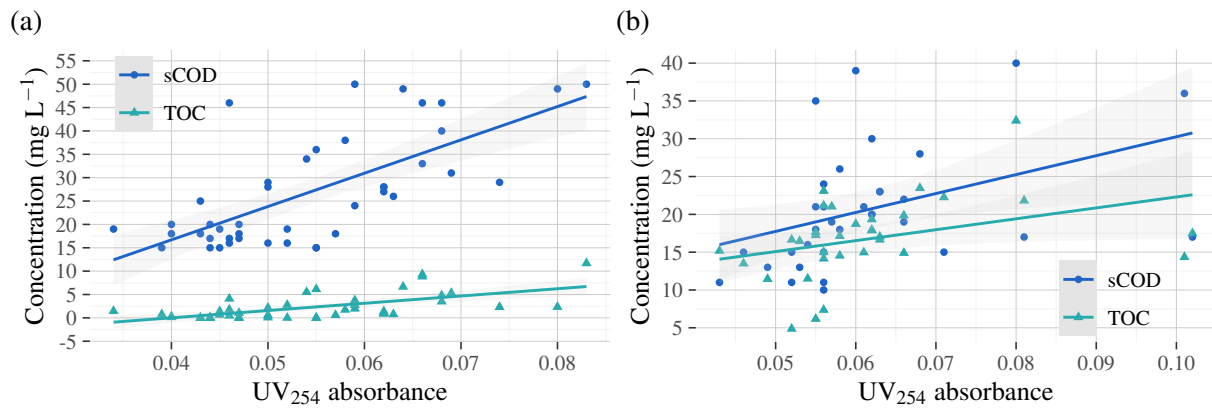


Figure 4.10: Relation between UV<sub>254</sub>, TOC and sCOD for the effluent of Phase I (a) and III (b).

These correlations were translated into relations for effluent monitoring, using only the highly correlated variables in Phase I and III (Figure 4.10). For Phase I, the relations are given by Equation 4.1 for the sCOD ( $p = 2.2 \cdot 10^{-7}$ ,  $R^2 = 0.47$ ) and Equation 4.2 for the TOC ( $p = 6.5 \cdot 10^{-6}$ ,  $R^2 = 0.37$ ). Similarly, the equations for Phase III are given by Equation 4.3 for the sCOD ( $p = 0.02$ ,  $R^2 = 0.14$ ) and Equation 4.4 for the TOC ( $p = 0.04$ ,  $R^2 = 0.1$ ).

$$sCOD = (713 \pm 115) \cdot UV_{254} - 12 \pm 6 \quad (4.1)$$

$$TOC = (156 \pm 30) \cdot UV_{254} - 6 \pm 2 \quad (4.2)$$

$$sCOD = (250 \pm 100) \cdot UV_{254} - 5 \pm 6 \quad (4.3)$$

$$TOC = (114 \pm 67) \cdot UV_{254} - 8 \pm 4 \quad (4.4)$$

## 4.5 *E. coli* removal efficiency

When reusing greywater, human health is an important concern. Although faecal indicator bacteria are not indicative of the removal of the major pathogens of risk for greywater, most guidelines, standards and regulations still focus on the removal of *E. coli* (Section 1.3.2). Therefore, the disinfection efficiency was determined through *E. coli* spike tests, since the synthetic GW does not normally contain *E. coli*. The added concentrations were about ten times higher than in real GW (Table 1.3).

### 4.5.1 Spike test 1: polymeric membranes

For the blank samples of the influent,  $>3 \cdot 10^6$  CFU  $100 \text{ mL}^{-1}$  coliforms were found ( $>300$  CFU with  $100 \mu\text{L}$  of dilution 1:10 plated). These can be any lactose-fermenting bacteria, however. In the effluent after membrane filtration, a total coliform concentration of  $3 \cdot 10^3$  CFU  $100 \text{ mL}^{-1}$  was found, along with  $2.1 \cdot 10^5$  CFU  $100 \text{ mL}^{-1}$  non-lactose fermenting gram-negative bacteria. For the spiked influent, a total coliform concentration of  $0.4 \cdot 10^8$ – $2.1 \cdot 10^8$  (average  $1.3 \cdot 10^8$ ) CFU  $100 \text{ mL}^{-1}$  was found, as expected. No lac-negative bacteria were found in the influent. No coliforms ( $<10^3$  CFU  $100 \text{ mL}^{-1}$ ,  $<1$  CFU  $100 \mu\text{L}^{-1}$ ) were detected in the effluent, but  $1.0 \cdot 10^4$ – $1.82 \cdot 10^5$  CFU  $100 \text{ mL}^{-1}$  lac-negative bacteria. Since no exact LRV could be calculated, *i.e.*, the LRV is possibly *at least* 5, a second spike test was performed on the polymeric membranes using three different methods.

### 4.5.2 Spike test 2: method comparison for polymeric membranes and UV

No colonies ( $<5 \cdot 10^3$  CFU  $100 \text{ mL}^{-1}$ ,  $<1$  CFU  $20 \mu\text{L}^{-1}$ ) were found after UV disinfection, nor for the samples plated on MacConkey agar. The latter might be due to an expired agar powder used. A thermotolerant coliform concentration of  $0.5 \cdot 10^4$ – $3 \cdot 10^4$  (average  $1.5 \cdot 10^4$ ) CFU  $100 \text{ mL}^{-1}$  was found in the influent, but none in the effluent ( $<5 \cdot 10^3$  CFU  $100 \text{ mL}^{-1}$ , m-FC agar). The CCA showed the most reliable results, with an *E. coli* influent concentration of  $0.4 \cdot 10^8$ – $2.05 \cdot 10^8$  (average  $1.3 \cdot 10^8$ ) CFU  $100 \text{ mL}^{-1}$ . No other coliforms were found. For the effluent, *E. coli* was only detected in 2 out of 4 duplicates, one for each MBR. The *E. coli* concentrations found were  $2.5 \cdot 10^4$ – $4.5 \cdot 10^4$  CFU  $100 \text{ mL}^{-1}$ . Using only influent-effluent duplicate couples where *E. coli* was detected, the log removal values (LRV) were calculated using Equation 1.1. The LRVs for the polymeric membranes were 3.7 for MBR 1 and 3.1 for MBR 2.

### 4.5.3 Spike test 3: ceramic membranes, UV and EC

The *E. coli* concentration of the influent for the third spike test was  $1 \cdot 10^7$ – $3.7 \cdot 10^7$  (average  $2.3 \cdot 10^7$ ) CFU  $100 \text{ mL}^{-1}$ , which is lower than the targeted  $10^8$  CFU  $100 \text{ mL}^{-1}$ . The effluent, spiked to  $10^4$  CFU  $100 \text{ mL}^{-1}$  was verified to contain  $2 \cdot 10^3$ , which is also lower. The effluent spiked to  $10^8$  CFU  $100 \text{ mL}^{-1}$ , however, contained  $1.2 \cdot 10^8$ – $3 \cdot 10^8$  (average  $2.1 \cdot 10^8$ ) CFU  $100 \text{ mL}^{-1}$ . For the effluent spiked to  $10^{10}$  CFU  $100 \text{ mL}^{-1}$ , the *E. coli* concentration found was  $0.94 \cdot 10^{10}$ – $1.4 \cdot 10^{10}$  (average  $1.1 \cdot 10^{10}$ ) CFU  $100 \text{ mL}^{-1}$ .

The *E. coli* concentrations detected in the effluent were  $2.6 \cdot 10^4$ – $6.4 \cdot 10^4$  (average  $4.0 \cdot 10^4$ ) CFU  $100 \text{ mL}^{-1}$ . The LRV for the ceramic membranes was calculated to be 2.7 for MBR 1 and 3.0 for MBR 2, which is lower than the LRVs found for the polymeric membranes. Again, no coliforms were detected in the effluent after the UV disinfection, even with the highest spike concentration ( $10^{10}$  CFU  $100 \text{ mL}^{-1}$ ) and filtering  $100 \text{ mL}$  through the membrane filters. Therefore, the effluent after UV disinfection was effectively  $0 \text{ CFU } 100 \text{ mL}^{-1}$ , and the LRV for this UV reactor was  $>10$ . While an increased turbidity can hinder UV penetration and disinfection efficiency (Subsection 1.4.2), the most concentrated spike solution had a turbidity of  $54.4 \text{ NTU}$  compared to the unspiked effluent ( $0.47 \text{ NTU}$ ) and still performed exceptionally well.

The electrochemical cell is a valid alternative to UV disinfection, since it could effectively disinfect the MBR effluent to a non-detectable concentration, *i.e.*,  $0 \text{ CFU } 100 \text{ mL}^{-1}$ . A summary of microbial effluent quality and the determined LRV for UV and EC disinfection, the ceramic membranes, and the polymeric membranes can be found in Table 4.5, while the *E. coli* concentration throughout the treatment system can be seen in Figure 4.11.

Table 4.5: Summary of *E. coli* spike tests 2 and 3 for the effluent quality after disinfection and the determined log removal values.

<b>Effluent quality</b>	
<i>E. coli</i> after EC ( $0.77 \text{ mg Cl}_2 \text{ L}^{-1}$ )	$0 \text{ CFU } 100 \text{ mL}^{-1}$
<i>E. coli</i> after UV ( $726 \text{ J L}^{-1}$ , $875 \text{ mJ cm}^{-2}$ )	$0 \text{ CFU } 100 \text{ mL}^{-1}$
<b>Log removal values</b>	
Polymeric membranes ( $0.4 \mu\text{m}$ )	3.1 – 3.7
Ceramic membranes ( $0.56 \mu\text{m}$ )	2.7 – 3.0
UV reactor ( $726 \text{ J L}^{-1}$ , $875 \text{ mJ cm}^{-2}$ )	$>10$

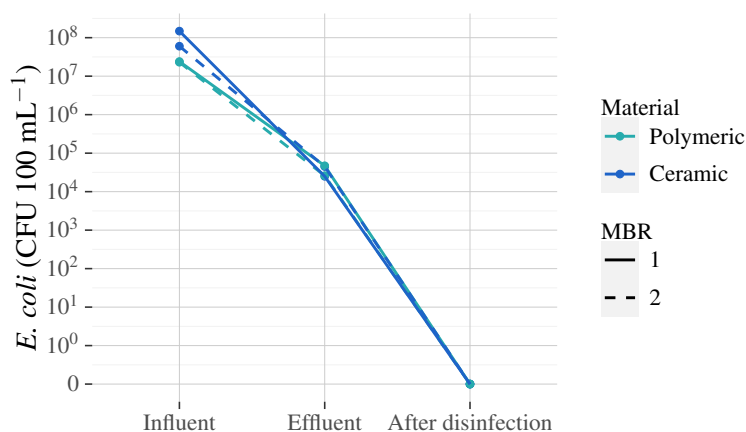


Figure 4.11: *E. coli* concentration throughout the treatment train.

## 4.6 UV reactor characteristics

Since an LRV for disinfection is not meaningful unless related to a certain UV dose (Subsection 1.4.2), the UV reactor was characterized in terms of residence time and applied UV dose.

### 4.6.1 UV reactor residence time

The UV reactor volume ( $V_{UV \text{ reactor}}$ ) was determined to be 196–198 mL, with an average of 197 mL. Therefore, the theoretical residence time  $\tau$  is 13.8 min to 14.3 min, with an average of 13.8 min. The inlet conductivity measured in the test tube was  $52.2 \text{ mS cm}^{-1}$ , which is lower than the measured conductivity in the free solution ( $100 \text{ mS cm}^{-1}$ ). This was caused by an interaction effect of the probe in the narrow test tube. This deviation has no effect on the results, since the outlet conductivity  $\kappa(t)$  will be normalized with  $\kappa_0$  following Equation 3.13. The cumulative residence time distribution (RTD) and RTD are shown in Figure 4.12.

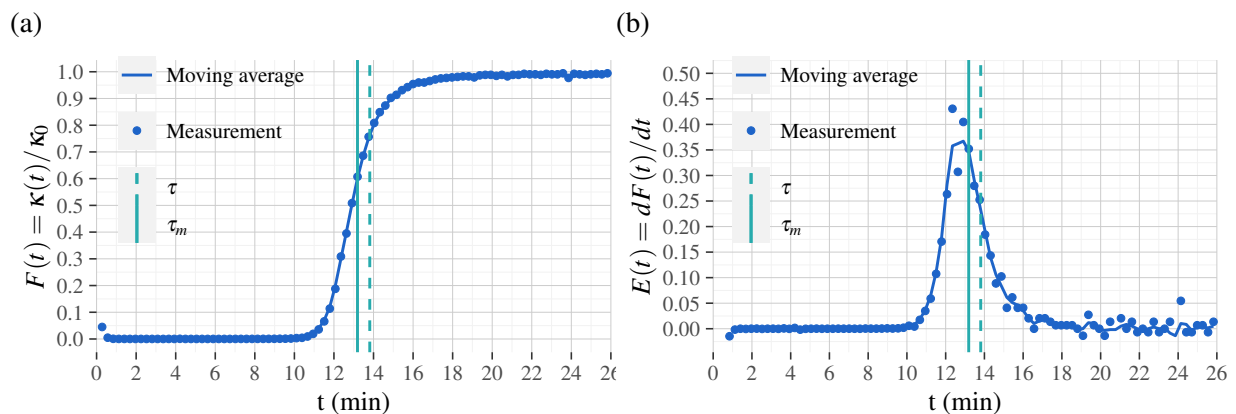


Figure 4.12: Cumulative RTD (a) and RTD (b) of the UV reactor, with  $\tau$  the hydraulic retention time (HRT), and  $\tau_m$  the mean residence time.

The mean residence time  $\tau_m$  was calculated using Equation 3.16 and found to be 13.19 minutes. The peak residence time occurs well before the theoretical residence time (Figure 4.12b). Furthermore, the RTD shows a long tail, which is additionally indicated by  $\tau_m$  not coinciding with the peak of the RTD.

## 4.6.2 UV dose

During irradiation, the pH and temperature of the actinometric iodide-iodate solution increased from 9.09 to 9.18 and from 22.0°C to 23.4°C, respectively. The measured absorbance at 300 nm of the solution prior to irradiation was 0.614. Therefore, the KI concentration was 0.579 M (Equation 3.18), which is close to 0.6 M and similar to the findings of Rahn [1997]. When correcting the quantum yield  $\Phi$  for the KI concentration and an average temperature of 22.7°C using Equation 3.22, a value of 0.780 mol I<sub>3</sub><sup>-</sup> einstein<sup>-1</sup> was obtained.

The absorbance of the actinometric solution at 352 nm before irradiation was found to be 0.089. The irradiated solution was sampled after 20 minutes and measured for absorbance at 352 nm immediately. Because the solution exceeded maximum absorbance, it had to be diluted by a factor 1:16, since absorbance and concentration are linearly related following the law of Lambert-Beer ( $A_{352} = \epsilon \cdot l \cdot c_{I_3^-}$ ). The absorbance of the undiluted solution was calculated to be 33.3. Using Equation 3.19, the volumetric UV dose at 254 nm ( $D_v$ ) was 726 J L<sup>-1</sup>. The diameter and height of the UV lamp casing were 4 and 12 cm, respectively. Using a surface area of 163.4 cm<sup>2</sup> and the UV reactor volume (Subsection 4.6.1), the UV dose at 254 nm was estimated to be 875 mJ cm<sup>-2</sup> (Equation 3.20). Following Equation 3.20, the lamp intensity was determined to be 1.11 mW cm<sup>-2</sup>. The UV-C output of the lamp was 2.3 W at 254 nm. Using this value and the estimated surface area, the lamp intensity was found to be 14 mW cm<sup>-2</sup>.

# 5

## Discussion

### 5.1 Treatment performance

During the entire experiment (all three Phases), nitrogen removal was limited to at most 67.7% (95<sup>th</sup> quantile), with an average of 53% during the period with the highest removal efficiency, being Phase III. Since the experimental setup was an aerated MBR, no denitrification would be expected, which was confirmed by the results (Subsection 4.3.3). The removal of nitrogen is purely based on immobilisation of nitrogen in sludge growth and subsequent removal of this sludge through the overflow. Increasing sludge wastage can therefore increase the nitrogen removal efficiency, but the sludge concentration was already limited by the available COD. Furthermore, increasing sludge wastage will decrease the water recovery, which may not be preferred. Better alternatives to obtain higher nitrogen removal efficiencies are to either increase the loading rates by increasing the treated wastewater volume or to decrease the reactor volume (Subsection 4.3.1). This way, sludge concentration would be increased, allowing for higher sludge wastage while maintaining the same recovery. However, both approaches were practical limitations of the greywater storage drum and the membrane dimensions, respectively. Another option would be to add carriers to the system to obtain a MBBMR (Section 1.5), as this would allow for denitrification in deeper, anoxic layers of the biofilm present on the carriers.

A noticeable treatment performance difference between Phase I and Phases II and III was found. The main cause was a difference in sludge quality and especially quantity. Since nitrogen was removed based on immobilisation, a higher MLSS concentration caused a higher removal efficiency. Furthermore, nematodes, ciliate protozoa, and slight algal growth was observed during Phases II and III (Supplementary figures B), which is an indicator of good sludge quality since these organisms could survive in Phases II and III, but not in Phase I.

The influent after storage showed lower tCOD and  $\text{PO}_4^{3-}$  concentrations compared to fresh synthetic greywater, fluctuations in the concentrations of other ions, and high concentrations of lac-positive bacteria in the spike test blanks. The plastic drum used for the influent was stored outside and filled with pebbles and sand before use in this setup. It was only rinsed with tap water and not disinfected, and the drum was left open to the laboratory atmosphere for the entire experiment. Therefore, contamination is likely and expected. Since the influent storage drums were never completely emptied or cleaned, any microbial biomass present would remain available to regrow once fresh greywater was added. These short cycles of fresh added GW and microbial proliferation likely caused the observed high variability in the turbidity, anoxic conditions, precipitation, and degradation.

For the  $\text{UV}_{254}$  correlations, the influent absorbances were most likely inaccurate due to filtration with a PA filter instead of an inorganic filter, *e.g.*, glass fibre [APHA, 2017]. Indeed, the polyamide (nylon) filters used release the highest amount of interfering organics [Karanfil *et al.*, 2003]. Furthermore, the older samples for TOC showed deviation due to prolonged storage before analysis. Different samples were used for the measurement of sCOD and other variables at CMET, and  $\text{UV}_{254}$  and TOC at PaInT, which might have decreased the quality of the correlation further, since the influent showed high variation.

The  $UV_{254}$  correlations for the effluent of Phase III were significant, but had a low indication for linear goodness of fit ( $R^2$ ), due to a higher variance. The samples of the effluent were not filtered with a PA filter. The difference between two Phases was most likely caused by the difference in sludge characteristics [APHA, 2017]. Furthermore, all correlations determined are specific to the greywater used and the sludge characteristics, *e.g.*, microbial community composition [APHA, 2017]. In fact, the same can be said for all results obtained within these experiments, as operational conditions will impact both treatment and membrane performance.

## 5.2 Membrane performance

The ceramic membranes developed lower pressures during operation compared to the polymeric membranes. This can be attributed to three factors: the lower flux and larger pore size of the ceramic membranes, and the different surface properties, *e.g.*, surface material, roughness, porosity and pore length of the ceramic membranes. The membrane performance in terms of fouling rate was 6.85x lower for the ceramic membranes, which corrects for differences in pore size and flux. The flux difference was corrected for by the use of the fouling resistance  $R_f$  instead of TMP, while the differences in pore size, porosity and pore length were corrected for by looking only at the fouling resistance, and not including the membrane resistance  $R_m$  (Equation 1.3). Therefore, the lower fouling rate was caused by the different surface material and roughness of the ceramic membranes. Indeed, the SiC membranes have a high hydrophilicity and a low iso-electric point (Table C.2). The iso-electric point was about 2 to 2.5 as given by the manufacturer, *i.e.*, a high negative surface charge at the synthetic greywater pH. This is a clear advantage of the ceramic membranes for decentralized applications, allowing longer operation without cleaning. However, the ceramic membranes should be researched further to see the effect of backwashing and to further assess fouling development, since no cleaning was performed in this experiment.

## 5.3 Disinfection performance

During the assessment of disinfection performance, high effluent concentrations of lac-negative bacteria were found in the blank. Since these bacteria were not present in the influent, it can be assumed that the contamination was caused by the reactor's MLSS. Indeed, the polymeric membranes were removed from the reactor when cleaning, which leaves the tubing exposed for contamination. Furthermore, the polymeric membranes were only cleaned manually during Phase II, which might have allowed for more significant bacterial regrowth after membrane filtration compared to regular chemical cleaning. The ceramic membranes can probably be cleaned effectively by backwashing, allowing for low-maintenance, which is an advantage when regarding decentralized greywater treatment. Because no cleaning was performed during this study, the efficacy of backwashing for this specific SiC membrane is not known.

The LRV for the polymeric membranes was 3.1–3.7, which is slightly lower compared to values found in literature (Section 1.6), which might be due to frequent cleaning. For the ceramic membranes, the LRV was 2.7–3.0, which was lower than the polymeric membrane LRV. This was expected, since the pore size of the ceramic membranes was a factor 1.4 larger. The lower LRV for ceramic membranes is not necessarily disadvantageous, since the main purpose of



membrane filtration is not disinfection but solids retention and removal, and both membranes performed equally well in terms of turbidity and TSS removal. Furthermore, the removal efficiency was not perfect, while *E. coli* dimensions are  $0.6 \times 2 \mu\text{m}$ , which is larger than the pore sizes of the membranes [Liu, 2019]. This was caused by imperfect pore size distributions compared to nominal pore sizes, and membrane surface defects.

To the best of the author's knowledge, no values are reported for ceramic membrane LRVs for the treatment of greywater using MBRs, so no comparison with literature could be made. Only one study concerning ceramic membranes for (non-biological) greywater treatment was found, but no LRV was given [Bhattacharya *et al.*, 2013]. The LRV, based on ranges of most probable numbers (MPN) per 100 mL for bacteria in the influent and effluent, was at the very least 0.8 and at best 1.5 for a clay-alumina membrane with pore size  $1 \mu\text{m}$  [Bhattacharya *et al.*, 2013].

The excellent performance of the UV reactor was likely caused by an over-dimensioning, since the UV lamp is designed for household ponds of size 7000 L. The flow rate of  $0.9 \text{ L h}^{-1}$  ( $14.25 \text{ mL min}^{-1}$ ) used in the spike tests was only a fraction of the maximum design flow rate of  $3000 \text{ L h}^{-1}$ . The UV dose was  $875 \text{ mJ cm}^{-2}$ , which is more than a factor 10 higher than the requirements in Table 1.5. It is unclear how much the required dose would increase when corrected for photoreactivation and other variables in Subection 1.4.2. However, it is evident that the UV reactor is over-dimensioned for *E. coli* removal, as expected from the results of *E. coli* removal (Section 4.5). The low flow rate, being only a fraction of the maximum design flow rate, led to an excessively long residence time and a decrease of energy efficiency. The required energy for disinfection was  $10.5 \text{ kWh m}^{-3}$ , which is very high compared to literature, being 0.4 to  $3.3 \text{ kWh m}^{-3}$  (Section 1.5).

The long tail of the residence time distribution, and the mean residence time being smaller than the hydraulic residence time are strong indications of a dead volume, which is very plausible considering the geometry of the UV reactor (Figure B.11). The UV reactor consists of two concentric cylinders with inflow and outflow connections on either side at different heights. Furthermore, the inner cylinder, containing the UV lamp, has its base elevated from the outer casing, allowing water to pass underneath. Therefore, the water can travel any of three different paths around the inner lamp casing (Figure B.11). It is most likely that the dead volume is situated somewhere in the longest paths. At high flow rates ( $3000 \text{ L h}^{-1}$ ) close to the intended UV reactor design, this dead volume would probably be negligible.

There is an obvious discrepancy between the two lamp intensity values. This can be explained by several factors. The irradiated area was simplified to the lamp casing surface, which was assumed to be cylindrical. A concentric water layer further from the lamp casing will have a larger surface area, and therefore a smaller UV flux. Therefore, the formula used in Equation 3.20 and the calculated surface area are not representative of reality. Furthermore, transmission effects of the lamp casing, and reflection effects of the water surface and UV reactor aluminium lining were not considered. The volumetric UV dose  $D_v$  will be the most accurate representation of disinfection intensity, since it is directly based on the number of photons with a wavelength of 254 nm absorbed per litre of water (Subsection 1.4.2).

## 5.4 Water fit for reuse

This study aims at non-potable reuse on a household-scale for, *e.g.*, toilet flushing. No local guidelines or regulations are present for household-scale decentralized general wastewater reuse in Belgium, since water reuse is limited to specific industrial cases, and the well known example of indirect potable reuse at the centralized WWTP of Torreele [Van Houtte and Verbauwhe, 2008]. To compare the treatment performance of the MBR system, the most stringent set of target values from Table 1.4 were chosen, which can be found in Table 5.1 together with the effluent results of the polymeric and ceramic membranes (Phases II and III). Since the reporting of an average and standard deviation is less meaningful when comparing with targets [Reynaert *et al.*, 2021], a range and average was given for each parameter of effluent quality.

The legislation for Italy is based on general wastewater treatment for reuse in toilet flushing [Alcalde Sanz *et al.*, 2014]. No frequency of monitoring is mentioned except annual reporting, which is the responsibility of the owner of the water recovery plant. The guidelines concerning the reuse of greywater in Western Australia for toilet flushing and clothes washing only apply to communal or public properties, not to a single domestic dwelling [Western Australia Department of Health, 2011]. Weekly monitoring of coliphages, Clostridia, *E. coli*, BOD, and TSS is required, with online monitoring for pH, turbidity, and UV dose intensity. The ISO standard was made primarily for non-sewered (*i.e.*, decentralized) sanitation systems treating human excreta for unrestricted urban reuse, although the input substances can be extended to include greywater [International Standards Organisation, 2018]. Controlled laboratory tests of 32 days on urine and faeces are required, with sampling roughly every week. Besides the parameters in Table 5.1, noise, odour, and air emissions require monitoring to obtain ISO certification. However, the aim of this study was not to comply to a certain water reuse criterion, but to be a proof-of-concept that an MBR system using ceramic membranes for greywater treatment can meet current target values for non-potable municipal water reuse.

Total phosphorus, residual chlorine, faecal coliforms, MS2 coliphage, Clostridia, protozoa, and *Salmonella* targets were defined in the selected water quality targets, but not measured in this study. Residual chlorine was not applicable since the disinfection was UV-based. Total phosphorus was not considered since the added concentration was only  $0.5 \text{ mg P L}^{-1}$ , excluding detergent contribution. To assess the disinfection performance, only the *E. coli* removal in terms of LRV and effluent concentration was determined.

From Table 5.1, it can be seen that the effluent quality easily met the defined targets for both membrane materials, except for nitrogen-related targets. Indeed, the maximum effluent TN concentration exceeds the target of Italy, while the TN removal efficiency requirement for the ISO standard is not met. The maximum ammonium concentration exceeds the target of Italy. However, the question is whether these targets are relevant for the application. For the ISO standard, the targets are set to prevent eutrophication of surface waters, since discharge to surface waters is included in the standard. For Italy, the regulations seem to be set as an intermediary of drinking water targets and agriculture irrigation. Should toilet flushing be considered, the only concern would be regrowth of micro-organisms due to the presence of nitrogen. The added urine would increase nitrogen concentrations back to levels equal or greater than that of the untreated greywater, since urine contains about  $9.8 \text{ g N L}^{-1}$  as urea [Larsen *et al.*, 2013].

Table 5.1: Comparison between the observed MBR effluent quality and a selection of non-potable water reuse quality targets.

Type	Phase II Polymeric membranes	Phase III Ceramic membranes		ISO 30500:2018 Category A <sup>a</sup> International standard Unrestricted use	Australia (2011) <sup>b</sup> Guideline Toilet flushing, clothes washing	Italy (2003) <sup>c</sup> Regulation Toilet flush- ing
Reuse purpose						
pH		7.6 – 8.0 (7.7)	7.6 – 8.1 (7.8)	6 – 9	6.5 – 8.5	6.0 – 9.5
$\kappa$	(mS cm <sup>-1</sup> )	0.9 – 1.3 (1.2)	1.0 – 1.4 (1.1)			≤3.0
Turbidity	(NTU)	0.27 – 3.83 (0.87)	0.33 – 3.27 (0.83)		≤2 (95 percentile) ≤5 (max)	
COD	(mg L <sup>-1</sup> )	15 – 28 (17)	10 – 40 (21)	≤50		≤100
BOD	(mg L <sup>-1</sup> )				≤10	≤20
TN	(mg L <sup>-1</sup> )	9.1 – 20.8 (14.8)	6.9 – 18.5 (11.6)			≤15
TN removal	(%)	10 – 65 (43)	29 – 73 (53)	70%		
NH <sub>4</sub> <sup>+</sup> -N	(mg L <sup>-1</sup> )	<0.2 – 10.8 (0.8)	<0.2 – 8.0 (0.8)			≤1.6
TP	(mg L <sup>-1</sup> )			80% load re- duction		≤2
TSS	(g L <sup>-1</sup> )	<0.01	<0.01	≤10	<10	≤10
Cl <sup>-</sup>	(mg L <sup>-1</sup> )	111.7 – 163.4 (149.7)	132.8 – 216.1 (147.1)			≤250
Residual chlorine	(mg L <sup>-1</sup> )	N/A	N/A		0.2 – 2	
UV dose	(mJ cm <sup>-1</sup> )	875	875		40-70	
Faecal coliforms	(CFU/100 mL)				<1	
<i>E. coli</i>	(CFU/100 mL)	0, >10 LRV	0, >10 LRV	≤1, ≥6 LRV	>5 LRV	≤10
Coliphage MS2	(PFU/100mL)			≤1, ≥7 LRV	<1, >6.5 LRV	
Clostridia	(CFU/100 mL)				<1	
Protozoa					>5 LRV	
<i>Salmonella</i>						N.D.

<sup>a</sup> Reynaert *et al.* [2020]<sup>b</sup> Western Australia Department of Health [2011]<sup>c</sup> Alcalde Sanz *et al.* [2014]

## 5.5 Comparison with MBBR

A comparison will be made between the MBR-UV and the MBBR-EC of colleague student Nele Driesen [Driesen, 2021]. The MBBR system was two-staged, using AnoxKaldnes K5 carriers with a filling ratio of 40%. The surface loading rate was  $3 \pm 1 \text{ kg COD m}^{-2} \text{ d}^{-1}$ , while the volumetric loading rate was  $1.1 \pm 0.3 \text{ kg COD m}^{-3} \text{ d}^{-1}$ . The same composition was used for the synthetic GW. Solids removal was based on conical settlers, and disinfection after settling occurred through an electrochemical cell (EC) with cation exchange membranes, producing  $0.77 \text{ mg L}^{-1}$  free chlorine species. Other characteristics of the EC and MBBR can be found in Driesen [2021], since those are out of the scope of this study.

The effluent quality and disinfection performance of both systems are summarized in Table 5.2. For the MBR, the data for Phase III is given (ceramic membranes). Carbon fractions and other ions besides phosphate and nitrogen species are not shown. No difference in  $\kappa$ , phosphate and nitrite was found.

Table 5.2: Comparison between MBR and MBBR effluent quality.

		MBR (ceramic)		MBBR	
pH		7.62 – 8.12	(7.83)	7.6 – 8.37	(8.1)
$\kappa$	( $\mu\text{S cm}^{-1}$ )	1005 – 1431	(1107)	756 – 1271	(1117)
Turbidity	(NTU)	0.33 – 3.27	(0.83)	0.91 – 71.2	(9.32)
COD	( $\text{mg L}^{-1}$ )	10 – 40	(21)	<15 – 172	(46)
TN	( $\text{mg L}^{-1}$ )	6.9 – 18.5	(11.6)	1 – 22	(14.3)
$\text{NH}_4^+\text{-N}$	( $\text{mg L}^{-1}$ )	<0.2 – 8.0	(0.8)	<0.2 – 15.4	(1.0)
$\text{NO}_2^-\text{-N}$	( $\text{mg L}^{-1}$ )	0.1 – 3.6	(0.7)	<0.03 – 4.9	(0.6)
$\text{NO}_3^-\text{-N}$	( $\text{mg L}^{-1}$ )	1.6 – 16.1	(8.6)	0.4 – 14.4	(10.0)
$\text{PO}_4^{3-}$	( $\text{mg L}^{-1}$ )	<0.1 – 4.2	(0.3)	<0.1 – 4.1	(<0.1)
TSS	( $\text{g L}^{-1}$ )	<0.01		<0.3 – 380	(31)
<i>E. coli</i>	(CFU 100 $\text{mL}^{-1}$ )	0		0 – 20	
LRV treatment		2.7 – 3.0		1.2 – 3.3	(2.2)
LRV disinfection		>10		4.3 – 5.3 <sup>a</sup> , >4.8 <sup>b</sup>	
Residual chlorine	( $\text{mg L}^{-1}$ )	N/A		0.77	
UV dose	( $\text{mJ cm}^{-2}$ )	875		N/A	
Disinfection energy use	( $\text{kWh m}^{-3}$ )	10.5		$5 \pm 1$	

<sup>a</sup> Effluent of MBBR

<sup>b</sup> Effluent of MBR

The average turbidity of the MBBR effluent was a factor 10 higher, which was also reflected in elevated TSS levels. For the MBR, the TSS of the effluent was below the quantification limit ( $<0.01 \text{ g L}^{-1}$ ), while the TSS of the MBBR was on average much higher ( $31 \text{ g L}^{-1}$ ) with extreme values of up to  $380 \text{ g L}^{-1}$ . The reliance of the MBBR on gravitational settling led to a vulnerability to bulking and floating sludge. Indeed, floating sludge caused high TSS levels and decreased disinfection performance through reaction of the reactive chlorine with organic matter. The MBR was more effective for TSS and turbidity removal, but this is likely accompanied by an increased energy demand required to overcome TMP. No energy efficiency was calculated.

The effluent COD concentration of the MBBR was on average about 2 times higher, with a 4 times higher observed maximum. Both reactor types have mechanisms of sludge retention, but the SRT of the MBR was more controllable through setting of the sludge wastage  $Q_w$ . It is likely that more biomass was present in the MBR, *i.e.*, the sludge loading rate was lower in the MBR, which caused an increased COD removal efficiency.

The TN removal was slightly higher for the MBR, but this is caused by the temporary increase in MLSS concentration during Phase III, with similar results between Phase II and the MBBR. Similar nitrate and average ammonium concentrations were observed, although with lower maximum ammonium concentrations for the MBR. This could indicate that the addition of carriers to the MBR would not necessarily improve nitrogen removal. However, the active biomass was mainly located on the carriers in the MBBR, while biomass in a moving bed biofilm membrane reactor (MBBMR) or hybrid MBR-MBBR would be present both on the carriers and as additional sludge suspended in the MLSS. This could lead to a decreased DO concentration in the MBBMR due to higher total biomass presence, which might initiate denitrification [Hocaoglu *et al.*, 2011], should the DO be sufficiently low to induce anoxic conditions in the carrier biofilms.

The LRV of both treatment trains without disinfection was similar, although the LRV for the MBR was more consistently high, in the sense that the average LRV for the MBBR was lower than the LRVs for both MBR 1 and 2. However, the main purpose of the treatment trains was solids retention and biological treatment. The UV showed a very high LRV since it was overdimensioned, with no effect of increased turbidity on disinfection performance. The EC struggled with the suspended organic matter in the MBBR effluent and showed a lower LRV than the UV reactor. However, the MBR effluent could effectively be disinfected by the EC. A LRV for the EC of  $>4.8$  was found for the disinfection of the MBR effluent. No LRV determination for the EC was performed with spiked MBR effluent. Therefore, a comparison is not straightforward.

In terms of energy use for disinfection, the UV lamp used about twice the energy per treated unit of water compared to the EC, being  $10.5 \text{ kWh m}^3$  compared to  $5 \pm 1 \text{ kWh m}^3$ . The flowrate of the UV could be increased since the UV dose was about a factor 10 higher than usual for disinfection. However, the UV dose does not typically decrease linearly with the flow rate [Friedler and Gilboa, 2010], so possible energy savings can not be determined. The EC energy use was high because of an increased internal resistance of the cell, due to high TSS concentrations of the MBBR effluent and precipitation caused by a high cathode pH.

# 6

## Conclusion

### 6.1 General conclusions

The main focus of this study was the reclamation of greywater for non-potable reuse and assessing the application potential on a small scale of an MBR treatment system with UV disinfection. The effluent quality met the most stringent available physicochemical and biological water quality targets for toilet flushing and unrestricted reuse, at a water recovery of 95% (Objectives 3 and 2). Only nitrogen removal was limited. However, this might be less relevant for, *e.g.*, toilet flushing, which is one of the most demanding uses in terms of water quantity (Table 1.1). The SiC ceramic membranes used can enable long operation cycles without the need for cleaning, through a lower degree of fouling accumulation, which is a strong advantage for small-scale systems compared to the widely used commercial polymeric membranes (Objective 1).

Despite initial optimization problems during Phase I, a stable reactor performance was obtained during Phases II and III (Objective 3). A good sludge quality was found to be essential to ensure ideal membrane performance and treatment efficiency. A high turbidity removal was observed, being 98.9% for the polymeric membranes and 99.2% for the ceramic membranes, despite differences in pore size. A high average COD removal was obtained of around 95% for both membranes. Nitrogen removal was based on sludge growth and wastage and limited to at most 67.7% (95<sup>th</sup> percentile) with an average of 48% for both membrane materials together. Precipitation and degradation occurred in the influent storage drum, which acted as a first step for the treatment of the synthetic greywater (Objective 3).

Looking at biological effluent quality, the UV reactor could reduce *E. coli* concentrations to non-detectable levels (Objective 2). The UV lamp was heavily over-dimensioned through design, leading to a high UV dose of 726 J L<sup>-1</sup> (875 mJ cm<sup>-2</sup>) and an LRV above 10 with no observed decrease under higher turbidity. The LRV for the polymeric membranes was 3.1–3.7, which is slightly lower compared to literature, but can be explained by frequent ex-situ cleaning and the accompanied increased susceptibility to regrowth. For the ceramic membranes lower LRVs of 2.7–3.0 were found, due to a difference in pore size. However, the LRVs of the membranes are less relevant since the UV reactor was the main point of disinfection.

Membrane fouling was observed and assessed during operation. The fouling rate for the ceramic membranes was a factor 6.85 lower compared to the polymeric C-PE membranes (Objective 1). This could be attributed to the difference in surface roughness and membrane material. The overall operation pressures were much lower for the ceramic membranes than for the polymeric membranes for the entire duration of the experiment, but this might have been partly due to the larger pore size and larger surface area. Microbial regrowth was observed when cleaning the membranes ex-situ, *e.g.*, chemical cleaning or rinsing under tap water. The SiC membranes are not expected to require removal from the MBR for cleaning, since they can be backwashed and are robust enough to enable manual brushing should this be required. However, no cleaning was performed to verify this.



To allow for on-line monitoring of effluent quality, correlations were determined between  $UV_{254}$  absorbance and TOC and sCOD (Objective 5). A strong linear correlation was found for the effluent during Phase I, which could have been used for monitoring. However, no significant correlation was found for Phase II and the correlations for Phase III were of lesser quality due to several factors, such as sample filtering with the wrong filter material, overdue analyses, prolonged storage, and the use of different samples for analysis with high sampling variability. Therefore, the determined correlations have limited use, in addition to being specific for the treatment system and greywater in question.

One of the main advantages of MBR is the retention of biomass, allowing for small reactor volumes with high sludge concentrations (Objective 4). During MBR operation, a lower mixed liquor suspended solids (MLSS) concentration of about 2.25 to 3 g MLSS L<sup>-1</sup> was found compared to conventional AS (4 g MLSS L<sup>-1</sup>) and typical MBR systems (12 g MLSS L<sup>-1</sup>). However, this was caused by a low organic loading rate limiting sludge growth and not by any inhibition or excessive die-off caused by detergents and biocides present in the greywater, contrary to expectations. Therefore, the retention of biomass in the system as an advantage of MBR is confirmed. The reactor volume could be lowered from 10 L to as low as 1.7 L, or the organics loading could be increased. This allows for a system with low space requirements, which is well suited for small-scale applications.

Lastly, the other advantages of MBR systems (Objective 4) were assessed by a comparison between the MBR setup and a moving bed biofilm reactor (MBBR) running on the same synthetic greywater [Driesen, 2021]. The MBBR volume was in total 17 L, with 5 L per stage and 7 L for the conical settler, which is in total about 10 times higher than the lowest feasible MBR volume. The effluent turbidity of the MBR was on average 10 times lower, with no quantifiable amount of TSS present. Therefore, it was able to provide an effluent of higher clarity compared to the MBBR, especially when sludge bulking is a problem. As a consequence, the electrochemical cell of the MBBR setup could effectively disinfect the MBR effluent to a non-detectable level of *E. coli*. The retention of activated sludge in the MBR was much more controllable compared to the MBBR, by setting of the sludge wastage.

Overall, the MBR-UV setup with ceramic membranes has shown excellent application potential for greywater treatment and reuse through its advantages for implementation on a small-scale. Further research could strengthen this position and allow for an effective implementation, alleviating water scarcity in Flanders and other regions of the world.



## 6.2 Perspectives

To allow a more thorough comparison between the SiC and C-PE membranes, the use of the current SiC ceramic membranes should be continued. This way, the fouling development can be evaluated in a more concise way, including the use of cleaning methods such as backwashing or manual brushing. Furthermore, many other materials are available for the use in top-layers of ceramic membranes and can be evaluated for their effectiveness for greywater treatment in an MBR, such as SiC membranes with different top-layer thicknesses or substrate pore sizes, Al<sub>2</sub>O<sub>3</sub> ceramic membranes, the combination of photocatalytic TiO<sub>2</sub> membranes with UV disinfection, zeolite based membranes, or even ceramic membranes made of natural materials such as clays.

Since nitrogen removal was limited, the use of carriers in a ceramic moving bed biofilm membrane reactor (CMBBMR) can be evaluated, to achieve simultaneous nitrification and denitrification. Another option would be to operate under intermittent aeration, introducing anoxic periods. To test the applicability of the treatment system, it should be evaluated on real greywater. Furthermore, a direct connection to a greywater supply could enable higher loading rates and assess the effect on MLSS concentration and treatment performance.

Lastly, the disinfection performance assessment should be extended to viruses, since they pose a non-negligible concern for human health. The LRV of the UV reactor for, *e.g.*, MS2 coliphage could be determined using the existing MBR-UV system with SiC ceramic membranes. Furthermore, since the UV reactor was heavily overdimensioned, the relation of reactor flow rate and UV dose could be determined to better understand exactly how much the UV reactor is overdimensioned. However, should a flow rate of 3000 L h<sup>-1</sup> still provide adequate disinfection, this is not feasible for a lab-scale reactor. Other options would be to assess lower power UV lamps, or even a small LED-UV diode array fit for the low flow rates used. However, the goal of this study was not to deliver a completely customized treatment system ready for application, but rather to be a proof-of-concept.

# A

## Sustainability

Approximately 7300 litres of drinking water were used during the entire experiment for the preparation of synthetic greywater, after which it was treated and disposed of down the drain. These 7300 litres are the non-potable water usage of 1 person for a period of 4 months [Vlaamse Milieumaatschappij, 2018]. It would have been more sustainable to treat real greywater and effectively reuse it for, *e.g.*, toilet flushing, since the effluent quality met the requirements. Furthermore, the reactors could have potentially treated 43000 litres of real greywater would the organic loading rate have been increased and the effluent quality stayed the same. This could have supplied 3.5 people for the entire duration of the experiment (204 days) with all of their daily water needs that do not require a potable water quality, such as toilet flushing, clothes washing, garden irrigation, and house cleaning. When considering only toilet flushing, the two MBRs could have supplied nearly 10 people with their daily toilet flush water.

Ghent is supplied in its drinking water by the water utility company Farys, which relies for 88% of its drinking water on the import of groundwater from the Walloon region of Belgium and the Netherlands [Vlaamse Milieumaatschappij, 2019a]. To treat and reuse greywater locally could reduce a person's potable water demand by roughly 52%, drastically reducing the number of kilometres our water needs to travel, saving both the energy needed for pumping over large distances and lowering the pressures on groundwater supplies [Rabaey and Van De Walle, 2020; Vlaamse Milieumaatschappij, 2018]. When looking at Flanders as a whole, a total of about 183 million m<sup>3</sup> of potable water could be saved on a yearly basis [Vlaamse Milieumaatschappij, 2019a], which is equal to 73000 olympic swimming pools.

# B Supplementary figures

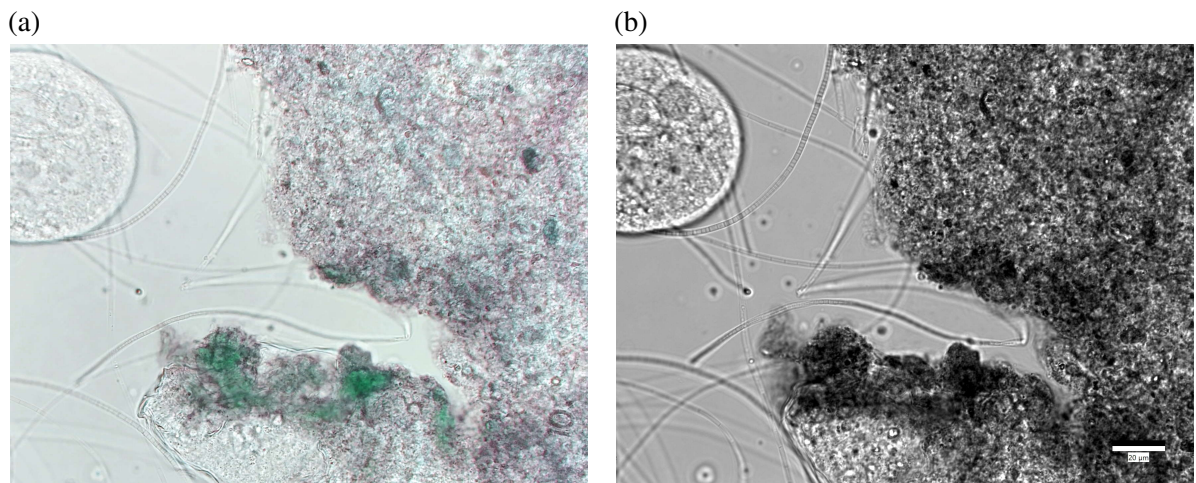


Figure B.1: Microscopic images of algae in the MBR. (a) Colour image. (b) Image taken with the microscopy camera, including scale. Filamentous bacteria and a ciliate can be seen.

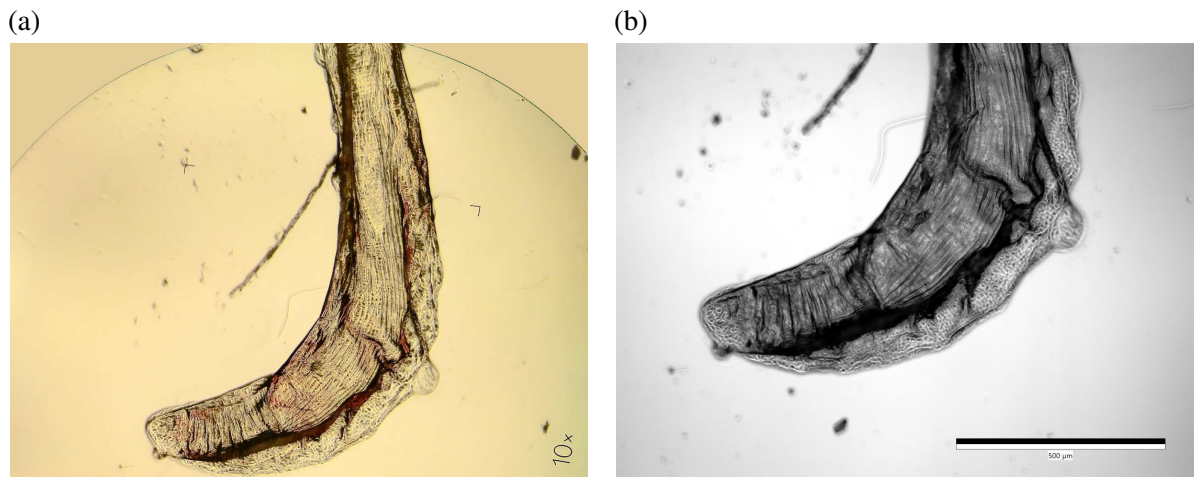


Figure B.2: Male nematode tail. (a) Colour image. (b) Image taken with the microscopy camera, including scale.



Figure B.3: Composite image of a female nematode, since the nematodes were too large to fit in view on the smallest magnification.

Figure B.4: Ciliate protozoa present in the MBR, feeding on the activated sludge. Filamentous bacteria were also visible.

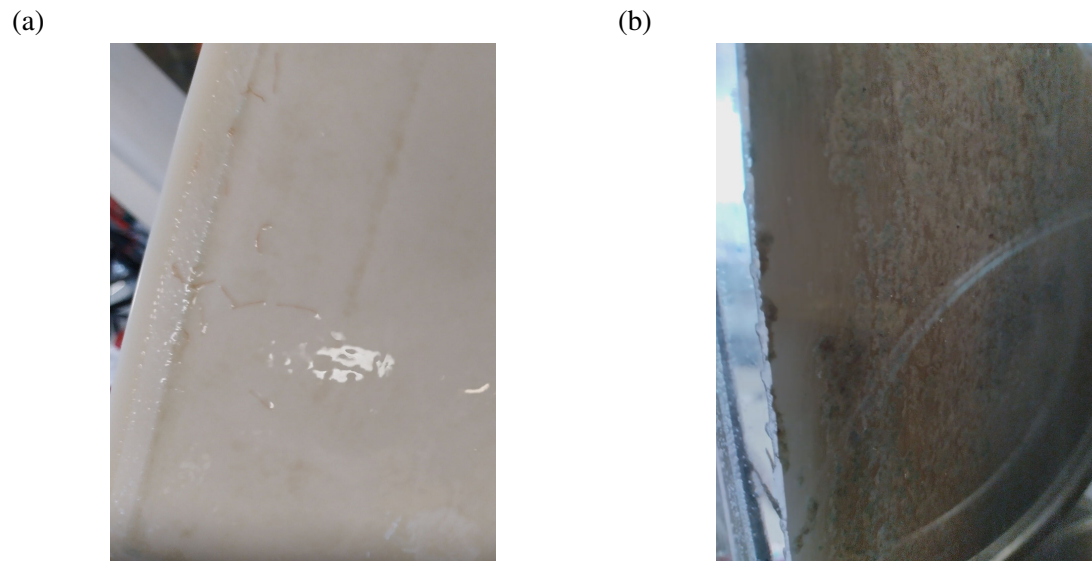


Figure B.5: Macroscopic view of (a) the red-coloured nematodes on the polymeric membrane, and (b) limited algae growth inside the MBR. The visible border on the left side of the polymeric membrane was 5 mm wide.

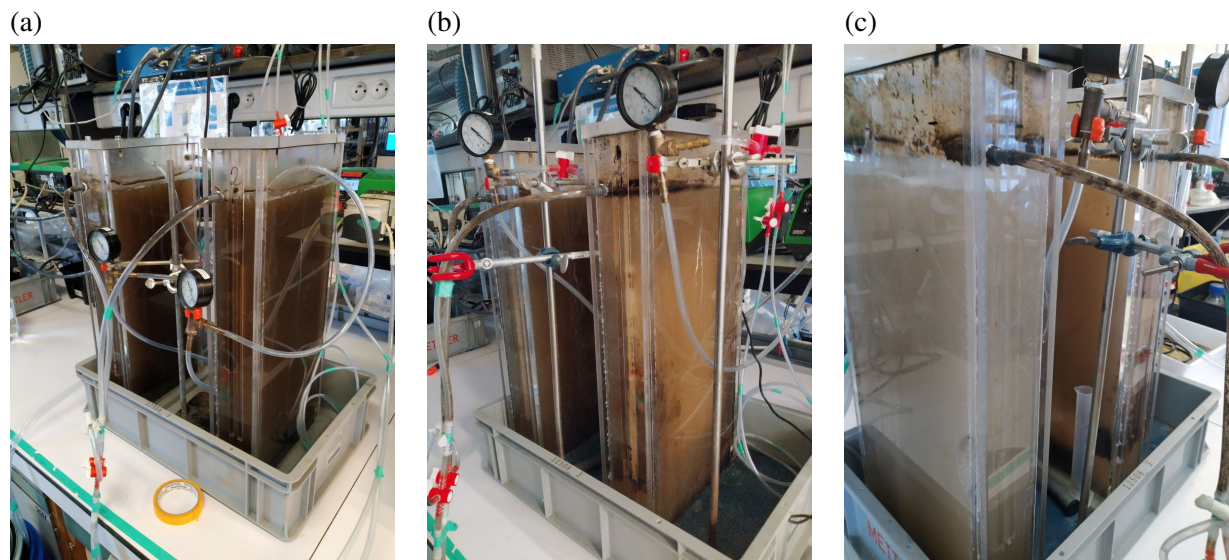


Figure B.6: Progression of the overflow events. (a) just after inoculation, day 0. (b) after the first overflow event, day 4. (c) after the fourth overflow event, day 8. The left reactor was MBR 1, the right MBR 2.



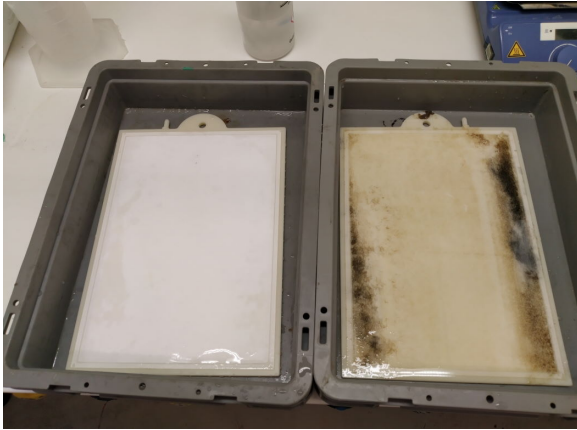


Figure B.7: Dispersed growth at the end of Phase I, after settling of the activated sludge.



Figure B.8: The ceramic membranes used in Phase III.

(a)



(b)

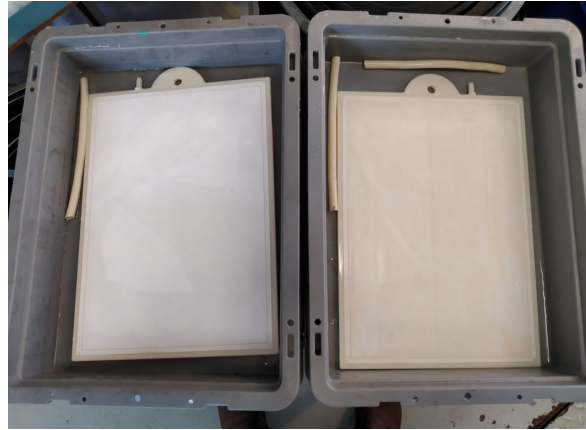


Figure B.9: The polymeric membranes used, before (a) and after (b) cleaning. The left membrane was yet unused.

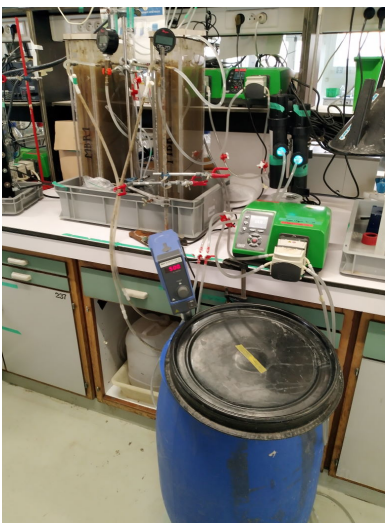


Figure B.10: Overview of the MBR setup.

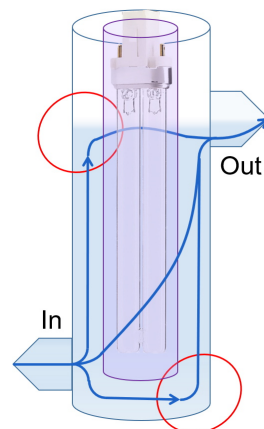


Figure B.11: Diagram of the UV reactor, with the violet cylinder being the UV lamp casing, the blue arrows indicating possible flow paths, and the red circles indicating the most likely locations of dead volume.

Table C.1: Main differences between membrane polymers of 6 polymer families, polytetrafluoroethylene not included. Adapted from Judd [2011] and Park *et al.* [2015]

Polymer family	Advantages	Disadvantages
Cellulose acetate (CA))	Fully hydrophilic (low fouling). Good controllability of pore size.	Biodegradability and poor tolerance to caustic cleaning chemicals. Limited chemical resistance, susceptible to hydrolysis below pH 4 and above pH 8.
Polypropylene (PP)	Satisfactory MF membranes. Low material costs.	Fully hydrophobic. Permeability may be low due to low pore density. Slightly wider pore size distribution. Cannot be made hydrophilic. Lower chlorine tolerance.
Polyethylene (PE)	Satisfactory MF membranes. Can be made hydrophilic through post-treatment. Good acid tolerance. Low material costs.	Fully hydrophobic. Permeability may be low due to low pore density. Slightly wider pore size distribution. Lower chlorine tolerance.
Poly(ether)sulfone (PS/PES)	Good controllability of pore size. Higher solubility of polymer, making it suitable for polymer blends. Generally the highest mechanical strength among polymers. High chemical resistance between pH 1.5 and 13.	Intermediately hydrophobic, but can be modified through additives (copolymers) or post-treatment.
Polyacrylonitrile (PAN)	Good controllability of pore size. Wide pH tolerance.	Intermediately hydrophobic, but can be modified through additives (copolymers) or post-treatment. Moderate chlorine tolerance.
Polyvinylidene difluoride (PVDF)	Good controllability of pore size. Combination of generally high strength, flexibility, and chemical resistance. Highly tolerant to chlorine.	Intermediately hydrophobic, but can be modified through additives (copolymers) or post-treatment, although this is more difficult for PVDF.

Table C.2: Main properties of different ceramic top-layer materials. Adapted from [Abdullayev et al. \[2019\]](#); [Gitis and Rothenberg \[2016\]](#).

Top-layer type	Advantages	Disadvantages	Applications
Alumina ( $\text{Al}_2\text{O}_3$ )	Abundant, good chemical and thermal stability, relatively good strength and thermal and electrical insulation properties. Multiple allotropes can be used for a desired pore size (boehmite, $\gamma\text{-Al}_2\text{O}_3$ , $\alpha\text{-Al}_2\text{O}_3$ ).	High sintering temperature ( $>1300\text{ }^\circ\text{C}$ ). Impurities cause cracking at relatively low stress values.	Excellent for low-cost applications not requiring high performance.
Silicon Carbide (SiC)	Superb fouling resistance due to hydrophilicity and a low iso-electric point <sup>a</sup>	High sintering temperatures ( $2000\text{ }^\circ\text{C}$ ) unless additives are added <sup>b</sup>	Ideal for applications with high fouling potential.
Silica ( $\text{SiO}_2$ )	Thin coating layer possible (30 nm) with true micropores ( $< 2\text{ nm}$ ).	Low reproducibility, high hydrothermal instability.	Molecular sieving and gas separation
Titania ( $\text{TiO}_2$ )	Excellent chemical resistance at both acidic and alkali pH. Photocatalytic properties under UV light. Low sintering temperatures ( $300\text{--}400\text{ }^\circ\text{C}$ ). Lower fouling susceptibility <sup>a</sup> (compared to $\text{Al}_2\text{O}_3$ and $\text{ZrO}_2$ ).	Self-standing membranes, <i>i.e.</i> no support layer, the entire membrane is $\text{TiO}_2$ , have poor structural stability and cannot be assembled in a module.	Mainly used for its photocatalytic properties.
Zirconia ( $\text{ZrO}_2$ )	High chemical stability, especially in alkali solutions.	Low thermal stability, cracking when heated above $1173\text{ }^\circ\text{C}$ . Only fit for top-layer construction.	Solid electrolyte membrane for high-temperature fuel cells.
Zeolites ( $[(\text{SiO}_2)(\text{AlO}_2)_x]\text{M}\cdot y\text{H}_2\text{O}$ )	Exceptional chemical and thermal stability, as well as catalytic activity. Also ion exchange and adsorption is possible, allowing for a multifunctional separation material. Natural zeolites can be sourced cheaply. Relatively low sintering temperatures ( $800\text{--}900\text{ }^\circ\text{C}$ ). Superior ammonia adsorption.	Relatively new for membrane separations, mechanical strength not comprehensively researched yet.	Gas separation, catalytic membrane reactors at high temperatures, water treatment.

*Continued on next page*



Table C.2 – Continued from previous page

Top-layer type		Advantages	Disadvantages	Applications
Kaolin ( $3\text{Al}_2\text{O}_3 \cdot 2\text{SiO}_2$ $\text{SiO}_2$ )	clay and	Easily sourceable, cheaply and widely available. Good pore structures and mechanical properties, low processing temperatures possible (400-700 °C).	Increased mechanical strength requires higher sintering temperatures (850–1550 °C).	Low cost water filtration applications, pore size 0.1 to 1.2 $\mu\text{m}$ , 30–50% porosity.
Attapulgitic clay		Large specific surface area, excellent mechanical strength, high adsorptive capacity along with high chemical and thermal stability, can be prepared without sintering. Can be made flexible with the addition of long-chain polymers. High permeability		UF applications (2 nm pore size, porosity above 60%).
Apatite ( $\text{Ca}_5(\text{PO}_4)_3(\text{F}, \text{Cl}, \text{OH})$ )		Low cost, cation exchange and adsorption possible, similar to zeolites.	Lower mechanical strength as self-standing membrane.	UF applications (83 nm pore size, porosity of 55%)
Fly ash ( $\text{SiO}_2$ , $\text{Al}_2\text{O}_3$ , $\text{Fe}_2\text{O}_3$ , and $\text{CaO}$ )		Abundant and very cheap waste product.	Highly variable composition of ash and by extension membrane. Additives such as bauxite are needed to improve mechanical and chemical stability, which increases sintering temperature above 1100 °C.	Low cost MF applications (<1 $\mu\text{m}$ , 30–52% porosity).

<sup>a</sup> Hofs *et al.* [2011]<sup>b</sup> Das *et al.* [2018]

## References

- Abdel-Shafy, H.I., Al-Sulaiman, A.M., 2014. Assessment of Physico-chemical Processes for Treatment and Reuse of Greywater. *Egyptian Journal of Chemistry* 57(3) 215–231, doi:<https://doi.org/10.21608/ejchem.2014.1042>.
- Abdullayev, A., Bekheet, M.F., Hanaor, D.A.H., Gurlo, A., 2019. Materials and Applications for Low-Cost Ceramic Membranes. *Membranes* 9(9) 105, doi:<https://doi.org/10.3390/membranes9090105>.
- Abed, S.N., Almuktar, S.A., Scholz, M., 2020. Impact of Storage Time on Characteristics of Synthetic Greywater for Two Different Pollutant Strengths to Be Treated or Recycled. *Water, Air, and Soil Pollution* 231(5) 211, doi:<https://doi.org/10.1007/s11270-020-04602-1>.
- Ahm, M., Thorndahl, S., Nielsen, J.E., Rasmussen, M.R., 2016. Estimation of combined sewer overflow discharge: a software sensor approach based on local water level measurements. *Water Science and Technology* 74(11) 2683–2696, doi:<https://doi.org/10.2166/wst.2016.361>.
- Ahn, K.H., Song, J.H., Cha, H.Y., 1998. Application of tubular ceramic membranes for reuse of wastewater from buildings. *Water Science and Technology* 38(4-5) 373–382, doi:<https://doi.org/10.2166/wst.1998.0671>.
- Aiyuk, S., Verstraete, W., 2004. Sedimentological evolution in an UASB treating SYNTHES, a new representative synthetic sewage, at low loading rates. *Bioresource Technology* 93(3) 269–278, doi:<https://doi.org/10.1016/j.biortech.2003.11.006>.
- Alcalde Sanz, L., Gawlik, B., European Commission Joint Research Centre, 2014. Water reuse in Europe: relevant guidelines, needs for and barriers to innovation., Publications Office of the European Union, Luxembourg, doi:<https://www.doi.org/10.2788/29234>.
- Alim, M.A., Rahman, A., Tao, Z., Samali, B., Khan, M.M., Shirin, S., 2020. Feasibility analysis of a small-scale rainwater harvesting system for drinking water production at Werrington, New South Wales, Australia. *Journal of Cleaner Production* 270 122437, doi:<https://doi.org/10.1016/j.jclepro.2020.122437>.
- Alloul, A., Ganigué, R., Spiller, M., Meerburg, F., Cagnetta, C., Rabaey, K., Vlaeminck, S., 2018. Capture-ferment-upgrade : a three-step approach for the valorization of sewage organics as commodities. *Environmental Science & Technology* 52(12) 6729–6742, doi:<http://doi.org/10.1021/acs.est.7b05712>.
- American Public Health Association, Baird, R., Eaton, A.D., Rice, E.W., Bridgewater, L., American Water Works Association, Water Environment Federation, 2017. Standard Methods for the Examination of Water and Wastewater, American Water Works Association.
- Arndt, F., Ehlen, F., Schütz, S., Anlauf, H., Nirschl, H., 2016. Influence of operating parameters and membrane materials on fouling of ceramic hollow fibre membranes. *Separation and Purification Technology* 171 289–296, doi:<https://doi.org/10.1016/j.seppur.2016.07.046>.

- Asano, T., Burton, F.L., Leverenz, H.L., Tsuchihashi, R., Tchobanoglous, G., 2007. *Water Reuse: Issues, Technologies, and Applications*, Metcalf & Eddy (AECOM), McGraw-Hill, New York.
- Atanasova, N., Dalmau, M., Comas, J., Poch, M., Rodriguez-Roda, I., Buttiglieri, G., 2017. Optimized MBR for greywater reuse systems in hotel facilities. *Journal of Environmental Management* 193 503–511, doi:<https://doi.org/10.1016/j.jenvman.2017.02.041>.
- Atasoy, E., Murat, S., Baban, A., Tiris, M., 2007. Membrane Bioreactor (MBR) Treatment of Segregated Household Wastewater for Reuse. *CLEAN – Soil, Air, Water* 35(5) 465–472, doi:<https://doi.org/10.1002/clen.200720006>.
- Azimi, Y., Allen, D.G., Seto, P., Farnood, R., 2014. Effect of Activated Sludge Retention Time, Operating Temperature, and Influent Phosphorus Deficiency on Floc Physicochemical Characteristics and UV Disinfection. *Industrial & Engineering Chemistry Research* 53(31) 12485–12493, doi:<https://doi.org/10.1021/ie5012068>.
- Baghaei Lakeh, R., Andrade, D., Miller, K.J., Du, B., Pham, J., Modabernia, M.M., Ng, P.Y., Nguyen, T.N., Nguyen, J.L., Mena, C., Anderson, K.R., Sharbatmaleki, M., 2017. A Case Study of Decentralized Off-Grid Water Treatment Using Reverse Osmosis, in *Volume 5: Education and Globalization*, American Society of Mechanical Engineers, doi:<https://doi.org/10.1115/IMECE2017-70828>.
- Beard, J.E., Bierkens, M.F.P., Bartholomeus, R.P., 2019. Following the Water: Characterising de facto Wastewater Reuse in Agriculture in the Netherlands. *Sustainability* 11(21) 5936, doi:<https://doi.org/10.3390/su11215936>.
- Benami, M., Busgang, A., Gillor, O., Gross, A., 2016. Quantification and risks associated with bacterial aerosols near domestic greywater-treatment systems. *Science of The Total Environment* 562 344–352, doi:<https://doi.org/10.1016/j.scitotenv.2016.03.200>.
- Besson, M., Berger, S., Tiruta-barna, L., Paul, E., Spérandio, M., 2021. Environmental assessment of urine, black and grey water separation for resource recovery in a new district compared to centralized wastewater resources recovery plant. *Journal of Cleaner Production* 301 126868, doi:<https://doi.org/10.1016/j.jclepro.2021.126868>.
- Bhattacharya, P., Sarkar, S., Ghosh, S., Majumdar, S., Mukhopadhyay, A., Bandyopadhyay, S., 2013. Potential of ceramic microfiltration and ultrafiltration membranes for the treatment of gray water for an effective reuse. *Desalination and Water Treatment* 51(22-24) 4323–4332, doi:<https://doi.org/10.1080/19443994.2013.770198>.
- Biesterbos, J.W.H., Dudzina, T., Delmaar, C.J.E., Bakker, M.I., Russel, F.G.M., von Goetz, N., Scheepers, P.T.J., Roeleveld, N., 2013. Usage patterns of personal care products: Important factors for exposure assessment. *Food and Chemical Toxicology* 55 8–17, doi:<https://doi.org/10.1016/j.fct.2012.11.014>.
- Boano, F., Caruso, A., Costamagna, E., Ridolfi, L., Fiore, S., Demichelis, F., Galvão, A., Piscoiro, J., Rizzo, A., Masi, F., 2020. A review of nature-based solutions for greywater treatment: Applications, hydraulic design, and environmental benefits. *Science of The Total Environment* 711 134731, doi:<https://doi.org/10.1016/j.scitotenv.2019.134731>.

- Bonthuys, G.J., Blom, P., van Dijk, M., 2020. Leveraging Asset Management Data for Energy Recovery and Leakage Reduction, in J.P. Liyanage, J. Amadi-Echendu, J. Mathew, eds., *Engineering Assets and Public Infrastructures in the Age of Digitalization*, 309–317, Springer International Publishing, doi:[https://doi.org/10.1007/978-3-030-48021-9\\_35](https://doi.org/10.1007/978-3-030-48021-9_35).
- Brown, R.R., Keath, N., Wong, T.H.F., 2009. Urban water management in cities: historical, current and future regimes. *Water Science and Technology* 59(5) 847–855, doi:<https://doi.org/10.2166/wst.2009.029>.
- Bu, Q., Wang, B., Huang, J., Deng, S., Yu, G., 2013. Pharmaceuticals and personal care products in the aquatic environment in China: A review. *Journal of Hazardous Materials* 262 189–211, doi:<https://doi.org/10.1016/j.jhazmat.2013.08.040>.
- Buekenhoudt, A., 2008. Stability of Porous Ceramic Membranes, in *Inorganic Membranes: Synthesis, Characterization and Applications*, Volume 13 of *Membrane Science and Technology*, 1–31, Elsevier, doi:[https://doi.org/10.1016/S0927-5193\(07\)13001-1](https://doi.org/10.1016/S0927-5193(07)13001-1).
- Burek, P., Satoh, Y., Fischer, G., Kahil, M.T., Scherzer, A., Tramberend, S., Nava, L.F., Wada, Y., Eisner, S., Flörke, M., Hanasaki, N., Magnuszewski, P., Cosgrove, B., Wiberg, D., 2016. *Water Futures and Solution - Fast Track Initiative (Final Report)*, IIASA Working Paper, IIASA, Laxenburg, Austria.
- Burmistrov, I., Agarkov, D., Bredikhin, S., Nepochatov, Y., Tiunova, O., Zadorozhnaya, O., 2013. Multilayered Electrolyte-Supported SOFC Based on NEVZ-Ceramics Membrane. *ECS Transactions* 57(1) 917–923, doi:<https://doi.org/10.1149/05701.0917ecst>.
- Butler, D., Friedler, E., Gatt, K., 1995. Characterising the quantity and quality of domestic wastewater inflows. *Water Science and Technology* 31(7) 13–24, doi:[https://doi.org/10.1016/0273-1223\(95\)00318-H](https://doi.org/10.1016/0273-1223(95)00318-H).
- Cai, Y.H., Schäfer, A.I., 2020. Renewable energy powered membrane technology: Impact of solar irradiance fluctuation on direct osmotic backwash. *Journal of Membrane Science* 598 117666, doi:<https://doi.org/10.1016/j.memsci.2019.117666>.
- California Department of Water Resources, 2016. *Municipal Recycled Water: A Resource Management Strategy of the California Water Plan*, , California natural resources agency.
- Collivignarelli, M., Abbà, A., Benigna, I., Sorlini, S., Torretta, V., 2017. Overview of the Main Disinfection Processes for Wastewater and Drinking Water Treatment Plants. *Sustainability* 10(2) 86, doi:<https://doi.org/10.3390/su10010086>.
- Coördinatiecommissie Integraal Waterbeleid, 2019. *Evaluatierapport waterschaarste en droogte 2018* (Dutch), retrieved 29/12/2020.  
URL <https://www.integraalwaterbeleid.be/nl/nieuws/downloads-van-nieuwsberichten/tussentijds-evaluatierapport-waterschaarste-en-droogte-2018-1/view>
- Cornejo, P.K., Zhang, Q., Mihelcic, J.R., 2016. How Does Scale of Implementation Impact the Environmental Sustainability of Wastewater Treatment Integrated with Resource Recovery? *Environmental Science & Technology* 50(13) 6680–6689, doi:<https://doi.org/10.1021/acs.est.5b05055>.

- Crook, M.J., Jefferson, B., Autin, O., MacAdam, J., Nocker, A., 2014. Comparison of ultraviolet light emitting diodes with traditional UV for greywater disinfection. *Journal of Water Reuse and Desalination* 5(1) 17–27, doi:<https://doi.org/10.2166/wrd.2014.022>.
- Cruz, H., Law, Y.Y., Gues, J.S., Rabaey, K., Batstone, D., Laycock, B., Verstraete, W., Pikaar, I., 2019. Mainstream ammonium recovery to advance sustainable urban wastewater management. *Environmental Science & Technology* 53(19) 11066–11079, doi:<http://doi.org/10.1021/acs.est.9b00603>.
- Dahlgren, E., Göçmen, C., Lackner, K., van Ryzin, G., 2013. Small Modular Infrastructure. *The Engineering Economist* 58(4) 231–264, doi:<https://doi.org/10.1080/0013791X.2013.825038>.
- Daigger, G.T., 2009. Evolving Urban Water and Residuals Management Paradigms: Water Reclamation and Reuse, Decentralization, and Resource Recovery. *Water Environment Research* 81(8) 809–823, doi:<https://doi.org/10.2175/106143009X425898>.
- Das, D., Baitalik, S., Haldar, B., Saha, R., Kayal, N., 2018. Preparation and characterization of macroporous SiC ceramic membrane for treatment of waste water. *Journal of Porous Materials* 25(4) 1183–1193, doi:<https://doi.org/10.1007/s10934-017-0528-5>.
- Databank Ondergrond Vlaanderen, s.d. Actuele grondwaterstandindicator (Dutch), retrieved 29/12/2020.  
URL <https://www.dov.vlaanderen.be/page/actuele-grondwaterstandindicator>
- Daud, S.M., Daud, W.R.W., Kim, B.H., Somalu, M.R., Bakar, M.H.A., Muchtar, A., Jahim, J.M., Lim, S.S., Chang, I.S., 2018. Comparison of performance and ionic concentration gradient of two-chamber microbial fuel cell using ceramic membrane (CM) and cation exchange membrane (CEM) as separators. *Electrochimica Acta* 259 365–376, doi:<https://doi.org/10.1016/j.electacta.2017.10.118>.
- De Nocker, L., Liekens, I., Broekx, S., 2017. Water, een kostbaar goed. Uitgevoerd in opdracht van de VMM (Dutch), , Vlaams Instelling voor Technologisch Onderzoek.  
URL <https://www.integraalwaterbeleid.be/nl/publicaties/afbeeldingen/vito-rapport-water-een-kostbaar-goed/view>
- De Paepe, J., De Paepe, K., Gòdia, F., Rabaey, K., Vlaeminck, S.E., Clauwaert, P., 2020. Bio-electrochemical COD removal for energy-efficient, maximum and robust nitrogen recovery from urine through membrane aerated nitrification. *Water Research* 185 116223, doi:<https://doi.org/10.1016/j.watres.2020.116223>.
- De Watergroep, 2019. Proefproject drinkwater uit regenwater (Dutch), retrieved 15/11/2020.  
URL <https://www.dewatergroep.be/nl-be/over-de-watergroep/nieuws/proefproject-drinkwater-uit-regenwater>
- de Wit, P., Kappert, E.J., Lohaus, T., Wessling, M., Nijmeijer, A., Benes, N.E., 2015. Highly permeable and mechanically robust silicon carbide hollow fiber membranes. *Journal of Membrane Science* 475 480–487, doi:<https://doi.org/10.1016/j.memsci.2014.10.045>.

- Delgado, N., Bermeo, L., Hoyos, D.A., Peñuela, G.A., Capparelli, A., Marino, D., Navarro, A., Casas-Zapata, J.C., 2020. Occurrence and removal of pharmaceutical and personal care products using subsurface horizontal flow constructed wetlands. *Water Research* 187 116448, doi:<https://doi.org/10.1016/j.watres.2020.116448>.
- di Chen, Y., Duan, X., Zhou, X., Wang, R., Wang, S., qi Ren, N., Ho, S.H., 2021. Advanced oxidation processes for water disinfection: Features, mechanisms and prospects. *Chemical Engineering Journal* 409 128207, doi:<https://doi.org/10.1016/j.cej.2020.128207>.
- Diaz-Elsayed, N., Rezaei, N., Guo, T., Mohebbi, S., Zhang, Q., 2019. Wastewater-based resource recovery technologies across scale: A review. *Resources, Conservation and Recycling* 145 94–112, doi:<https://doi.org/10.1016/j.resconrec.2018.12.035>.
- Ding, A., Liang, H., Li, G., Derlon, N., Szivak, I., Morgenroth, E., Pronk, W., 2016. Impact of aeration shear stress on permeate flux and fouling layer properties in a low pressure membrane bioreactor for the treatment of grey water. *Journal of Membrane Science* 510 382–390, doi:<https://doi.org/10.1016/j.memsci.2016.03.025>.
- Domènech, L., Saurí, D., 2010. Socio-technical transitions in water scarcity contexts: Public acceptance of greywater reuse technologies in the Metropolitan Area of Barcelona. *Resources, Conservation and Recycling* 55(1) 53–62, doi:<https://doi.org/10.1016/j.resconrec.2010.07.001>.
- Domènech, L., Saurí, D., 2011. A comparative appraisal of the use of rainwater harvesting in single and multi-family buildings of the Metropolitan Area of Barcelona (Spain): social experience, drinking water savings and economic costs. *Journal of Cleaner Production* 19(6-7) 598–608, doi:<https://doi.org/10.1016/j.jclepro.2010.11.010>.
- Domínguez Henao, L., Turolla, A., Antonelli, M., 2018. Disinfection by-products formation and ecotoxicological effects of effluents treated with peracetic acid: A review. *Chemosphere* 213 25–40, doi:<https://doi.org/10.1016/j.chemosphere.2018.09.005>.
- Driesen, N., 2021. Aiming for a water independent household by direct reuse of greywater using an integrated MBBR-EC treatment train, [unpublished master's thesis], Ghent University.
- Dubowski, Y., Alfiya, Y., Gilboa, Y., Sabach, S., Friedler, E., 2020. Removal of organic micropollutants from biologically treated greywater using continuous-flow vacuum-UV/UVC photo-reactor. *Environmental Science and Pollution Research* 27(7) 7578–7587, doi:<https://doi.org/10.1007/s11356-019-07399-7>.
- Eggimann, S., Truffer, B., Feldmann, U., Maurer, M., 2018. Screening European market potentials for small modular wastewater treatment systems - an inroad to sustainability transitions in urban water management? *Land Use Policy* 78 711–725, doi:<https://doi.org/10.1016/j.landusepol.2018.07.031>.
- Eggimann, S., Truffer, B., Maurer, M., 2016. Economies of density for on-site waste water treatment. *Water Research* 101 476–489, doi:<https://doi.org/10.1016/j.watres.2016.06.011>.

- Emmerton, C.A., Cooke, C.A., Hustins, S., Silins, U., Emelko, M.B., Lewis, T., Kruk, M.K., Taube, N., Zhu, D., Jackson, B., Stone, M., Kerr, J.G., Orwin, J.F., 2020. Severe western Canadian wildfire affects water quality even at large basin scales. *Water Research* 183 116071, doi:<https://doi.org/10.1016/j.watres.2020.116071>.
- Eom, J.H., Yeom, H.J., Kim, Y.W., Song, I.H., 2015. Ceramic Membranes Prepared from a Silicate and Clay-mineral Mixture for Treatment of Oily Wastewater. *Clays and Clay Minerals* 63(3) 222–234, doi:<https://doi.org/10.1346/CCMN.2015.0630305>.
- Eriksson, E., Andersen, H.R., Madsen, T.S., Ledin, A., 2009. Greywater pollution variability and loadings. *Ecological Engineering* 35(5) 661–669, doi:<https://doi.org/10.1016/j.ecoleng.2008.10.015>.
- Escudero, J., Muñoz, J.L., Morera-Herreras, T., Hernandez, R., Medrano, J., Domingo-Echaburu, S., Barceló, D., Orive, G., Lertxundi, U., 2021. Antipsychotics as environmental pollutants: An underrated threat? *Science of The Total Environment* 769 144634, doi:<https://doi.org/10.1016/j.scitotenv.2020.144634>.
- Etchepare, R., van der Hoek, J.P., 2015. Health risk assessment of organic micropollutants in greywater for potable reuse. *Water Research* 72 186–198, doi:<https://doi.org/10.1016/j.watres.2014.10.048>.
- Fang, J., Liu, H., Shang, C., Zeng, M., Ni, M., Liu, W., 2014. *E. coli* and bacteriophage MS2 disinfection by UV, ozone and the combined UV and ozone processes. *Frontiers of Environmental Science & Engineering* 8(4) 547–552, doi:<https://doi.org/10.1007/s11783-013-0620-2>.
- Fenner, R.A., Komvuschara, K., 2005. A New Kinetic Model for Ultraviolet Disinfection of Greywater. *Journal of Environmental Engineering* 131(6) 850–864, doi:[https://doi.org/10.1061/\(ASCE\)0733-9372\(2005\)131:6\(850\)](https://doi.org/10.1061/(ASCE)0733-9372(2005)131:6(850)).
- Ficheux, A.S., Gomez-Berrada, M.P., Roudot, A.C., Ferret, P.J., 2019. Consumption and exposure to finished cosmetic products: A systematic review. *Food and Chemical Toxicology* 124 280–299, doi:<https://doi.org/10.1016/j.fct.2018.11.060>.
- Fielding, K.S., Dolnicar, S., Schultz, T., 2019. Public acceptance of recycled water. *International Journal of Water Resources Development* 35(4) 551–586, doi:<https://doi.org/10.1080/07900627.2017.1419125>.
- Finley, S., Barrington, S., Lyew, D., 2009. Reuse of Domestic Greywater for the Irrigation of Food Crops. *Water, Air, and Soil Pollution* 199(1-4) 235–245, doi:<https://doi.org/10.1007/s11270-008-9874-x>.
- Flint, C.G., Koci, K.R., 2021. Local resident perceptions of water reuse in Northern Utah. *Water Environment Research* 93(1) 123–135, doi:<https://doi.org/10.1002/wer.1367>.
- Fogler, H.S., 2016. *Elements of Chemical Reaction Engineering, Chapter Residence Time Distributions of Chemical Reactors*, 767–806, Prentice Hall, Boston, fifth Edition.
- Folkman, S., 2018. *Water main break rates in the USA and Canada: A comprehensive study*. Mechanical and Aerospace Engineering Faculty Publications. .



- Fountoulakis, M.S., Markakis, N., Petousi, I., Manios, T., 2016. Single house on-site grey water treatment using a submerged membrane bioreactor for toilet flushing. *Science of The Total Environment* 551-552 706–711, doi:<https://doi.org/10.1016/j.scitotenv.2016.02.057>.
- French, A.P., Taylor, E.F., 1978. *An Introduction to Quantum Physics*, M.I.T. Introductory Physics Series, CRC Press, Taylor & Francis Group, Boca Raton, Florida, first Edition.
- Friedler, E., F. Chavez, D., Alfiya, Y., Gilboa, Y., Gross, A., 2021. Impact of Suspended Solids and Organic Matter on Chlorine and UV Disinfection Efficiency of Greywater. *Water* 13(2) 214, doi:<https://doi.org/10.3390/w13020214>.
- Friedler, E., Gilboa, Y., 2010. Performance of UV disinfection and the microbial quality of greywater effluent along a reuse system for toilet flushing. *Science of The Total Environment* 408(9) 2109–2117, doi:<https://doi.org/10.1016/j.scitotenv.2010.01.051>.
- Friedler, E., Shwartzman, Z., Ostfeld, A., 2008. Assessment of the reliability of an on-site MBR system for greywater treatment and the associated aesthetic and health risks. *Water Science and Technology* 57(7) 1103–1110, doi:<https://doi.org/10.2166/wst.2008.248>.
- Gao, M., Zhang, L., Guo, B., Zhang, Y., Liu, Y., 2019. Enhancing biomethane recovery from source-diverted blackwater through hydrogenotrophic methanogenesis dominant pathway. *Chemical Engineering Journal* 378 122258, doi:<https://doi.org/10.1016/j.cej.2019.122258>.
- Garcia-Hidalgo, E., von Goetz, N., Siegrist, M., Hungerbühler, K., 2017. Use-patterns of personal care and household cleaning products in Switzerland. *Food and Chemical Toxicology* 99 24–39, doi:<https://doi.org/10.1016/j.fct.2016.10.030>.
- García-Sánchez, M., Güereca, L.P., 2019. Environmental and social life cycle assessment of urban water systems: The case of Mexico City. *Science of The Total Environment* 693 133464, doi:<https://doi.org/10.1016/j.scitotenv.2019.07.270>.
- Gassie, L.W., Englehardt, J.D., 2017. Advanced oxidation and disinfection processes for onsite net-zero greywater reuse: A review. *Water Research* 125 384–399, doi:<https://doi.org/10.1016/j.watres.2017.08.062>.
- Giresunlu, E., Beler Baykal, B., 2016. A case study of the conversion of grey water to a flush water source in a Turkish student residence hall. *Water Supply* 16(6) 1659–1667, doi:<https://doi.org/10.2166/ws.2016.078>.
- Gitis, V., Rothenberg, G., 2016. *Ceramic Membranes: New Opportunities and Practical Applications*, Wiley, doi:<https://www.doi.org/10.1002/9783527696550>.
- Gomez, V., Majamaa, K., Pocurull, E., Borrull, F., 2012. Determination and occurrence of organic micropollutants in reverse osmosis treatment for advanced water reuse. *Water Science and Technology* 66(1) 61–71, doi:<https://doi.org/10.2166/wst.2012.166>.
- Gomez-Berrada, M.P., Ficheux, A.S., Dahmoul, Z., Roudot, A.C., Ferret, P.J., 2017. Exposure assessment of family cosmetic products dedicated to babies, children and adults. *Food and Chemical Toxicology* 103 56–65, doi:<https://doi.org/10.1016/j.fct.2017.02.024>.

- Gonçalves, R.F., de Oliveira Vaz, L., Peres, M., Merlo, S.S., 2020. Microbiological risk from non-potable reuse of greywater treated by anaerobic filters associated to vertical constructed wetlands. *Journal of Water Process Engineering* 39 101751, doi:<https://doi.org/10.1016/j.jwpe.2020.101751>.
- Goodwin, D., Raffin, M., Jeffrey, P., Smith, H.M., 2019. Collaboration on risk management: The governance of a non-potable water reuse scheme in London. *Journal of Hydrology* 573 1087–1095, doi:<https://doi.org/10.1016/j.jhydrol.2017.07.020>.
- Gorgich, M., Mata, T.M., Martins, A., Caetano, N.S., Formigo, N., 2020. Application of domestic greywater for irrigating agricultural products: A brief study. *Energy Reports* 6 811–817, doi:<https://doi.org/10.1016/j.egyr.2019.11.007>.
- Gross, A., Maimon, A., Alfiya, Y., Friedler, E., 2015. *Greywater Reuse*, CRC Press, Boca Raton, FL.
- Guo, T., Englehardt, J., Wu, T., 2014. Review of cost versus scale: Water and wastewater treatment and reuse processes. *Water Science and Technology* 69(2) 223–234, doi:<https://doi.org/10.2166/wst.2013.734>.
- Hartley, K., Tortajada, C., Biswas, A.K., 2019. A formal model concerning policy strategies to build public acceptance of potable water reuse. *Journal of Environmental Management* 250 109505, doi:<https://doi.org/10.1016/j.jenvman.2019.109505>.
- Hasan, M.M., Shafiquzzaman, M., Nakajima, J., Ahmed, A.K.T., Azam, M.S., 2015. Application of a Low Cost Ceramic Filter to a Membrane Bioreactor for Greywater Treatment. *Water Environment Research* 87(3) 233–241, doi:<https://doi.org/10.1002/j.1554-7531.2015.tb00141.x>.
- Hasik, V., Anderson, N.E., Collinge, W.O., Thiel, C.L., Khanna, V., Wirick, J., Piacentini, R., Landis, A.E., Bilec, M.M., 2017. Evaluating the Life Cycle Environmental Benefits and Trade-Offs of Water Reuse Systems for Net-Zero Buildings. *Environmental Science & Technology* 51(3) 1110–1119, doi:<https://doi.org/10.1021/acs.est.6b03879>.
- Health Canada, 2010. *Canadian Guidelines for Domestic Reclaimed Water for Use in Toilet and Urinal Flushing*, Working Group on Domestic Reclaimed Water of the Federal-Provincial-Territorial Committee on Health and the Environment, Ottawa, Ont.
- Hering, J.G., Waite, T.D., Luthy, R.G., Drewes, J.E., Sedlak, D.L., 2013. A Changing Framework for Urban Water Systems. *Environmental Science & Technology* 47(19) 10721–10726, doi:<https://doi.org/10.1021/es4007096>.
- Hernández Leal, L., Temmink, H., Zeeman, G., Buisman, C.J.N., 2010. Bioflocculation of grey water for improved energy recovery within decentralized sanitation concepts. *Bioresource Technology* 101(23) 9065–9070, doi:<https://doi.org/10.1016/j.biortech.2010.07.047>.
- Hijnen, W.A.M., Beerendonk, E.F., Medema, G.J., 2006. Inactivation credit of UV radiation for viruses, bacteria and protozoan (oo)cysts in water: A review. *Water Research* 40(1) 3–22, doi:<https://doi.org/10.1016/j.watres.2005.10.030>.

- Hocaoglu, S.M., Atasoy, E., Baban, A., Orhon, D., 2013. Modeling biodegradation characteristics of grey water in membrane bioreactor. *Journal of Membrane Science* 429 139–146, doi:<https://doi.org/10.1016/j.memsci.2012.11.012>.
- Hocaoglu, S.M., Insel, G., Cokgor, E.U., Orhon, D., 2011. Effect of low dissolved oxygen on simultaneous nitrification and denitrification in a membrane bioreactor treating black water. *Bioresource Technology* 102(6) 4333–4340, doi:<https://doi.org/10.1016/j.biortech.2010.11.096>.
- Hocaoglu, S.M., Orhon, D., 2010. Fate of proteins and carbohydrates in membrane bioreactor operated at high sludge age. *Journal of Environmental Science and Health* 45(9) 1101–1108, doi:<https://doi.org/10.1080/10934529.2010.486342>.
- Hoffmann, S., Feldmann, U., Bach, P.M., Binz, C., Farrelly, M., Frantzeskaki, N., Hiessl, H., Inauen, J., Larsen, T.A., Lienert, J., Londong, J., Lüthi, C., Maurer, M., Mitchell, C., Morgenroth, E., Nelson, K.L., Scholten, L., Truffer, B., Udert, K.M., 2020. A Research Agenda for the Future of Urban Water Management: Exploring the Potential of Nongrid, Small-Grid, and Hybrid Solutions. *Environmental Science & Technology* 54(9) 5312–5322, doi:<http://doi.org/10.1021/acs.est.9b05222>.
- Hofs, B., Ogier, J., Vries, D., Beerendonk, E.F., Cornelissen, E.R., 2011. Comparison of ceramic and polymeric membrane permeability and fouling using surface water. *Separation and Purification Technology* 79(3) 365–374, doi:<https://doi.org/10.1016/j.seppur.2011.03.025>.
- Hourlier, F., Masse, A., Jaouen, P., Lakel, A., Gerente, C., Faur, C., Le Cloirec, P., 2010. Formulation of synthetic greywater as an evaluation tool for wastewater recycling technologies. *Environmental Technology* 31(2) 215–223, doi:<https://doi.org/10.1080/09593330903431547>.
- Huang, X., Qu, Y., Cid, C.A., Finke, C., Hoffmann, M.R., Lim, K., Jiang, S.C., 2016. Electrochemical disinfection of toilet wastewater using wastewater electrolysis cell. *Water Research* 92 164–172, doi:<https://doi.org/10.1016/j.watres.2016.01.040>.
- Hubadillah, S.K., Othman, M.H.D., Matsuura, T., Ismail, A.F., Rahman, M.A., Harun, Z., Jaafar, J., Nomura, M., 2018. Fabrications and applications of low cost ceramic membrane from kaolin: A comprehensive review. *Ceramics International* 44(5) 4538–4560, doi:<https://doi.org/10.1016/j.ceramint.2017.12.215>.
- Huelgas, A., Funamizu, N., 2010. Flat-plate submerged membrane bioreactor for the treatment of higher-load graywater. *Desalination* 250(1) 162–166, doi:<https://doi.org/10.1016/j.desal.2009.05.007>.
- Huelgas-Orbecido, A., Funamizu, N., 2019. Membrane System for Gray Water, 185–193, Springer Japan, Tokyo, doi:[https://doi.org/10.1007/978-4-431-56835-3\\_13](https://doi.org/10.1007/978-4-431-56835-3_13).
- Hyde, K., Smith, M., 2018. Greywater Recycling and Reuse, Chapter 16, 211–221, John Wiley & Sons, Ltd, doi:<https://doi.org/10.1002/9781119260493.ch16>.
- Hyde, K., Smith, M.J., Adeyeye, K., 2016. Developments in the quality of treated greywater supplies for buildings, and associated user perception and acceptance. *International Journal of Low-Carbon Technologies* 12(2) 136–140, doi:<https://doi.org/10.1093/ijlct/ctw006>.

- Ice, G.G., Neary, D.G., Adams, P.W., 2004. Effects of Wildfire on Soils and Watershed Processes. *Journal of Forestry* 102(6) 16–20, doi:<https://doi.org/10.1093/jof/102.6.16>.
- International Standards Organisation, 2014. ISO 9308-1:2014. Water quality - Enumeration of *Escherichia coli* and coliform bacteria - Part 1: Membrane filtration method for waters with low bacterial background flora, International Organization for Standardization, Geneva, Switzerland.
- International Standards Organisation, 2018. ISO 30500:2018. Non-sewered sanitation systems - Prefabricated integrated treatment units - General safety and performance requirements for design and testing., International Organization for Standardization, Geneva, Switzerland.
- Issaoui, M., Limousy, L., 2019. Low-cost ceramic membranes: Synthesis, classifications, and applications. *Comptes Rendus Chimie* 22(2-3) 175–187, doi:<https://doi.org/10.1016/j.crci.2018.09.014>.
- Issaoui, M., Limousy, L., Lebeau, B., Bouaziz, J., Fourati, M., 2016. Design and characterization of flat membrane supports elaborated from kaolin and aluminum powders. *Comptes Rendus Chimie* 19(4) 496–504, doi:<https://doi.org/10.1016/j.crci.2015.10.011>.
- Jabornig, S., 2014. Overview and feasibility of advanced grey water treatment systems for single households. *Urban Water Journal* 11(5) 361–369, doi:<https://doi.org/10.1080/1573062X.2013.783086>.
- Jabornig, S., Favero, E., 2013. Single household greywater treatment with a moving bed biofilm membrane reactor (MBBMR). *Journal of Membrane Science* 446 277–285, doi:<https://doi.org/10.1016/j.memsci.2013.06.049>.
- Jabornig, S., Podmirseg, S.M., 2015. A novel fixed fibre biofilm membrane process for on-site greywater reclamation requiring no fouling control. *Biotechnology and Bioengineering* 112(3) 484–493, doi:<https://doi.org/10.1002/bit.25449>.
- Jedidi, I., Saïdi, S., Khemakhem, S., Larbot, A., Elloumi-Ammar, N., Fourati, A., Charfi, A., Salah, A.B., Amar, R.B., 2009. Elaboration of new ceramic microfiltration membranes from mineral coal fly ash applied to waste water treatment. *Journal of Hazardous Materials* 172(1) 152–158, doi:<https://doi.org/10.1016/j.jhazmat.2009.06.151>.
- Jeong, H., Broesicke, O.A., Drew, B., Crittenden, J.C., 2018. Life cycle assessment of small-scale greywater reclamation systems combined with conventional centralized water systems for the City of Atlanta, Georgia. *Journal of Cleaner Production* 174 333–342, doi:<https://doi.org/10.1016/j.jclepro.2017.10.193>.
- Judd, S., 2011. *The MBR book: principles and applications of membrane bioreactors for water and wastewater treatment*, Butterworth-Heinemann, Oxford, second Edition.
- Karanfil, T., Erdogan, I., Schlautman, M.A., 2003. Selecting Filter Membranes for measuring DOC and UV254. *Journal - American Water Works Association* 95(3) 86–100, doi:<https://doi.org/10.1002/j.1551-8833.2003.tb10317.x>.

- Khemakhem, S., Ben Amar, R., Larbot, A., 2007. Synthesis and characterization of a new inorganic ultrafiltration membrane composed entirely of Tunisian natural illite clay. *Desalination* 206(1-3) 210–214, doi:<https://doi.org/10.1016/j.desal.2006.03.567>.
- Kiparsky, M., Sedlak, D.L., Thompson Jr, B.H., Truffer, B., 2013. The innovation deficit in urban water: the need for an integrated perspective on institutions, organizations, and technology. *Environmental Engineering Science* 30(8) 395–408, doi:<https://doi.org/10.1089/ees.2012.0427>.
- Kiparsky, M., Thompson, B.H., Binz, C., Sedlak, D.L., Tummers, L., Truffer, B., 2016. Barriers to Innovation in Urban Wastewater Utilities: Attitudes of Managers in California. *Environmental Management* 57(6) 1204–1216, doi:<https://doi.org/10.1007/s00267-016-0685-3>.
- Kowalski, W., 2009. *Ultraviolet Germicidal Irradiation Handbook: UVGI for Air and Surface Disinfection*, Springer Berlin Heidelberg, doi:<https://doi.org/10.1007/978-3-642-01999-9>.
- Kroll, S., Weemaes, M., Van Impe, J., Willems, P., 2018. A Methodology for the Design of RTC Strategies for Combined Sewer Networks. *Water* 10(11) 1675, doi:<https://doi.org/10.3390/w10111675>.
- Kusumawardhana, A., Zlatanovic, L., Bosch, A., van der Hoek, J.P., 2021. Microbiological Health Risk Assessment of Water Conservation Strategies: A Case Study in Amsterdam. *International Journal of Environmental Research and Public Health* 18(5) 2595, doi:<https://doi.org/10.3390/ijerph18052595>.
- Kwarciak-Kozłowska, A., 2020. Methods used for the removal of disinfection by-products from water, in M.N.V. Prasad, ed., *Disinfection By-products in Drinking Water*, 1–21, Elsevier, doi:<https://doi.org/10.1016/B978-0-08-102977-0.00001-9>.
- Lamine, M., Samaali, D., Ghrabi, A., 2012. Greywater treatment in a submerged membrane bioreactor with gravitational filtration. *Desalination and Water Treatment* 46(1-3) 182–187, doi:<https://doi.org/10.1080/19443994.2012.677553>.
- Lane, P.N.J., Feikema, P.M., Sherwin, C.B., Peel, M.C., Freebairn, A.C., 2010. Modelling the long term water yield impact of wildfire and other forest disturbance in Eucalypt forests. *Environmental Modelling & Software* 25(4) 467–478, doi:<https://doi.org/10.1016/j.envsoft.2009.11.001>.
- Larsen, T.A., Gujer, W., 1996. Separate management of anthropogenic nutrient solutions (human urine). *Water Science and Technology* 34(3-4) 87–94, doi:<https://doi.org/10.2166/wst.1996.0420>.
- Larsen, T.A., Hoffmann, S., Lüthi, C., Truffer, B., Maurer, M., 2016. Emerging solutions to the water challenges of an urbanizing world. *Science* 352(6288) 928–933, doi:<https://doi.org/10.1126/science.aad8641>.
- Larsen, T.A., Udert, K.M., Lienert, J., 2013. *Source Separation and Decentralization for Wastewater Management*, IWA Publishing, doi:<https://doi.org/10.2166/9781780401072>.

- Lemos, D., Dias, A.C., Gabarrell, X., Arroja, L., 2013. Environmental assessment of an urban water system. *Journal of Cleaner Production* 54 157–165, doi:<https://doi.org/10.1016/j.jclepro.2013.04.029>.
- Leong, C., Lebel, L., 2020. Can conformity overcome the yuck factor? explaining the choice for recycled drinking water. *Journal of Cleaner Production* 242 118196, doi:<https://doi.org/10.1016/j.jclepro.2019.118196>.
- Li, G.Q., Wang, W.L., Huo, Z.Y., Lu, Y., Hu, H.Y., 2017. Comparison of UV-LED and low pressure UV for water disinfection: Photoreactivation and dark repair of *Escherichia coli*. *Water Research* 126 134–143, doi:<https://doi.org/10.1016/j.watres.2017.09.030>.
- Li, K., 2007. *Ceramic Membranes for Separation and Reaction*, John Wiley & Sons, Ltd, doi:<https://www.doi.org/10.1002/9780470319475>.
- Liberman, N., Shandalov, S., Forgacs, C., Oron, G., Brenner, A., 2016. Use of MBR to sustain active biomass for treatment of low organic load grey water. *Clean Technologies and Environmental Policy* 18(4) 1219–1224, doi:<https://www.doi.org/10.1007/s10098-016-1112-4>.
- Lienert, J., Bürki, T., Escher, B.I., 2007. Reducing micropollutants with source control: substance flow analysis of 212 pharmaceuticals in faeces and urine. *Water Science and Technology* 56(5) 87–96, doi:<https://doi.org/10.2166/wst.2007.560>.
- Lin, H., Gao, W., Meng, F., Liao, B.Q., Leung, K.T., Zhao, L., Chen, J., Hong, H., 2012. Membrane Bioreactors for Industrial Wastewater Treatment: A Critical Review. *Critical Reviews in Environmental Science and Technology* 42(7) 677–740, doi:<https://doi.org/10.1080/10643389.2010.526494>.
- Linden, K.G., Mohseni, M., 2014. Advanced Oxidation Processes: Applications in Drinking Water Treatment, in S. Ahuja, ed., *Comprehensive Water Quality and Purification*, 148–172, Elsevier, Waltham, doi:<https://doi.org/10.1016/B978-0-12-382182-9.00031-1>.
- Lindqvist, K., Lidén, E., 1997. Preparation of alumina membranes by tape casting and dip coating. *Journal of the European Ceramic Society* 17(2-3) 359–366, doi:[https://doi.org/10.1016/S0955-2219\(96\)00107-0](https://doi.org/10.1016/S0955-2219(96)00107-0).
- Liu, D., 2019. *Escherichia coli*, in T.M. Schmidt, ed., *Encyclopedia of Microbiology* (Fourth Edition), 171–182, Academic Press, Oxford, fourth Edition, doi:<https://doi.org/10.1016/B978-0-12-801238-3.02291-1>.
- Lundie, S., Peters, G.M., Beavis, P.C., 2004. Life Cycle Assessment for Sustainable Metropolitan Water Systems Planning. *Environmental Science & Technology* 38(13) 3465–3473, doi:<https://doi.org/10.1021/es034206m>.
- Luo, T., Young, R., Reig, P., 2015. *Aqueduct Projected Water Stress Country Rankings*, World Resources Institute.
- Ma, J., Dai, R., Chen, M., Khan, S.J., Wang, Z., 2018. Applications of membrane bioreactors for water reclamation: Micropollutant removal, mechanisms and perspectives. *Bioresource Technology* 269 532–543, doi:<https://doi.org/10.1016/j.biortech.2018.08.121>.

- Madsen, T., Miljøstyrelsen, D., 2001. Environmental and Health Assessment of Substances in Household Detergents and Cosmetic Detergent Products, Danish Environmental Protection Agency.
- Marlow, D.R., Moglia, M., Cook, S., Beale, D.J., 2013. Towards sustainable urban water management: A critical reassessment. *Water Research* 47(20) 7150–7161, doi:<https://doi.org/10.1016/j.watres.2013.07.046>.
- Masi, F., Bresciani, R., Rizzo, A., Edathoot, A., Patwardhan, N., Panse, D., Langergraber, G., 2016. Green walls for greywater treatment and recycling in dense urban areas: a case-study in Pune. *Journal of Water, Sanitation and Hygiene for Development* 6(2) 342–347, doi:<https://doi.org/10.2166/washdev.2016.019>.
- Maurer, M., 2009. Specific net present value: An improved method for assessing modularisation costs in water services with growing demand. *Water Research* 43(8) 2121–2130, doi:<https://doi.org/10.1016/j.watres.2009.02.008>.
- Maurer, M., Wolfram, M., Anja, H., 2010. Factors affecting economies of scale in combined sewer systems. *Water Science and Technology* 62(1) 36–41, doi:<https://doi.org/10.2166/wst.2010.241>.
- Mbavarira, T.M., Grimm, C., 2021. A Systemic View on Circular Economy in the Water Industry: Learnings from a Belgian and Dutch Case. *Sustainability* 13(6) 3313, doi:<https://doi.org/10.3390/su13063313>.
- McCarty, P.L., Bae, J., Kim, J., 2011. Domestic Wastewater Treatment as a Net Energy Producer - Can This be Achieved? *Environmental Science & Technology* 45(17) 7100–7106, doi:<https://doi.org/10.1021/es2014264>.
- McDonald, R.I., Weber, K., Padowski, J., Flörke, M., Schneider, C., Green, P.A., Gleeson, T., Eckman, S., Lehner, B., Balk, D., Boucher, T., Grill, G., Montgomery, M., 2014. Water on an urban planet: Urbanization and the reach of urban water infrastructure. *Global Environmental Change* 27 96–105, doi:<https://doi.org/10.1016/j.gloenvcha.2014.04.022>.
- Meindertsma, W., van Sark, W.G.J.H.M., Lipchin, C., 2010. Renewable energy fueled desalination in Israel. *Desalination and Water Treatment* 13(1-3) 450–463, doi:<https://doi.org/10.5004/dwt.2010.1004>.
- Merlet, R.B., Pizzoccaro-Zilamy, M.A., Nijmeijer, A., Winnubst, L., 2020. Hybrid ceramic membranes for organic solvent nanofiltration: State-of-the-art and challenges. *Journal of Membrane Science* 599 117839, doi:<https://doi.org/10.1016/j.memsci.2020.117839>.
- Metcalf & Eddy, Burton, F.L., Stensel, H.D., Tchobanoglous, G., 2013. *Wastewater engineering: treatment and resource recovery*, New York : McGraw-Hill Higher Education ; London : McGraw-Hill, fifth Edition.
- Molden, D., ed., 2007. *Water for Food, Water for Life: A Comprehensive Assessment of Water Management in Agriculture*, Comprehensive assessment of water management in agriculture, Earthscan; International Water Management Institute.



- Müller, A., Stahl, M.R., Greiner, R., Posten, C., 2014. Performance and dose validation of a coiled tube UV-C reactor for inactivation of microorganisms in absorbing liquids. *Journal of Food Engineering* 138 45–52, doi:<https://doi.org/10.1016/j.jfoodeng.2014.04.013>.
- Naddeo, V., Scannapieco, D., Belgiorno, V., 2013. Enhanced drinking water supply through harvested rainwater treatment. *Journal of Hydrology* 498 287–291, doi:<https://doi.org/10.1016/j.jhydrol.2013.06.012>.
- Napoli, C., Rioux, B., 2016. Evaluating the economic viability of solar-powered desalination: Saudi Arabia as a case study. *International Journal of Water Resources Development* 32(3) 412–427, doi:<https://doi.org/10.1080/07900627.2015.1109499>.
- Nel, N., Jacobs, H.E., 2019. Investigation into untreated greywater reuse practices by suburban households under the threat of intermittent water supply. *Journal of Water, Sanitation and Hygiene for Development* 9(4) 627–634, doi:<https://doi.org/10.2166/washdev.2019.055>.
- Nyamutswa, L., Zhu, B., Navaratna, D., Collins, S., Duke, M., 2018. Proof of Concept for Light Conducting Membrane Substrate for UV-Activated Photocatalysis as an Alternative to Chemical Cleaning. *Membranes* 8(4) 122, doi:<https://doi.org/10.3390/membranes8040122>.
- Öberg, G., Metson, G.S., Kuwayama, Y., A. Conrad, S., 2020. Conventional Sewer Systems Are Too Time-Consuming, Costly and Inflexible to Meet the Challenges of the 21st Century. *Sustainability* 12(16) 6518, doi:<https://doi.org/10.3390/su12166518>.
- Opher, T., Friedler, E., 2016. Comparative LCA of decentralized wastewater treatment alternatives for non-potable urban reuse. *Journal of Environmental Management* 182 464–476, doi:<https://doi.org/10.1016/j.jenvman.2016.07.080>.
- Oteng-Peprah, M., de Vries, N.K., Acheampong, M.A., 2018. Greywater characterization and generation rates in a peri urban municipality of a developing country. *Journal of Environmental Management* 206 498–506, doi:<https://doi.org/10.1016/j.jenvman.2017.10.068>.
- Pabi, S., Amarnath, A., Goldstein, R., Reekie, L., 2013. Electricity use and management in the municipal water supply and wastewater industries, , Electric Power Research Institute and Water Research Foundation.
- Palmarin, M.J., Young, S., 2019. Comparison of the treatment performance of a hybrid and conventional membrane bioreactor for greywater reclamation. *Journal of Water Process Engineering* 28 54–59, doi:<https://doi.org/10.1016/j.jwpe.2018.12.012>.
- Palmarin, M.J., Young, S., Chan, J., 2020. Recovery of a hybrid and conventional membrane bioreactor following long-term starvation. *Journal of Water Process Engineering* 34 101027, doi:<https://doi.org/10.1016/j.jwpe.2019.101027>.
- Palmer, N., 2011. Desalination 'Comes of Age' Across Arid Australia. *Water and Wastewater International* 26(3) 54–61.
- Park, H.D., Chang, I.S., Lee, K.J., 2015. Principles of Membrane Bioreactors for Wastewater Treatment, Taylor & Francis Ltd.

- Penn, R., Schütze, M., Alex, J., Friedler, E., 2017. Impacts of onsite greywater reuse on wastewater systems. *Water Science and Technology* 75(8) 1862–1872, doi:<https://doi.org/10.2166/wst.2017.057>.
- Puchongkawarin, C., Gomez-Mont, C., Stuckey, D.C., Chachuat, B., 2015. Optimization-based methodology for the development of wastewater facilities for energy and nutrient recovery. *Chemosphere* 140 150–158, doi:<https://doi.org/10.1016/j.chemosphere.2014.08.061>.
- Rabaey, K., Van De Walle, A., 2020. De "water-kilometer" kan een instrument zijn om Vlaanderen beter te wapenen tegen de droogte (Dutch), In: Knack.  
URL <https://www.knack.be/nieuws/belgie/de-water-kilometer-kan-een-instrument-zijn-om-vlaanderen-beter-te-wapenen-tegen-de-droogte/article-opinion-1604231.html>
- Rabaey, K., Vandekerckhove, T., Van de Walle, A., Sedlak, D.L., 2020. The third route: Using extreme decentralization to create resilient urban water systems. *Water Research* 185 116276, doi:<https://doi.org/10.1016/j.watres.2020.116276>.
- Ragazzo, P., Chiuccini, N., Piccolo, V., Spadolini, M., Carrer, S., Zanon, F., Gehr, R., 2020. Wastewater disinfection: long-term laboratory and full-scale studies on performic acid in comparison with peracetic acid and chlorine. *Water Research* 184 116169, doi:<https://doi.org/10.1016/j.watres.2020.116169>.
- Rahn, R.O., 1997. Potassium Iodide as a Chemical Actinometer for 254 nm Radiation: Use of Iodate as an Electron Scavenger. *Photochemistry and Photobiology* 66(4) 450–455, doi:<https://doi.org/10.1111/j.1751-1097.1997.tb03172.x>.
- Rahn, R.O., Stefan, M.I., Bolton, J.R., Goren, E., Shaw, P.S., Lykke, K.R., 2003. Quantum Yield of the Iodide–Iodate Chemical Actinometer: Dependence on Wavelength and Concentration. *Photochemistry and Photobiology* 78(2) 146, doi:[https://doi.org/10.1562/0031-8655\(2003\)078<0146:qyotic>2.0.co;2](https://doi.org/10.1562/0031-8655(2003)078<0146:qyotic>2.0.co;2).
- Ramprasad, C., Smith, C.S., Memon, F.A., Philip, L., 2017. Removal of chemical and microbial contaminants from greywater using a novel constructed wetland: GROW. *Ecological Engineering* 106 55–65, doi:<https://doi.org/10.1016/j.ecoleng.2017.05.022>.
- Ray, P.A., Kirshen, P.H., Vogel, R.M., 2010. Integrated Optimization of a Dual Quality Water and Wastewater System. *Journal of Water Resources Planning and Management* 136(1) 37–47, doi:[https://doi.org/10.1061/\(ASCE\)WR.1943-5452.0000004](https://doi.org/10.1061/(ASCE)WR.1943-5452.0000004).
- Reynaert, E., Greenwood, E.E., Ndwandwe, B., Riechmann, M.E., Sindall, R.C., Udert, K.M., Morgenroth, E., 2020. Practical implementation of true on-site water recycling systems for hand washing and toilet flushing. *Water Research* 7 100051, doi:<https://doi.org/10.1016/j.wroa.2020.100051>.
- Reynaert, E., Hess, A., Morgenroth, E., 2021. Making Waves: Why water reuse frameworks need to co-evolve with emerging small-scale technologies. *Water Research* 11 100094, doi:<https://doi.org/10.1016/j.wroa.2021.100094>.

- Rezaei, N., Diaz-Elsayed, N., Mohebbi, S., Xie, X., Zhang, Q., 2019. A multi-criteria sustainability assessment of water reuse applications: a case study in Lakeland, Florida. *Environmental Science: Water Research and Technology* 5(1) 102–118, doi:<https://doi.org/10.1039/c8ew00336j>.
- Rice, J., Wutich, A., White, D.D., Westerhoff, P., 2016. Comparing actual de facto wastewater reuse and its public acceptability: A three city case study. *Sustainable Cities and Society* 27 467–474, doi:<https://doi.org/10.1016/j.scs.2016.06.007>.
- Richardson, T.G., Bailey, H., 1995. Indirect potable reuse - a watershed management technique, Volume 2, 1031–1035.
- Richter, H., Voigt, I., Fischer, G., Puhlfürß, P., 2003. Preparation of zeolite membranes on the inner surface of ceramic tubes and capillaries. *Separation and Purification Technology* 32(1-3) 133–138, doi:[https://doi.org/10.1016/S1383-5866\(03\)00025-X](https://doi.org/10.1016/S1383-5866(03)00025-X).
- Rittmann, B., 2001. *Environmental biotechnology : principles and applications*, McGraw-Hill, Boston.
- Rodda, N., Salukazana, L., Jackson, S.A.F., Smith, M.T., 2011. Use of domestic greywater for small-scale irrigation of food crops: Effects on plants and soil. *Physics and Chemistry of the Earth, Parts A/B/C* 36(14-15) 1051–1062, doi:<https://doi.org/10.1016/j.pce.2011.08.002>.
- Rodríguez-Chueca, J., Ormad, M.P., Mosteo, R., Sarasa, J., Ovelleiro, J.L., 2015. Conventional and Advanced Oxidation Processes Used in Disinfection of Treated Urban Wastewater. *Water Environment Research* 87(3) 281–288, doi:<https://doi.org/10.2175/106143014X13987223590362>.
- Royal Meteorological Institute of Belgium, s.d. *Klimaatatlas: Gemiddelde Jaarlijkse Neerslag 1981-2010 (Dutch)*, retrieved 15/11/2020.  
URL <https://www.meteo.be/nl/klimaat/klimaatatlas/klimaatkaarten/neerslag/neerslaghoeveelheid/jaarlijks>
- Sahoo, G.C., Halder, R., Jedidi, I., Oun, A., Nasri, H., Roychoudhury, P., Majumdar, S., Bandyopadhyay, S., Amar, R.B., 2016. Preparation and characterization of microfiltration apatite membrane over low cost clay-alumina support for decolorization of dye solution. *Desalination and Water Treatment* 57(57) 1–10, doi:<https://doi.org/10.1080/19443994.2016.1186565>.
- Santasmasas, C., Rovira, M., Clarens, F., Valderrama, C., 2013. Grey water reclamation by decentralized MBR prototype. *Resources, Conservation and Recycling* 72 102–107, doi:<https://doi.org/10.1016/j.resconrec.2013.01.004>.
- Scheumann, R., Kraume, M., 2009. Influence of hydraulic retention time on the operation of a submerged membrane sequencing batch reactor (SM-SBR) for the treatment of greywater. *Desalination* 246(1-3) 444–451, doi:<https://doi.org/10.1016/j.desal.2008.03.066>.
- Schoen, M.E., Jahne, M.A., Garland, J., 2018. Human health impact of non-potable reuse of distributed wastewater and greywater treated by membrane bioreactors. *Microbial Risk Analysis* 9 72–81, doi:<https://doi.org/10.1016/j.mran.2018.01.003>.

- Schoen, M.E., Jahne, M.A., Garland, J., 2020. A risk-based evaluation of onsite, non-potable reuse systems developed in compliance with conventional water quality measures. *Journal of Water and Health* 18(3) 331–344, doi:<https://doi.org/10.2166/wh.2020.221>.
- Schuetze, T., 2013. Rainwater harvesting and management - policy and regulations in Germany. *Water Supply* 13(2) 376–385, doi:<https://doi.org/10.2166/ws.2013.035>.
- Schwaller, C., Keller, Y., Helmreich, B., Drewes, J.E., 2021. Estimating the agricultural irrigation demand for planning of non-potable water reuse projects. *Agricultural Water Management* 244 106529, doi:<https://doi.org/10.1016/j.agwat.2020.106529>.
- Sedlak, D.L., Drewes, J.E., Luthy, R.G., 2013. Introduction: Reinventing Urban Water Infrastructure. *Environmental Engineering Science* 30(8) 393–394, doi:<https://doi.org/10.1089/ees.2013.3008>.
- Shabangu, T.H., Hamam, Y., Adedeji, K.B., 2020. Decision support systems for leak control in urban water supply systems: A literature synopsis. *Procedia CIRP* 90 579–583, doi:<https://doi.org/10.1016/j.procir.2020.01.120>.
- Shaikh, I.N., Ahammed, M.M., 2020. Quantity and quality characteristics of greywater: A review. *Journal of Environmental Management* 261 110266, doi:<https://doi.org/10.1016/j.jenvman.2020.110266>.
- Sharvelle, S., Ashbolt, N., Clerico, E., Holquist, R., Levernz, H., Olivieri, A., 2017. Risk-Based Framework for the Development of Public Health Guidance for Decentralized Non-Potable Water Systems. *Proceedings of the Water Environment Federation* 6(8) 3799–3809, doi:<https://doi.org/10.2175/193864717822158189>.
- Shukla, P.R., Skea, J., Slade, R., van Diemen, R., Haughey, E., Malley, J., Pathak, M., Portugal Pereira, J., eds., 2019. *Climate Change and Land: an IPCC special report on climate change, desertification, land degradation, sustainable land management, food security, and greenhouse gas fluxes in terrestrial ecosystems*, Chapter Technical Summary, Intergovernmental Panel on Climate Change.
- Shukla, S., Tare, V., 2019. *Handbook of Environmental Materials Management*, Chapter Assessment of Some Aspects of Provisioning Sewerage Systems: A Case Study of Urban Agglomerations in Ganga River Basin, 3–34, Springer International Publishing, Cham, doi:[10.1007/978-3-319-73645-7\\_3](https://doi.org/10.1007/978-3-319-73645-7_3).
- Siggins, A., Burton, V., Ross, C., Lowe, H., Horswell, J., 2016. Effects of long-term greywater disposal on soil: A case study. *Science of The Total Environment* 557-558 627–635, doi:<https://doi.org/10.1016/j.scitotenv.2016.03.084>.
- Simpson, N.P., Simpson, K.J., Shearing, C.D., Cirolia, L.R., 2019. Municipal finance and resilience lessons for urban infrastructure management: a case study from the Cape Town drought. *International Journal of Urban Sustainable Development* 11(3) 257–276, doi:<https://doi.org/10.1080/19463138.2019.1642203>.
- Skambraks, A.K., Kjerstadius, H., Meier, M., Åsa Davidsson, Wuttke, M., Giese, T., 2017. Source separation sewage systems as a trend in urban wastewater management: Drivers for

- the implementation of pilot areas in Northern Europe. *Sustainable Cities and Society* 28 287–296, doi:<https://doi.org/10.1016/j.scs.2016.09.013>.
- Sun, C., Leiknes, T., Weitzenböck, J., Thorstensen, B., 2010. Development of a biofilm-MBR for shipboard wastewater treatment: The effect of process configuration. *Desalination* 250(2) 745–750, doi:<https://doi.org/10.1016/j.desal.2008.11.034>.
- Tadkaew, N., Hai, F.I., McDonald, J.A., Khan, S.J., Nghiem, L.D., 2011. Removal of trace organics by MBR treatment: The role of molecular properties. *Water Research* 45(8) 2439–2451, doi:<https://doi.org/10.1016/j.watres.2011.01.023>.
- Tang, X., Wen, Y., He, Y., Jiang, H., Dai, X., Bi, X., Wagner, M., Chen, H., 2020. Full-scale semi-centralized wastewater treatment facilities for resource recovery: operation, problems and resolutions. *Water Science and Technology* 82(2) 303–314, doi:<https://doi.org/10.2166/wst.2020.169>.
- Tay, M.F., Lee, S., Xu, H., Jeong, K., Liu, C., Cornelissen, E.R., Wu, B., Chong, T.H., 2020. Impact of salt accumulation in the bioreactor on the performance of nanofiltration membrane bioreactor (NF-MBR)+Reverse osmosis (RO) process for water reclamation. *Water Research* 170 115352, doi:<https://doi.org/10.1016/j.watres.2019.115352>.
- Ternes, T., Joss, A., 2006. *Human Pharmaceuticals, Hormones and Fragrances - The Challenge of Micropollutants in Urban Water Management*, IWA Publishing, doi:10.2166/9781780402468.
- Tideway, 2020. *Tideway Annual Report FY 2019-20*, Bazalgette Tunnel Ltd., Cottons Centre, Cottons Lane, London.  
URL <https://www.tideway.london>
- Trinh, T., van den Akker, B., Coleman, H.M., Stuetz, R.M., Le-Clech, P., Khan, S.J., 2012. Removal of endocrine disrupting chemicals and microbial indicators by a decentralised membrane bioreactor for water reuse. *Journal of Water Reuse and Desalination* 2(2) 67–73, doi:<https://doi.org/10.2166/wrd.2012.010>.
- UNESCO World Water Assessment Programme, 2015. *The United Nations world water development report 2015: water for a sustainable world*, UNESCO World Water assessment Programme, United Nations Educational, Scientific and Cultural Organization, Paris, France.
- UNESCO World Water Assessment Programme, 2018. *The United Nations world water development report 2018: nature-based solutions for water*, United Nations Educational, Scientific and Cultural Organization, Paris, France.
- United Nations, Department of Economic and Social Affairs, Population Division, 2018. *World Urbanization Prospects: The 2018 Revision*, United Nations, New York NY.
- United Nations, Department of Economic and Social Affairs, Population Division, 2019a. *World Population Prospects 2019*, custom data acquired via website.
- United Nations, Department of Economic and Social Affairs, Population Division, 2019b. *World Population Prospects 2019: Highlights*, United Nations, New York NY.

- U.S. EPA, 2012. 2012 Guidelines for Water Reuse. EPA/600/R-12/618.
- Van Houtte, E., Verbauwhede, J., 2008. Operational experience with indirect potable reuse at the Flemish Coast. *Desalination* 218(1-3) 198–207, doi:<https://doi.org/10.1016/j.desal.2006.08.028>.
- Verliefde, A., Cornelissen, E., Amy, G., Van der Bruggen, B., van Dijk, H., 2007. Priority organic micropollutants in water sources in Flanders and the Netherlands and assessment of removal possibilities with nanofiltration. *Environmental Pollution* 146(1) 281–289, doi: <https://doi.org/10.1016/j.envpol.2006.01.051>.
- Vlaamse Milieumaatschappij, 2018. Watergebruik door huishoudens - het watergebruik in 2016 bij de Vlaming thuis (Dutch), retrieved 29/12/2020.  
URL <https://www.vlaanderen.be/publicaties/watergebruik-door-huishoudens-het-watergebruik-in-2016-bij-de-vlaming-thuis>
- Vlaamse Milieumaatschappij, 2019a. Drinkwatervoorziening in Vlaanderen: organisatie en een blik vooruit (Dutch).  
URL [https://www.vmm.be/water/drinkwater/drinkwatervoorziening\\_in\\_vlaanderen\\_organisatie\\_en\\_een\\_blik\\_vooruit\\_tw.pdf/view](https://www.vmm.be/water/drinkwater/drinkwatervoorziening_in_vlaanderen_organisatie_en_een_blik_vooruit_tw.pdf/view)
- Vlaamse Milieumaatschappij, 2019b. Riolerings- en zuiveringsgraden (Dutch).  
URL <https://www.vmm.be/data/riolerings-en-zuiveringsgraden>
- Vlaamse Milieumaatschappij, 2020a. Afwegingskader prioritair watergebruik tijdens droogte (Dutch), retrieved 29/12/2020.  
URL <https://www.vmm.be/water/projecten/afwegingskader-prioritair-watergebruik-tijdens-droogte>
- Vlaamse Milieumaatschappij, 2020b. Hittegolven en andere temperatuursextremen (Dutch), retrieved 31/12/2020.  
URL <https://www.milieuraapport.be/milieuthemas/klimateverandering/temperatuur/hittegolven-en-temperatuursextremen>
- Vlaamse Milieumaatschappij, 2020c. Impact droogte op drinkwater (Dutch), retrieved 31/12/2020.  
URL <https://www.vmm.be/water/droogte/impact-droogte-op-drinkwater>
- von Recklinghausen, M., 1914. The ultra-violet rays and their application for the sterilization of water. *Journal of the Franklin Institute* 178(6) 681–704, doi:[https://doi.org/10.1016/S0016-0032\(14\)90419-7](https://doi.org/10.1016/S0016-0032(14)90419-7).
- Vuppaladadiyam, A.K., Merayo, N., Prinsen, P., Luque, R., Blanco, A., Zhao, M., 2019. A review on greywater reuse: quality, risks, barriers and global scenarios. *Reviews in Environmental Science and Bio/Technology* 18(1) 77–99, doi:<https://doi.org/10.1007/s11157-018-9487-9>.
- Wang, S., Liu, H., Gu, J., Sun, H., Zhang, M., Liu, Y., 2019. Technology feasibility and economic viability of an innovative integrated ceramic membrane bioreactor and reverse osmosis process for producing ultrapure water from municipal wastewater. *Chemical Engineering Journal* 375 122078, doi:<https://doi.org/10.1016/j.cej.2019.122078>.

- Weber, K.T., Yadev, R., Davis, J., Blair, K., Schnase, J., Carroll, M., Gill, R., 2017. The NASA RECOVER Decision Support System: Geography of Wildfires Across the West, , The National Aeronautics and Space Administration.
- Western Australia Department of Health, 2011. Guidelines for the Non-potable Uses of Recycled Water in Western Australia 2011.
- Westhof, L., Köster, S., Reich, M., 2016. Occurrence of micropollutants in the wastewater streams of cruise ships. *Emerging Contaminants* 2(4) 178–184, doi:<https://doi.org/10.1016/j.emcon.2016.10.001>.
- Willems, P., Renson, I., 2019. We spelen met water (Dutch), retrieved 31/12/2020. URL [https://www.standaard.be/cnt/dmf20191208\\_04756786?](https://www.standaard.be/cnt/dmf20191208_04756786?)
- Winward, G.P., Avery, L.M., Frazer-Williams, R., Pidou, M., Jeffrey, P., Stephenson, T., Jefferson, B., 2008. A study of the microbial quality of grey water and an evaluation of treatment technologies for reuse. *Ecological Engineering* 32(2) 187–197, doi:<https://doi.org/10.1016/j.ecoleng.2007.11.001>.
- World Health Organization, 2006. Excreta and greywater use in agriculture, in *Guidelines for the safe use of wastewater, excreta and greywater, Volume 4*, WHO Press, World Health Organization, 20 Avenue Appia, 1211 Geneva 27, Switzerland.
- Wu, B., 2019. Membrane-based technology in greywater reclamation: A review. *Science of The Total Environment* 656 184–200, doi:<https://doi.org/10.1016/j.scitotenv.2018.11.347>.
- Yang, B., Zhang, S., Pang, X., Lu, J., Wu, Z., Yue, Y., Wang, T., Jiang, Z., Lv, J., 2020. Separation of serum proteins and micellar casein from skim goat milk by pilot-scale 0.05- $\mu\text{m}$  pore-sized ceramic membrane at 50°C. *Journal of Food Process Engineering* 43(2) e13334, doi:<https://doi.org/10.1111/jfpe.13334>.
- Yangali-Quintanilla, V., Maeng, S.K., Fujioka, T., Kennedy, M., Amy, G., 2010. Proposing nanofiltration as acceptable barrier for organic contaminants in water reuse. *Journal of Membrane Science* 362(1-2) 334–345, doi:<https://doi.org/10.1016/j.memsci.2010.06.058>.
- Yazdanshenas, M., Soltanieh, M., Tabatabaei Nejad, S.A.R., Fillaudeau, L., 2010. Cross-flow microfiltration of rough non-alcoholic beer and diluted malt extract with tubular ceramic membranes: Investigation of fouling mechanisms. *Journal of Membrane Science* 362(1-2) 306–316, doi:<https://doi.org/10.1016/j.memsci.2010.06.041>.
- Yu, M., Bishop, T., Ogtrop, F.V., 2019. Assessment of the Decadal Impact of Wildfire on Water Quality in Forested Catchments. *Water* 11(3) 533, doi:<https://doi.org/10.3390/w11030533>.
- Yusuf, Z., Abdul Wahab, N., Sahlan, S., 2015. Fouling control strategy for submerged membrane bioreactor filtration processes using aeration airflow, backwash, and relaxation: a review. *Desalination and Water Treatment* 57(38) 17683–17695, doi:<https://doi.org/10.1080/19443994.2015.1086893>.
- Zang, J., Kumar, M., Werner, D., 2021. Real-world sustainability analysis of an innovative decentralized water system with rainwater harvesting and wastewater reclamation. *Journal*



of Environmental Management 280 111639, doi:<https://doi.org/10.1016/j.jenvman.2020.111639>.

Zeuner, B., Ovtar, S., Persson, Å.H., Foghmoes, S., Berendt, K., Ma, N., Kaiser, A., Negra, M.D., Pinelo, M., 2020. Surface treatments and functionalization of metal-ceramic membranes for improved enzyme immobilization performance. *Journal of Chemical Technology and Biotechnology* 95(4) 993–1007, doi:<https://doi.org/10.1002/jctb.6278>.